PL ISSN 1897-2691
PL ISBN 978-83-65719-63-8

MANAGEMENT OF TECHNOLOGICAL PROCESSES IN ENERGY TECHNOLOGIES

MONOGRAFIE, STUDIA, ROZPRAWY

M120

MANAGEMENT OF TECHNOLOGICAL PROCESSES IN ENERGY TECHNOLOGIES

under the general editorship of Anatoliy M. Pavlenko

Politechnika Świętokrzyska
Kielce 2019

MONOGRAFIE, STUDIA, ROZPRAWY

M120

MANAGEMENT OF TECHNOLOGICAL PROCESSES IN ENERGY TECHNOLOGIES

under the general editorship of Anatoliy M. Pavlenko

Kielce 2019

MONOGRAFIE, STUDIA, ROZPRAWY NR M120

Redaktor Naukowy serii
INŻYNIERIA ŚRODOWISKA I ENERGETYKA
dr hab. Lidia DĄBEK, prof. PŚk

Recenzenci
professor Natalia FIALKO
The National Academy of Sciences of Ukraine

professor Ibrahim SERDAR
European Scientifically-Educational Academy Poltava Ukraine

Redakcja
Aneta STARZYK

Projekt okładki
Tadeusz UBERMAN

Wydanie monografii finansowane w ramach projektu z programu Ministra
Nauki i Szkolnictwa Wyższego pod nazwą „Regionalna Inicjatywa Doskonałości”
w latach 2019-2022, nr projektu 025/RID/2018/19, kwota finansowania 12 000 000 zł

Ministerstwo Nauki
i Szkolnictwa Wyższego

PL ISSN 1897-2691
PL ISBN 978-83-65719-63-8

Wydawnictwo Politechniki Świętokrzyskiej
25-314 Kielce, al. Tysiąclecia Państwa Polskiego 7
tel./fax 41 34 24 581
e-mail: wydawca@tu.kielce.pl
www.wydawnictwo.tu.kielce.pl

Contents

Preface

The level of development of modern society is largely determined by energy production and consumption.

Of all the industries of human economic activity – energetics has the greatest impact on our lives. Mistakes in this area have serious consequences. Heat and light in homes, traffic and work in industry – all this requires energy consumption. In recent years high priority acquire it is these negative trends. First of all, there was a strong tendency to increase in the cost of energy. With existing energy systems and technologies use of energy and with existing schemes of consumption, most industrially developed countries have come to the level when a further increase in energy production costs begin to exceed the profit. Secondly, the problem of environmental pollution and the risk of exploitation of equipment of energy producing that is still local, take regional or global. Thus at the present time humanity faces a dilemma: on the one hand, cannot be achieved without the energy of material well-being of people, on the other – preserve the current rate of consumption can lead to the destruction of the environment and as a consequence – to reduce the standard of living and the threat to our existence. In order to smooth contradictions between energetics, economy and ecology, it is necessary to achieve a proper understanding of the current situation, possible and desirable directions of its development. Need a broad public discussion, which should be supported by intensive research to determine the schemes energetics of the future.

These are the challenges facing researchers and students of our faculty. In their scientific research and in the educational process energetics problems considered together various directions of research: energy consumption, renewable energy sources, ecology and of course the development of energy- and the material-saving technologies. Some of the results of research carried out by scientists of the faculty, we propose for discussion.

Anatoliy Pavlenko, Dr. Sci., professor

Department of Building Physics and Renewable Energy
Kielce University of Technology

Chapter 1

ANALYSIS OF ASPECTS AND SIMULATION MODELING OF THE THERMAL ENERGY MARKET IN UKRAINE

Valerii I. Deshko, Dmitro S. Karpenko

National Technical University of Ukraine
"Igor Sikorsky Kyiv Polytechnic Institute"

1.1. INTRODUCTION

The organization of the heat energy market within the state is an integral part of the functioning of the state economy in the energy sector. Unfortunately, at present stage of the development of Ukraine’s energy sector there are many technical, economic and legal issues that need to be addressed to build an effective model of the Thermal Energy Market. At the same time, it is necessary to consider the questions of constructing models of the heat energy market taking into account such features of our state as: significant territories, heterogeneity of the climate, technical state of heat supply networks, general economic and social situation, etc.

At the moment, fluctuations in prices on world markets for fossil fuels have led to the rapid development of technologies in the Renewable Energy Sector (RES). The diversity of these technologies every year shows the rapid growth of the level of competitiveness in the field of energy in the general sense. For example, in the states of Europe, taking into account the tough environmental policy, the direction of RES has been rapidly developing. In this regard, the question arises of the effective use of surplus resources, which are formed as a result of natural processes or the work of enterprises of various spheres of the state’s economy. Among the priority directions of utilization of surplus local resources, the tool of the Thermal Energy Market (TEM) can be distinguished. The transformation of local resources into heat energy is a technologically simple process, while the final price of products can be much lower than traditional heat energy production methods. Consequently, the creation of competitive conditions in the area of heat supply can lead to an increase in the quality of heat energy as a commodity for the consumer, reduction of tariffs for heat energy, and increase of the level of reliability of heat supply. Moreover, due to the effective use of local resources, the creation of the TEM can partly lead to Ukraine’s energy independence.

A prerequisite for studying the issue of creating TEM is the ineffectiveness of the existing heat supply system at all its stages of operation from the production of thermal energy to its use by consumers. The sphere of energy, from an economic point of view, has the type of a natural monopoly, that is, such a model of functioning of the system should lead to maximum economic welfare within this system [1]. But, based on current realities, it should be noted that the theoretical calculations, which indicate the effectiveness of the monopoly in this sector of the economy, do not coincide with the practical results of such enterprises. The absence of a motivating factor in the functioning of such a model results from a lack of competition, therefore, the level of performance of such a system can be estimated in advance as low. The system can not work without a person's participation, therefore it should be understood that the problem of lack of a motivational factor is primarily social. The monopolization of energy sector in Ukraine leads to inefficient use of resources at the stage of heat energy production, and as a result, to the overestimated tariffs for this type of products both for domestic consumers and for industrial-budget enterprises.

It is important to solve a number of problems before creating the TEM in Ukraine. In addition, it is important to determine the model of the market on the basis of which its functioning will take place. The most significant contribution to the reform of the heat supply model is the arrival of private energy companies in the sphere of generation of thermal energy. The main mission of the creation of the TEM is the creation of real tariffs for heat energy, namely for heating and hot water, which can lead to an increase in the level of efficiency of energy consumption and an increase in the state of well-being of the population in the state.

The term "heat energy" in accordance with the Law of Ukraine "About heat supply" is defined as the goods produced on the objects of the heat supply sector for heating, hot water, other economic and technological needs of consumers, intended for sale [2].

Thermal energy, as a commodity, has a certain number of essential features that are prerequisites for the operation of the heat energy market itself:

1. Thermal energy is limited in the distance of transport with centralized heat supply, as well as the use of decentralized heat supply plants – small CHP plants and boiler houses, as there are processes of irreversibility (the second law of thermodynamics). This means that it is economically inexpedient to accumulate thermal energy during a considerable time interval under the existing conditions in Ukraine, and consequently, the level of production and consumption, in general, should be equal to each other at any given time.
2. Thermal energy is a heterogeneous commodity, since it can be consumed in different aggregate states of the coolant with different heat engineering

parameters. The use of heat energy should be subject to both quantitative and qualitative assessment, depending on the type of heat load (process steam, heating, ventilation, hot water), for example, by analyzing exergy indicators.

3. Thermal energy supplied to a common system with several suppliers may be defined as the product of a particular supplier only on source leads.
4. The level of thermal energy consumption has a pronounced seasonal character. This is mainly due to the uneven schedule of heating loads.

The existing structure of the subjects of relations in the field of heat supply in general terms is determined by:

1. Suppliers of fuel and energy resources.
2. Equipment suppliers and energy service organizations.
3. Heat generating or heat supplying organizations.
4. Organization of the heating network.
5. Consumers of thermal energy.
6. Governmental regulation and control in the field of heat supply.

Consequently, the term "heat energy market", in the simplest sense, can be defined as a set of economic relations between suppliers of fuel and energy resources, suppliers of equipment and energy service organizations, heat generating organizations, heat supply network organizations, public regulators and regulators in the field of heat supply, and consumers thermal energy [3].

According to the current legislation, the term "heat energy market" is defined as the sphere of heat energy turnover as a commodity for which there is demand and supply.

1.2. THE SPHERE OF HEAT SUPPLY IN UKRAINE

The level of energy efficiency of municipal heat supply systems has been rapidly decreasing over the past years. The method of conducting economic activity by these enterprises calls into question the correctness of the principle of the organization of the system of heat supply in Ukraine.

In most cases, in Ukraine, on a certain heat supply system, there is one enterprise that simultaneously performs the functions of production, transportation and supply of heat energy. That is, the company has a monopoly position within this system. The field of energy, from an economic point of view, has the nature of a natural monopoly, that is, such a model of functioning of the system should lead to maximum economic prosperity within this system. But, based on current realities, it should be noted that the theoretical calculations, which indicate the effectiveness of the monopoly in this sector of the economy, do not coincide with the practical results of such enterprises. The absence of a motivating factor in the functioning of such a model results from a lack of competition, therefore, the level of performance of such a system can be estimated in advance as low. The system can not work without a person's participation, therefore it should be understood that the problem of lack of a motivational factor is primarily social.

The necessity to create a Thermal Energy Market can be justified by three unresolved problems:

1. In Ukraine, there are surplus resources that have potential energy in one form or another arising from the production process of any production or agricultural activity, but which are not utilized. This problem has a direct impact on the ecological and economic indicators of enterprises separately, and in Ukraine as a whole.
2. Lack of full use of the territorial potential of Ukraine for the production of thermal and electric energy from renewable energy sources.
3. Lack of civilized and competitive relations in the heat supply sector of Ukraine, which leads to high tariffs for heat energy for consumers.

To date, there is a significant number of thermal energy technologies that can solve the first two problems mentioned above. Depending on the price conjuncture of the energy market and how it is used, one or another technology may prevail. In Table 1.1 shows the main types of resources for the production of thermal and electric energy.

Table 1.1. The main types of resources for the production of thermal and electric energy

Type of resource	Technology
Solar energy	Solar systems
	Photovoltaics
Wind energy	Wind turbines
Biomass	Burning
	Gasification
	Reeteering
Energy of geothermal waters and earth's interior	Heat exchange with the environment
Hydroenergy	Electric generators
Fossil fuels	Burning
	Gasification
Atomic energy	Nuclear reactions of fission and synthesis

Some of the types of resources have their own varieties, which in turn are used by the appropriate technology, with the observance of technical and technological parameters to obtain the maximum level of energy efficiency of transformation into heat or electric energy.

Ukraine has a significant potential to use all of the above types of resources, which needs to take into account the local nature of this potential. The heat energy market, taking into account its localization, allows for the possibility of utilization of surplus resources and the use of renewable energy sources.

The heat supply sector has a number of peculiarities in terms of the process of production, transportation and use of heat energy. Speaking about the heat energy market, the ownership and management of trunk heating networks, distribution heat networks, central heating units and individual heat points (ITPs) should be distinguished as such activities falling within the concept of a natural monopoly [4]. This type of activity should be strictly controlled by the state bodies of management and control in the field of heat supply, with the provision of a certain level of profitability of these organizations.

In turn, competitive activities in the field of heat supply should include:

- design, construction and operation of heat energy sources,
- supply and use of fuel and energy resources,
- production and supply of equipment and energy service activities,
- energy sales and marketing activities.

In the markets for thermal energy, quite a variety of forms of competition are possible.

Competition of suppliers of Fuel and Energy Resources (FER). In the production of thermal energy, in almost all cases, the main cost item is the price of FERs that take part in the conversion process to the final product (thermal energy). The cheapest kind of fuel or energy (UAH/Gcal) will be in high demand among heat generating organizations.

Competition of projects. This is the most advanced type of competition in the heat energy market at the moment. First of all, it is about competition of projects of new heat sources, intended to cover growing loads in separate regions, replacement of more cost sources with less cost, projects to increase the reliability of heat supply, as well as projects to increase energy efficiency for different groups of consumers. The criterion for choosing another project could be whether the amount of annual reduction in the cost of producing heat energy, or the payback period of the project relative to the existing costs.

Competition of equipment suppliers. There are a large number of manufacturers and suppliers of equipment that is used directly in the technological processes of the heat energy sector. The competitiveness of this equipment is manifested in its level of energy and ecological efficiency, the level of technological perfection, the number of functions, the resource of work and the price of it.

Competition of energy service companies. This type of competition takes place directly during the operation of equipment, and provides for competition among organizations that are able to solve the problems of reducing the cost of production of thermal energy, increasing the energy efficiency of the generation, transportation and consumption of heat energy, and the introduction of advanced technologies.

Competition of heat-generating (heat supply) organizations. Implementation of this form of direct competition requires the solution of a significant number of technical, organizational and legal issues. The solution to these issues involves the organization of a particular model of the Thermal Energy Market. Thus, competition of heat sources is possible in principle only in large looped junctions and centralized heat supply systems. Since the organization of the thermal network is a natural monopoly, it is necessary that the process of production and transportation be divided into two independent organizations, in addition, the organization of the heat network should provide work in the system without discrimination and be subject to the state regulation and control authority in the field of heat supply, and not have their own large heat sources [5]. The free access of producers to the unified heating system should be legislated. Then, in the presence of excess heat generating capacity, the market operator (the organization of the heat network) can perform economically appropriate switching of loads, for example, according to the criterion of the minimum cost of generation (selling price) during this period. Actually, this kind of competition is the result of competition of projects, as there always are processes of fluctuations in prices for energy resources and technology.

All considered types of competition in the market of thermal energy are integral parts of it. The emphasis on thermal energy as a commodity needs to be shifted, since the above forms of competition determine the entire list of goods and services in the market, without which the functioning of this market is impossible. Taken together, all these form and determine the level of competitiveness of a different entity.

In Ukraine, the level of localization of the heat supply system is determined as follows:

- autonomous heat supply system (power of heat sources up to 1 Gcal/h),
- decentralized heat supply system (from 1 Gcal/year to 3 Gcal/year),
- a system of moderately centralized heat supply (from 3 Gcal/h to 20 Gcal/h),
- district heating system (from 20 Gcal/h) [3].

Depending on the localization of the heat supply system, one or another structure of interconnections between the entities prevails.

In the autonomous system of heat supply, the scheme of relations has a fairly simple view, where the consumer of heat energy himself serves as a heat supply and organization of the heating network. At the same time, the processes of construction and operation of equipment are almost, or not at all, controlled by the state. At this level, competition arises between suppliers of fuel and energy resources, suppliers of equipment and energy service organizations. The block diagram is shown in Figure 1.1.

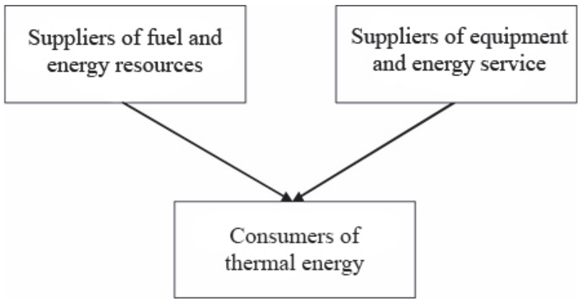

Figure 1.1. Structural scheme of subjects of relations in autonomous systems of heat supply

The decentralized heat supply system implies the presence of not very large thermal networks, but in the majority of cases, the activity of thermal network companies is excluded because the heat network is usually owned either by the consumer of thermal energy or by the heat supply organization. Compared to autonomous heat supply systems, decentralized is subject to state control and supervision. The structural scheme of the relationship in a decentralized heating system is shown in Figure 1.2.

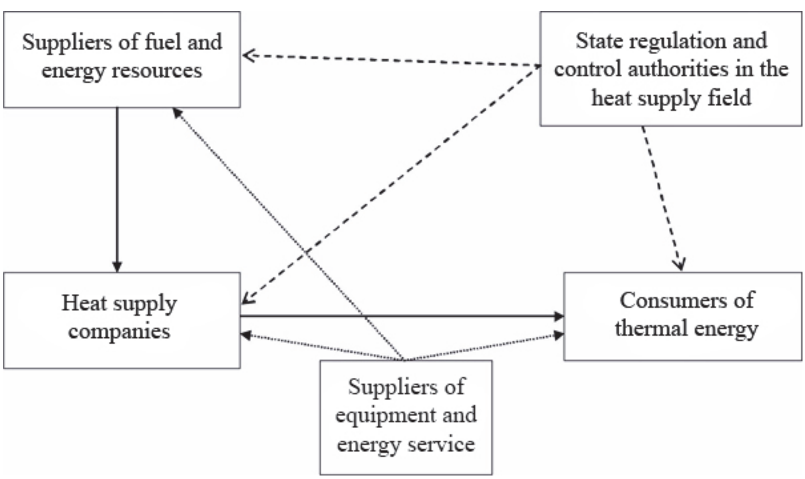

Figure 1.2. Structural scheme of subjects of relations in decentralized systems of heat supply

The system of moderately centralized heat supply is a transition from decentralized to centralized and includes the features of both systems. As the subject of the system appears the organization of the heating network, but in some cases, interconnections between heat supplying organizations and consumers of heat energy can be traced directly without the participation of the heat network organizations. Structural schemes of relationships between subjects of moderately centralized and centralized heat supply systems are presented in Figure 1.3.

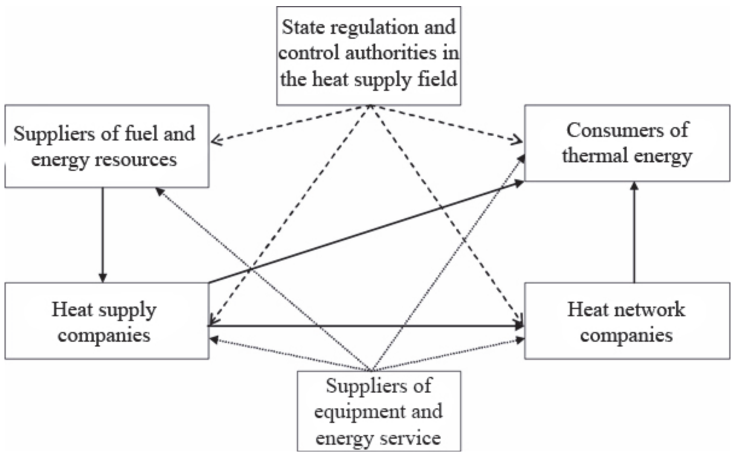

Figure 1.3. Structural scheme of subjects of relations in moderately centralized (centralized) heat supply systems

1.3. MODELS OF THE THERMAL ENERGY MARKET

There are several basic models of the Thermal Energy Market, which in one form or another already operate in developed countries of the world, and therefore one of these models can be imposed on the above differentiation of heat supply systems in Ukraine:

- **heat energy sales model through a single wholesale reseller or sole purchaser**; this model involves obtaining rights to the grid or heat supply companies to purchase heat energy at free market prices in any heat generating organization connected to this heating network and sell it to a customer connected to the heating network at prices that are formed on the basis of competitive bidding from the side of the heat generating organizations, and the norms of profit of the organizations of the thermal network regulated by the state authorities in the field of heat supply [6]. This model is the most promising in terms of the creation of the Thermal Energy Market, because it provides free conditions for entry into the market and participation in the process of its functioning;

- **model of direct provision of heat supply services using own/leased networks**; this model involves direct interaction between the heat-generating organization and the consumer on the basis of direct heat supply contracts. Unfortunately, this model, as such, does not anticipate competition, is a prerequisite for the creation of monopolies, and can not be considered effective;
- **the model of direct provision of heat and hot water supply services to consumers with transit through networks of a third party organization**; this model is somewhat similar to a single buyer model, where the owner of this heat network acts as a buyer. This model in the realities of Ukraine may be a transition to a single buyer model.

The listed models of the heat energy market can be based on the systems of heat supply according to their differentiation by the level of localization, in addition to the autonomous system of heat supply, since it does not provide for the possibility of functioning of the market as such.

The model of sales of heat energy through a single wholesale reseller most effectively fits into the framework of the relationship of subjects of the centralized system of heat supply. In turn, the model of direct provision of heat services to consumers with transit through the networks of a third-party organization can be the basis of the systems of moderately centralized heat supply and act as a transitional model for the organization of the market based on a centralized heat supply system. The direct heat supply model with the use of own or leased networks can function within the limits of decentralized heat supply.

1.4. ANALYSIS OF LITERARY DATA

The Law of Ukraine "On Heat Supply" provides for the possibility of creating and functioning of the heat energy market [3]. However, the general definition of the concept of the market of thermal energy and the absence of any mechanisms for its functioning do not allow to consider the market of thermal energy in Ukraine as a systemic phenomenon. An assessment of the possibility of introducing competition in heat supply systems in terms of all components from equipment and fuel to the final product in the form of thermal energy is analyzed in [4]. Organizational structures of the relationship between the entities of the Thermal Energy Market in Ukraine and other countries of the world are analyzed in works [8, 9]. Considering the conditions of operation of heat supply systems in different countries of the world, one can notice that there is no complete unambiguousness in the strategy of development of this sphere. Each of the states is guided by its rules in the field of heat supply, based on the technical and legal conditions that exist at the moment.

The paper [7] analyzes the state of the development of the district heating system in Ukraine in terms of the potential of alternative energy sources and their use in creating a competitive heat energy market. A large variety of energy sources leads Ukraine to their effective use, so the analysis of the amount of resources is an important characteristic when planning energy development of the country. An analysis of heat energy market models in different countries of the European Union is presented in [10]. The "single buyer" model in the first stage is the easiest to implement for countries that have a monopoly position in the field of heat and power. The structural distribution of energy sources used for thermal energy production in the states of the European Union is analyzed. Principles of pricing and setting tariffs for heat energy, as well as legal aspects of the operation of Thermal Energy Markets in the European Union states are analyzed in [11]. The main specific features of the Thermal Energy Market, in contrast to other markets, and thermal energy as a commodity are determined [12]. The paper [13] presents the experience of Poland in terms of the implementation and operation of the heat energy market. The main problems and conditions of the functioning of the heat energy market are presented in [14]. The technical aspects that need to be provided at the stages of production, transportation and supply of thermal energy are given. The peculiarities of the work of the most common model of the Thermal Energy Market of the "single buyer" are given. This model is the easiest in terms of implementation and operation, but there are problems that are related to the "length of money" [15]. The methods of calculating the effective radius of heat supply for thermal networks of centralized systems are presented [16, 17]. On the basis of this work it becomes possible to determine the level of localization of the heat energy market. In the works [18–20] the modern technical state and prospects of the reformation of the heat supply systems in Ukraine are analyzed.

1.5. PROBLEMS OF THE HEAT SUPPLY SECTOR IN UKRAINE

There are a number of problems and peculiarities that are taking place in the present day with the work of various types of heat supply systems in Ukraine and which are a barrier to creating an effective market system:

1. The heat supply system, as an energy sector, is a socially responsible process, in particular, for objects of the social sphere and the population. Therefore, an important indicator for heat supply systems is the level of reliability of such systems. In the absence of the market of thermal energy as such, the level of responsibility of monopoly structures may not provide an adequate level of reliability of heat supply systems.
2. Thermal networks have significant physical deterioration, which leads to significant losses of heat energy in the process of transportation (sometimes

more than 30%). Since the amount of heat energy losses is one of the determining indicators of the level of efficiency of the heat supply system in terms of functioning of the market, the solution of this problem is a priority. On the example of Poland, it becomes clear the priority of solving this problem, when in Poland in 1992, the state of the heating networks was disastrous and a decision was made to restore them. After the modernization in Warsaw, it was possible to reduce the level of heat losses of the fluid by 68%, the loss of thermal energy from 20% to 12% of the thermal load, increase the reliability of thermal supply and increase the resource of heat networks [13].

3. The low level of personnel qualification in the energy sector, which results from the monopolization of the market and the lack of motivation for the development of professional qualities of workers, causes considerable losses in the design, construction, operation and repair of equipment.
4. Absence of responsible bodies (operators) of control or dispatch control of the system of heat supply at the level of local markets of thermal energy. Any model of the energy market, where there is competition, involves the technical regulation of the system, depending on the loads that take place at the present time due to its features of thermal energy as a commodity.
5. One of the most priority issues when creating a market is the level of infrastructure development. This indicator depends directly on the density of thermal loads in the area, and the level of heat energy losses in the heating networks, which are the determining criteria for the estimation of the level of localization and loopiness of the system [16]. An analysis of the need to install new thermal networks, or the creation of the so-called “Rings” relies on technical and economic calculations, where one of the criteria should be the above-mentioned indicator. Actually, the optimization task should be defined as follows: the definition of the dependence of the scale of the local heat energy market on the density of thermal loads, while ensuring the level of regulatory losses in the heating network.
6. Lack of separation of functions of production and transportation of heat energy between different organizations. The need to solve this problem is that activities in the process of transportation of thermal energy fall into this type of market structure as a natural monopoly, and the process of generation of thermal energy can be technically, economically and legally organized in a competitive environment.
7. Significant barriers, in terms of legislative framework, when entering the market. An important issue is to ensure the free access of investors to the construction and operation of heat generation facilities. According to the current legislation on heat supply, the process of connecting to the heating networks

should be unhindered, but in practice these positions are not fulfilled because of the imperfection of the mechanisms for their implementation.

8. Lack of standards for the quality of heat energy as a commodity. Ambiguity in the process of accounting for thermal energy in terms of non-compliance with different temperature levels (as a measure of comfort level) in heating rooms with the same amounts of consumed thermal energy. Functions of observance of parameters can be assigned to power sales companies.
9. The low level of the provision of commercial accounting of heat energy by consumers makes them pay for the use of heat energy due to overestimated payment standards, which results in consumer overpayments. At the same time, in consequence, the level of disorientation in the processing of statistical data that is used to estimate macroeconomic indicators increases. The problem of availability of thermal energy counters for apartments is still not solved, and entails some difficulties in the work of energy-saving organizations with domestic consumers.
10. High level of non-payment by consumers and freezing of assets of heat-generating companies. This problem can reduce the intensity of market and technology development, while the market efficiency can not be maximized.
11. Cross-subsidization policy. The process of compensating by the state the difference in tariffs for the population in relation to tariffs for budgetary institutions and industry entails distortions in economic relations between organizations, and as a consequence of a decrease in the level of well-being of the heat energy market, which is the main indicator of the level of efficiency of the market itself.
12. Lack of marketing activity in the field of heat supply. The lack of awareness of domestic consumers about the possibilities to improve the process of using heat energy through energy efficiency measures.

Creation of the heat energy market in Ukraine involves solving the above-mentioned problems at a high level of quality, with the increased attention given to the issue of the theoretical determination of the level of localization of the Thermal Energy Market, depending on the density of thermal loads within the specified territories. Actually, when creating the market of thermal energy, the scale of the heat supply system should be maximal, ensuring normative losses of thermal energy. Then there will be more market entry opportunities where the level of competition will be significant, which is likely to result in low tariffs for services such as heating and hot water supply in this region.

1.6. SIMULATION MODEL OF THE THERMAL ENERGY MARKET

In order to understand the principle of the functioning of the heat supply system based on competition, it is necessary to present a simple model that would demonstrate the need for the implementation of such a system.

In this paper, the efficiency of the system in two alternative variants is analyzed: when working in the system of one producer (monopoly), and when the number of heat energy producers within the system of heat supply (competition) changes.

To simulate and optimize the processes of functioning of the Thermal Energy Market, there is the author software "Thermal Energy Market" that allows designing existing heat supply systems and imposing on them new objects in the form of heat energy producers, heat networks and consumers. With the help of a topographic editor, all the objects of the heat supply system are located on the city map, which allows you to create a geographical relation between all objects.

For each producer, heat network and consumer, technical and economic indicators are determined on the basis of which the calculation is made. It is also necessary to define the characteristics of the model, such as: market share for each producer, relative thermal energy consumption schedule, capital costs for market creation, and loss compensation coefficient for the main producer. On the basis of a definite project in the topographic editor, the model settings and tune-ups of the objects of the heating system under consideration are carried out market simulation, which involves determining the auction results. The auction organized determines the manufacturers who can sell the claimed amount of heat energy at the declared price.

The financial results of each producer are analyzed, while indicators of total benefits to the consumer and total profits of independent producers are formed [1]. The sum of these two indicators determines the absolute efficiency of the heat energy market, which is the target function of this model. Optimization of this target function is determined by the variation of the market share coefficient, which determines the degree of entry of producers into the market.

1.6.1. Purpose and tasks of the research

The purpose of the work is to determine the level of heat supply efficiency when creating a local heat energy market based on the simulation model at given volumes of thermal energy consumption, the number of producers in the system, and restrictions on the possibility of entering the market. Determine the optimal level of performance that will reflect the best conditions for entry into the market of independent producers.

To achieve the goal you need to solve the following tasks:

- formulation of conditions for market functioning when creating a model;
- execution of the simulation model on the basis of certain conditions in the variation of the market share factor, and the definition of the main financial indicators;
- analysis of the dependencies of the indicators of the benefits from the implementation of the heat energy market, taking into account the compensation of losses of the main producer, the amount of profits of independent producers, and the efficiency of the market of thermal energy from the factor of market share;
- to estimate the benefits of functioning of the market in optimal conditions in comparison with the state of monopoly, to represent the value of the reduction of the price of heat energy.

1.6.2. Technical means for creation of the market of thermal energy

The process of creating a Thermal Energy Market in Ukraine can not be considered only in terms of benefits that are generated when implementing the competitive environment in the heat supply system. TEM is a local market that is limited to the territory of the city and has no impact on the markets that are located in other Ukrainian cities. This aspect describes the need to transfer responsibility for market introduction from state authorities to local self-government bodies, which is part of the decentralization policy in Ukraine.

The effectiveness of an TEM is determined by the following indicators:

- availability and cost of local resources for use in the production of heat energy;
- ecological and economic incentives for the use of certain resources for the production of thermal energy;
- the level of success of conducting business in the field of heat supply, which is a benefit to the manufacturer;
- assistance of local self-government bodies to the development and operation of TEM;
- technical condition of heat networks;
- efficiency of the process of operator control of TEM;
- the level of technical and economic efficiency before the creation of TEM;
- correctness of technical decisions at the stage of implementation of TEM.

All the above indicators in the amount and give the benefit that is formed as a result of the functioning of the TEM. This benefit is mainly reflected in the reduction of the tariff for heat energy for the end user, which is one of the goals of the implementation of TEM.

But, it is very important to consider TEM in terms of a single whole, as a microeconomic unit. This means that the result of the creation of the market is the capital costs to bring it to the state of operation, and the result of the market is operating costs and profit. In this case, profit is considered exactly as the level of efficiency of TEM, which is the sum of the benefits of independent producers and consumers. Also, the key indicator should be the payback period of TEM, which is crucial in terms of making a decision on the creation of a market in the process of its design.

To determine the components of the creation of TEM in terms of technical means, it is necessary to divide into four main areas of responsibility in accordance with the structure of the heat supply system:

1. Zone of producers, which is characterized by the objects of heat generation and heating networks on the boundary of the physical separation of heat-carrier manufacturers and heat supply companies.
2. District of the district heating organization, which is characterized by trunk and distribution heat networks on the boundary of physical separation of heat carriers both from the side of producers and from the side of consumers. Also, here are the means of operator control and control of the process of heat supply.
3. The consumer zone, which is characterized by objects of thermal energy consumption and heating networks on the boundary of the physical separation of heat carriers of the consumer and heat supply organization.
4. The zone of state control over the processes of functioning of the TEM. This area is relevant to the organization of TEM in terms of conducting auctions for the purchase and sale of thermal energy. It is assumed that on the basis of the TEM, a government will be created as an integral part of local self-government bodies, which will have the functions of legal regulation of the functioning of TEM in general.

Based on this classification, an important issue is raised about the sources of financing of technical facilities, which are fixed in one of the four areas of responsibility stated above. There may be several options for the solution of this issue, therefore, since the result of the calculations does not depend on the sources of funding, this aspect is not considered here.

The technical means for the creation of TEM is a means, without which the functioning of the Thermal Energy Market is impossible.

Accordingly, to the above classification of areas of responsibility, a list of technical means for the creation and operation of TEM is given:

1. Zone of producers:
   – the heat network to the location of the producer's heat-carrier separation and the heat supply organization, if necessary, $C_{\mathrm{HN}}^{\mathrm{P}}$;
   – surface heat exchanger, $C_{\mathrm{HE}}^{\mathrm{P}}$;
   – a thermal energy counter, $C_{\mathrm{TEC}}^{\mathrm{P}}$;
   – automation means for controlling the power of heat generation, $C_{\mathrm{A}}^{\mathrm{P}}$.

   The amount of capital costs for the creation of TEM in the manufacturer's zone will be, UAH:

$$C_{\Sigma}^{\mathrm{P}} = C_{\mathrm{HM}}^{\mathrm{P}} + C_{\mathrm{HE}}^{\mathrm{P}} + C_{\mathrm{TEC}}^{\mathrm{P}} + C_{\mathrm{A}}^{\mathrm{P}} \tag{1.1}$$

2. Zone of district heat supply organization:
   – main and distribution heat networks for replacing or renovation those with unsatisfactory technical condition and for laying new ones for increasing the scale of TEM, $C_{\mathrm{HN}}^{\mathrm{HSO}}$;
   – Central Heat Points (CTP) for separating the circuit of main and distribution networks, $C_{\mathrm{CTP}}^{\mathrm{HSO}}$;
   – means of automation and dispatching for control and management of regulation of the power of thermal energy flows in the heat network, $C_{\mathrm{AD}}^{\mathrm{HSO}}$.

   The amount of capital expenditures for the creation of RTE in the heat supply organization's zone will be, UAH:

$$C_{\Sigma}^{\mathrm{HSO}} = C_{\mathrm{HN}}^{\mathrm{HSO}} + C_{\mathrm{CTP}}^{\mathrm{HSO}} + C_{\mathrm{AD}}^{\mathrm{HSO}} \tag{1.2}$$

3. Zone of consumers:
   – a heat network to the location of the separation of heat carriers of consumers and the heat supply organization, if necessary, $C_{\mathrm{HN}}^{\mathrm{C}}$;
   – an Individual Heat Point (ITP), which includes: a surface heat exchanger, a heat energy meter, automation means for controlling consumption power, $C_{\mathrm{ITP}}^{\mathrm{C}}$.

   The amount of capital costs for the creation of RTE in the consumer area will be, UAH:

$$C_{\Sigma}^{\mathrm{C}} = C_{\mathrm{HN}}^{\mathrm{C}} + C_{\mathrm{ITP}}^{\mathrm{C}} \tag{1.3}$$

4. The zone of state control over the processes of operation of the TEM involves the costs of establishing state authorities for the introduction and control of TEM within the city.

   Consequently, the total amount of capital expenditures will be TEM, UAH:

$$C_{\Sigma}^{\mathrm{TEM}} = C_{\Sigma}^{\mathrm{P}} + C_{\Sigma}^{\mathrm{HSO}} + C_{\Sigma}^{\mathrm{C}} + C_{\Sigma}^{\mathrm{SC}} \tag{1.4}$$

where $C_{\sum}^{SC}$ is amount of expenses for creation of the state control unit of the functioning of the TEM, UAH.

Determining capital costs in a specific city where it is planned to create an TEM can be carried out according to the above scheme, but it should be understood that due to different initial conditions, the size of capital costs may differ.

1.6.3. General principles of the formation of the heat energy market

In Figure 1.4 presents a schematic diagram of the components of the target function of the model of the Thermal Energy Market.

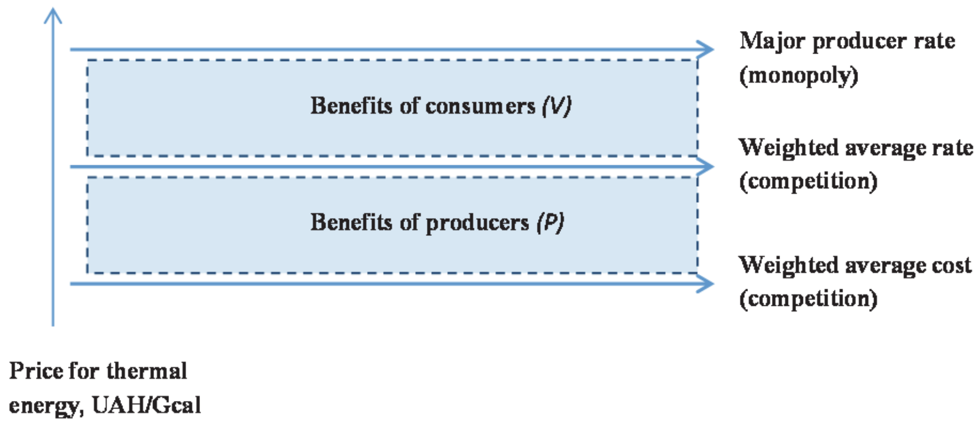

Figure 1.4. Principal scheme of the components of the target function of the model of the Thermal Energy Market

This model is static and does not describe the conjunctural changes in the market during its work. Articles of expenditure for each of the manufacturers are defined throughout the time and are unchanged. The static model shows the fundamental trends in the heat energy market, and does not take into account dynamic or unpredictable processes that may arise. Such processes can be:

1. The impossibility of supply of heat energy by the manufacturer who won the auction due to technical problems.
2. Changing the prices of resources in time, which are laid in the costs of producers.
3. Loss of thermal energy in the heating network depending on the location of the producers.
4. Change the rules of the auction or legislative restrictions on the market.
5. Instability of weather conditions.

For the functioning of the heat energy market there are conditions that must be fulfilled to ensure the fulfillment of the priority tasks that are facing it.

1. The density of heat capacity in the zone of one heat supply system must meet the requirements [16, 17]. For the density of heat capacities it is possible to accept the amount of thermal energy that was produced per year within the limits of this local heat supply system. These limits can be defined as the total length of the heating system, or as the total area of the heating networks and consumers, which is engaged in the zone of this system of heat supply.

   This indicator can be expressed in various variations, because, in fact, it defines the same essentially characteristic. Unfortunately, it is problematic to determine the exact level of this indicator, since it depends heavily on the economic situation in the region in which the heat energy market operates.

   Necessary task is to determine the lower boundary level of the density of thermal power in the zone of one heating system. Solving this problem will allow determining the fate of district heating systems in the whole of Ukraine, where the market for thermal energy can not function.

   The system of heat supply, as an energy sector, is a socially responsible structure, in particular, for objects of the social sphere and the population. Therefore, the necessary level of reliability is important.

2. After determining the heat supply systems that are suitable for creating the Thermal Energy Market, it is necessary to provide technical conditions for the proper operation of the heat supply system:
   – generation, transportation and consumption contours must be physically separated;
   – installation of the automation system, which performs operations on management and control of the main indicators of the system;
   – creation of the position of the technical operator of the system, which performs the switching according to the results of the auction conducted within the heat supply system. The organization of control over the flow of heat energy between manufacturers is an important issue, which is connected with the provision of automated systems on each of the objects, because it is necessary to ensure that the distribution of heat energy, which is determined by the results of auctions;
   – ensuring the minimum percentage of wear of heat networks within the system;
   – legislative provision of free access to the connection to the heat supply system, subject to fulfillment of all technical conditions, both from the generation side and from the side of the consumer.

In terms of consumers, the quality of thermal energy for the consumer plays an important role. The quality of the supply of heat energy is determined by the comfortable conditions of staying indoors. For this, consumers need to be provided with monitoring, regulating and recording of heat energy. Speaking of the population as a consumer of thermal energy, the process of interaction with them is simplified, if the population acts as an association of co-owners of an apartment building.

3. Determination of rules for the process of conducting tenders at the auction on the purchase and sale of heat energy.

   The heat transfer function relies on the main manufacturer in the system, since, as a rule, heat networks are in their ownership. Therefore, it is important to monitor the demolition of heat networks and timely repair of individual areas. To do this, it is necessary to provide certain incentives for the overall percentage of losses in the heat network to be feasible in the functioning of the market.

1.6.4. Calculation of the full cost of thermal energy producers

For each of the producers, the calculation of full-cost functions and the forecast tariff taking into account the profitability of each of the heat energy suppliers was performed.

The full cost function for each technology is presented in the following way [21]:

$$TC = (A_1 + A_2 + A_3)\ x\ Q + (B_1 + B_2 + B_3 + B_4) \tag{1.5}$$

where: TC – total cost of the production of thermal energy per year, UAH; A_1 – specific cost of the energy resource for the production of thermal energy, UAH/Gcal; A_2 – specific cost of delivery of energy resources for the production of thermal energy, UAH/Gcal; A_3 – specific cost of the electricity for the production of thermal energy, UAH/Gcal; B_1 – fixed cost for salaries of working personnel for heat energy production per year, UAH; B_2 – fixed cost for other costs on heat energy production per year, UAH; B_3 – fixed depreciation costs for heat energy production per year, UAH; B_4 – fixed cost for the administration salaries for the production of thermal energy per year, UAH; Q – amount of thermal energy produced per year, Gcal.

Characteristics of full costs, which are compiled on the basis of cost items, are given in Table 1.2.

Table 1.2. Articles of expenditure of heat energy producers

Cost	Type of cost
Fuel consumption	Variable (UAH/Gcal)
Logistics	Variable (UAH/Gcal)
Electricity consumption	Variable (UAH/Gcal)
Salary of workers	Fixed (UAH/year)
Administrative costs	Fixed (UAH/year)
Amortisation	Fixed (UAH/year)
Oher costs	Fixed (UAH/year)

In this model of the local heat energy market, as a constraint, the notion of market share is introduced, that is, the maximum limit of the amount of thermal energy that can be released by each producer for each month. Market share for *i*-th manufacturer (except for the main) is determined by the coefficient of market share:

$$Q^{s}_{m_{i,j}} = Q_{d_j} \cdot q \tag{1.6}$$

where: $Q^{s}_{m_{i,j}}$ – market share for *i*-th producer by *j*-th month, Gcal; Q_{d_j} – demand for thermal energy in *j*-th month, Gcal; q – coefficient of market share.

For the formation of the matrix of the potential for the production of thermal energy in the market, the following conditions are used:

- if $Q^{p}_{m_i} < Q^{s}_{m_{i,j}}$ then $Q^{b}_{m_{i,j}} = Q^{p}_{m_i}$,
- if $Q^{p}_{m_i} \geq Q^{s}_{m_{i,j}}$ then $Q^{b}_{m_{i,j}} = Q^{s}_{m_{i,j}}$

where: $Q^{p}_{m_i}$ – energy production potential for *i*-th producer by *j*-th month, Gcal; $Q^{b}_{m_{i,j}}$ – bid amount of thermal energy for the *i*-th producer of the *j*-th month, Gcal.

1.6.5. Estimated thermal energy tariff

Consequently, each producer, having the full cost function and the level of planned profit, based on market conditions and the possible amount of heat sold, calculates the forecasted heat energy tariff, and submits as a bid for the auction. The estimated heat energy tariff for each producer will be:

$$T_i = \frac{A_i \cdot \sum_n^{j=1} Q^b_{m_{i,j}} + B_i + P_i}{\sum_n^{j=1} Q^b_{m_{i,j}}} \tag{1.7}$$

where: T_i – estimated heat energy tariff for each producer, UAH/Gcal; A_i – total variable cost of i-th producer, UAH/Gcal; B_i – total fixed cost of i-th producer, UAH; P_i – total profit of i-th producer, UAH.

1.6.6. Organization of an auction on the sale and purchase of thermal energy

On the basis of submitted bids of producers, which specify such parameters as T_i and $Q^b_{m_{i,j}}$ an auction is conducted, which determines the winners who will be submitted to sold thermal energy in the i-th month.

Bids are sorted by price suggestions in the direction of increase. The sum of the winners' applications for the j-th month is determined by the condition:

$$\sum_n^{i=1} Q^b_{m_{i,j}} = Q_{d_j} \tag{1.8}$$

where n is the number of the last winning producer.

If the bid of the last winning producer does not completely cover the demand for the j-th month, then only the part of the bid volume of thermal energy is taken into account:

$$Q^b_{m_{n,j}} = Q_{d_j} - \sum_{n\text{-}1}^{i=1} Q^b_{m_{i,j}} \tag{1.9}$$

where $Q^b_{m_{n,j}}$ is part of the bid volume of thermal energy of the last winning producer covering the demand for the j-th month.

As a result of the auction conducted, a matrix of producers-winners of the auction is formed.

Based on the matrix of producers-winners of the auction, the total cost of the consumed heat energy in the j-th month is:

$$C_{d_j} = \sum_n^{i=1} \left(Q^b_{m_{i,j}} \cdot T_i \right) \tag{1.10}$$

where C_{d_j} is total cost of consumed thermal energy in the j-th month, UAH.

Weighted average tariff for thermal energy release in the j-th month:

$$T_j^{wa} = \frac{C_{d\,j}}{Q_{d\,j}} \tag{1.11}$$

1.6.7. Optimizing producer costs

Within the city, where the TEM model is considered, one producer can own several objects of heat generation. Each of the objects of heat generation is characterized by its function of expenses and the level of planned profit in accordance with capital costs for the construction of the facility, the technology of thermal energy production, and features of the operation process. In the case of the last manufacturer-winner there is a situation where the planned amount of thermal energy output is higher than the actual according to the results of the auction, therefore there is the problem of optimal distribution of the amount of heat energy produced between the heat-generating units within the limits of one producer for the reduction of specific production costs 1 Gcal of thermal energy [22].

Consequently, there is the task of optimizing the costs of the enterprise, where the target function is the amount of total costs for the production of thermal energy. For this task, the target function has the form [23]:

$$TC(x_1, x_2, .., x_n) = \sum_{i=1}^{n} \left(AVC_i \cdot x_i + TFC_i \right) \rightarrow \min \tag{1.12}$$

where: $TC(x_1, x_2, ..., x_n)$ – function of total expenses for heat energy production per year, UAH; AVC_i – average variable costs per unit of output of the i-th object of the company's heat production, UAH/Gcal; TFC_i – total fixed costs for the year i-th object of the company's heat production, UAH; n – number of objects of heat generation of the given enterprise; x – quantity of heat energy i-th object of heat generation.

For this optimization problem, there are the following limitations:

$$\begin{cases} \sum_{i=1}^{n} x_i = Q_{prod}^{f.gen.} \\ x_1 \le Q_1^{b.gen.} \\ x_2 \le Q_2^{b.gen.} \\ \quad \dots \\ x_n \le Q_n^{b.gen.} \end{cases} \qquad x_i \ge 0 \text{ , } i = 1, 2, \dots, n$$

where: $Q_{prod}^{f.\,gen}$ – the actual amount of thermal energy that a producer can sell in accordance with the results of the auction, Gcal; $Q_i^{b.\,gen.}$ – bid amount of thermal energy that the object of heat generation can produce in accordance with the share of the producer's market and the internal distribution of heat energy within the enterprise, Gcal.

Since the problem considered is the form of the general problem of linear programming, for it the use of the simplex method [23].

Let's write the problem which is considered in the form of the main problem, for finding the maximum of the function:

$$TC_1 = \sum_{i=1}^{n} \left(-AVC_i \cdot x_i - TFC_i \right) \tag{1.13}$$

Under conditions:

$$\begin{cases} \sum_{i=1}^{n} x_i = Q_{prod}^{f.\,gen.} \\ x_1 + x_{n+1} = Q_1^{b.\,gen.} \\ x_2 + x_{n+2} = Q_2^{b.\,gen.} \\ \dots \\ x_n + x_{2 \cdot n} = Q_n^{b.\,gen.} \end{cases}$$

$$x_i \geq 0,\ i = 1, 2, \dots, n$$

The transformed system of equations is written in the vector form:

$$x_1 P_1 + x_2 P_2 + \ldots + x_{2n} P_{2n} = P_0 \tag{1.14}$$

where

$$P_1 = \begin{bmatrix} 1 \\ 1 \\ 0 \\ \dots \\ 0 \\ 0 \end{bmatrix};\ P_2 = \begin{bmatrix} 1 \\ 0 \\ 1 \\ \dots \\ 0 \\ 0 \end{bmatrix} \dots P_{n+1} = \begin{bmatrix} 1 \\ 0 \\ 0 \\ \dots \\ 0 \\ 0 \end{bmatrix};$$

$$P_{n+2} = \begin{bmatrix} 0 \\ 0 \\ 0 \\ \dots \\ 0 \\ 0 \end{bmatrix}; \dots P_{2n+1} = \begin{bmatrix} 0 \\ 0 \\ 0 \\ \dots \\ 1 \\ 0 \end{bmatrix}; \; P_{2n+2} = \begin{bmatrix} 0 \\ 0 \\ 0 \\ \dots \\ 0 \\ 1 \end{bmatrix};$$

$$P_0 = \begin{bmatrix} Q_0^{f.gen.} \\ Q_1^{b.gen.} \\ Q_2^{b.gen.} \\ \dots \\ Q_{n\text{-}1}^{b.gen.} \\ Q_n^{b.gen.} \end{bmatrix}$$

Among the defined vectors $P_1, P_2, \dots, P_{2n}$ are n unit vectors $P_{n+1}, P_{n+2}, \dots, P_{2n}$, so for this task you can directly write down the reference plan and, accordingly, find its solution by a simplex method. In this way, we can compile the first table of the first iteration (Table 1.3).

Table 1.3. Simplex table of the first iteration

i	**Basis**	$\boldsymbol{C_b}$	$\boldsymbol{P_0}$	$\boldsymbol{-AVC_1}$	$\boldsymbol{-AVC_2}$	**…**	$\boldsymbol{-AVC_n}$	**0**	**…**	**0**	**0**
				$\boldsymbol{P_1}$	$\boldsymbol{P_2}$	**…**	$\boldsymbol{P_{n+1}}$	$\boldsymbol{P_{n+2}}$	**…**	$\boldsymbol{P_{2n+1}}$	$\boldsymbol{P_{2n+2}}$
1	P_{n+2}	0	$Q_{prod}^{f.\,gen}$	1	1	…	1	0	…	0	0
2	P_{n+3}	0	$Q_1^{b.\,gen.}$	1	0	…	0	0	…	0	0
…	…	…	…	…	…	…	…	…	…	…	…
n	P_{2n+2}	0	$Q_n^{f.\,gen.}$	0	0	…	0	0	…	1	0
$n+1$	P_{2n+2}	0	$Q_n^{f.\,gen.}$	0	0	…	0	0	…	0	1
$n+2$											

On the basis of the formulated simplex table is calculated according to the rules of calculation in the simplex method of the problem of linear programming [23], defining the values of the target function and the unknown variables.

Thus, the determined optimal values of the amount of thermal energy for each of the objects of heat generation allow to objectively predict the financial results of the manufacturer, which is considered in the model within the TEM.

The identified methodology is part of the copyright software "Thermal Energy Market" [24], which is designed to simulate the technical and economic processes in the heat energy market based on real objects or objects that are being designed.

1.6.8. Financial results of producers in the Thermal Energy Market

After conducting auctions for each month of the heating season, each of the producers will have a financial result that will reflect the success of the work of this manufacturer in the heat energy market. The main indicators that characterize the success of the company in the market of thermal energy are:

- total revenue of the *i*-th producer,
- total cost of *i*-th producer,
- total profit of the *i*-th producer,
- the difference between the planned profit and the actual profit of the *i*-th producer,
- the profitability of the *i*-th producer.

Considering the situation in Ukraine with regard to the systems of heat supply, it is necessary to take into account that in almost all large cities of Ukraine there are municipal companies that perform the function of the heat supplier and are in fact monopolists. By creating market relations in the heat supply systems of such cities, it is natural that the demand that covered the utility will decrease, and therefore the financial success of these enterprises will also be reduced. It is also possible that the utility will suffer losses.

Since municipal companies are the main suppliers of heat energy in cities, it is necessary to introduce a mechanism to stimulate these enterprises in the event of losses due to constant costs.

There are several ways to ensure this condition:

1. Full compensation of damages.
2. Partial compensation of damages with a constant percentage of compensation.
3. Partial compensation of damages with a stimulating percentage of compensation.

For simplicity, the first version of damages is selected in this model, distributing this value relative to the annual volume of released thermal energy in the market.

The annual average weighted tariff for heat energy, taking into account the compensation of losses to the main producer, is:

$$T^{wac} = \frac{\sum_{n}^{j=1} C_{d\,j} + U_1}{\sum_{n}^{j=1} Q_{d\,j}} \qquad (1.15)$$

where U_1 is the value of losses of the main producer per year, UAH.

The benefits from the implementation of the heat energy market need to be considered in terms of the difference in the value of the consumed thermal energy and the average weighted tariffs for thermal energy in its operation and absence. On the other hand, the total amount of profits of producers is considered. The sum of these two indicators is a target function of the model of the Thermal Energy Market.

1.6.9. Losses in heat networks

When creating the Thermal Energy Market, there are questions related to the use of existing heat networks in the city's heat supply system and the construction of new ones that would form a unified system for increasing the market size and, consequently, its absolute efficiency. Determination of heat losses in networks is necessary for the analysis of the technical and economic feasibility of the implementation of the heat energy market within the city. The following parameters have an impact on this indicator:

– the density of thermal capacity, which is characterized by the total amount of heat energy consumption in the heat supply system referenced to the total length of the heating networks;
– type of laying of parts of heating networks;
– the state of wear of thermal networks;
– the diameter of the pipelines;
– material and insulation thickness;
– temperature schedule in the heat supply system;
– weather conditions.

When transporting thermal energy from producers to consumers, heat energy losses are determined by the difference between the total amount of produced and consumed heat energy. This difference is one of the items of the cost price of heat energy as a commodity for the consumer, hence the costs of surplus energy production by producers are included in the fare according to the model.

Heat losses during the season can be determined by two methods: empirical and theoretical. The empirical method involves calculating the energy balance of the heat supply system on the basis of heat meters. The sum of the displays of heat meters of all producers for the selected period shows the total amount of energy produced, and the sum of meter readings in all consumers determines the total amount of heat energy consumed. When designing the market for thermal energy, the use of the empirical method is impossible, so only the theoretical calculation of losses is able to give an adequate assessment in accordance with the characteristics of the sections of heat networks.

In the model for calculation of heat energy losses in the city's heat supply system, within the framework of the heat energy market, three main types of laying of heat network areas are used in Ukraine:

- above ground,
- underground channel,
- underground non-channel.

For each of the above types of gasket sections of heat networks, an extensive method of calculating specific energy losses is determined.

Above ground. Specific heat losses from 1 m of the length of the feeder and return pipelines are:

$$q_{l1} = \frac{t_1 - t_e}{R_1} \tag{1.16}$$

$$q_{l2} = \frac{t_2 - t_e}{R_2} \tag{1.17}$$

where: t_e – average environmental temperature during the heating season, °C; q_{l1} – specific losses of thermal energy in the supply pipeline, W/m; q_{l2} – specific losses of heat energy in the return pipeline, W/m; t_1 – average coolant temperature in the feeding pipe during the heating season, °C; t_2 – average coolant temperature in the return line during the heating season, °C; R_1 – linear coefficient of thermal resistance of the supply pipeline, m · K/W; R_2 – linear coefficient of thermal resistance of the return pipeline, m · K/W.

The linear coefficient of thermal resistance is determined by the coefficient of thermal conductivity of the insulation material, the thickness of the insulation and the coefficient of heat transfer of the outer surface:

$$R = R_{ins} + R_{\alpha} = \frac{1}{2\pi\lambda_{ins}} \ln\frac{d_{ins}}{d_p} + \frac{1}{\pi d_{ins}\alpha} \tag{1.18}$$

where: R_{ins} – linear coefficient of thermal resistance of insulation, m · K/W; R_α – linear coefficient of thermal resistance of the outer surface, m · K/W; λ_{ins} – coefficient of thermal conductivity of insulation material, W/m · K; d_{ins} – external diameter of the pipe with insulation, m; d_p – external diameter of the pipe without insulation, m; α – heat transfer coefficient of the outer surface of the wall of the pipeline, W/m^2 · K.

The coefficient of heat transfer of the outer surface of the wall of the pipeline is determined by the following formula:

$$\alpha = 11.6 + 7\sqrt{w} \tag{1.19}$$

where w is average air speed during the heating season, m/s.

Underground non-channel. The linear coefficient of thermal resistance is determined by the sum of coefficients of thermal resistance of insulation and soil:

$$R = R_{ins} + R_s = \frac{1}{2\pi\lambda_{ins}} \ln\frac{d_{ins}}{d_p} + \frac{1}{2\pi\lambda_s} \ln\frac{4h}{d_p} \tag{1.20}$$

where: R_s – linear coefficient of thermal resistance of soil, m · K/W; λ_s – coefficient of thermal conductivity of the soil, W/m · K; h – depth of laying pipes in the ground, m.

In the case of an underground non-channel gasket there is a mutual influence of feed and return pipelines. Such influence is taken into account by an additional conditional coefficient of thermal resistance:

$$R_0 = \frac{1}{2\pi\lambda_s} \ln\sqrt{1+\left(\frac{2h}{b}\right)^2} \tag{1.21}$$

where b is distance between the axes of the feeder and the return pipelines, m.

Thus, the specific thermal losses of 1 m of the length of the feeder and return pipelines are by Shubin's methodology [25]:

$$q_{l1} = \frac{(t_1 - t_s)R_2 - (t_2 - t_s)R_0}{R_1 R_2 - R_0^2} \tag{1.22}$$

$$q_{l2} = \frac{(t_2 - t_s)R_1 - (t_1 - t_s)R_0}{R_1 R_2 - R_0^2} \tag{1.23}$$

where t_s is average temperature of the soil during the heating season, °C.

Underground channel. To calculate the heat loss in the channel it is necessary to determine the temperature value in the channel. The air temperature in the channel is determined from the equation of thermal balance:

$$\frac{t_1 - t_{ch}}{R_1} + \frac{t_2 - t_{ch}}{R_2} = \frac{t_{ch} - t_s}{R_{ch}} \tag{1.24}$$

where: R_{ch} – linear coefficient of thermal resistance of the walls of the channel, m · K/W; t_{ch} – average air temperature in the channel during the heating season, °C.

When channel laying of two-pipe thermal networks, the thermal resistance between the air of the channel and the ground is determined through the equivalent diameter of the channel.

Thus, the linear coefficient of thermal resistance of the walls of the channel is:

$$R_{ch} = R_{ch.w} + R_s = \frac{1}{2\pi\lambda_{ch}} \ln\frac{d_e + \delta_{ch}}{d_e} + \frac{1}{2\pi\lambda_s} \ln\frac{4h}{d_e + \delta_{ch}} \tag{1.25}$$

where: $R_{ch.w.}$ – linear coefficient of thermal resistance of the channel walls, m · K/W; d_e – equivalent channel diameter, m; δ_{ch} – thickness of the wall of the overlap of the channel, m; λ_{ch} – coefficient of thermal conductivity of the overlap of the channel, W/m · K; h – depth of laying of the channel in the ground, m.

Average air temperature in the channel:

$$t_{ch} = \frac{\dfrac{t_1}{R_1} + \dfrac{t_2}{R_K} + \dfrac{t_s}{R_{ch}}}{\dfrac{1}{R_1} + \dfrac{1}{R_2} + \dfrac{1}{R_{ch}}} \tag{1.26}$$

Having determined the linear coefficients of the thermal resistance of the feeder and return pipelines, the specific thermal losses from 1 m of the length of the thermal network make up, W/m:

$$q_{l1} = \frac{t_1 - t_{ch}}{R_1} \tag{1.27}$$

$$q_{l2} = \frac{t_2 - t_{ch}}{R_2} \tag{1.28}$$

Total losses of heat energy in the supply and return pipelines are:

$$Q^s = Q_1 + Q_2 = (q_{l1} \cdot l \cdot (1+\beta) + q_{l2} \cdot l \cdot (1+\beta)) \cdot 24 \cdot n \cdot 0.86 \cdot 10^{-6} \quad (1.29)$$

where: Q^s – heat loss on the supply and return pipelines during the heating season, Gcal; Q_1 – losses of heat energy in the heat supply network of the supply pipeline during the heating season, Gcal; Q_2 – loss of heat energy in the section of the heating network of the return pipeline during the heating season, Gcal; l – length of the heat network section in a two-pipe dimension, m; β – a coefficient that takes into account local energy losses ($\beta \approx 0.2 \ldots 0.3$); n – number of days in the heating season.

After determining the heat energy losses on all sections of the heat supply system of the city's heat supply system, the full losses for the heating season are:

$$Q^{c.n.} = \sum_{i=1}^{k} Q_i^s \quad (1.30)$$

where k is number of sections of heat networks in the system of heat supply.

1.6.10. Model results

The main purpose of the simulation is to determine the optimal coefficient of market share for a certain number of heat energy producers and the consumed amount of heat energy per year by customers on the market.

The benefits from the implementation of the heat energy market need to be considered in terms of the difference in the value of the consumed heat energy and the average weighted tariffs for thermal energy in its operation and absence. It is this difference that serves as the target function for optimizing the operation of the heat energy market, where the market share factor is limited.

In the absence of the Thermal Energy Market, the forecast tariff for the main producer is:

$$T_1 = \frac{A_i \cdot \sum_n^{j=1} Q_{d\,j} + B_i + P_i}{\sum_n^{j=1} Q_{d\,j}} \quad (1.31)$$

Difference in tariffs for thermal energy in the functioning and absence of the market of thermal energy, UAH/Gcal:

$$\Delta T = T_1 - T^{wac} \quad (1.32)$$

Benefit from introduction of the Thermal Energy Market for consumers, taking into account the compensation of losses of the main producer, UAH:

$$V = \Delta T \cdot \sum_{n}^{j=1} Q_{d\,j} \tag{1.33}$$

Benefit from introduction of the Thermal Energy Market for producers, taking into account the compensation of losses of the main producer U_1, UAH:

$$P = \sum_{n}^{i=1} TP_i - U_1 \tag{1.34}$$

The efficiency of the Thermal Energy Market is the benefits of the introduction of the heat energy market, taking into account the compensation of losses of the main producer and the amount of profits of independent producers, UAH:

$$E = V + P \tag{1.35}$$

Based on this, the discounted value of cash flows for TEM will be, UAH:

$$\mathrm{NPV}_r = -C_{\Sigma}^{\mathrm{TEM}} + \sum_{t=1}^{n} \frac{(E)}{\left(1 + \frac{i}{100}\right)^t} \tag{1.36}$$

where: i – the discount rate, which is a function of the cost of alternative investment, the level of inflation for the selected period, etc., %; t – current period (year); n – estimated billing period (years).

Discounted payback period T is determined by the formula:

$$T = (r-1) + \frac{/\mathrm{NPV}_{r-1}/}{\mathrm{NPV}_r - \mathrm{NPV}_{r-1}}, \text{ years} \tag{1.37}$$

where r is the year, when NPV > 0.

Simple payback period will be:

$$T^s = \frac{C_{\Sigma}^{\mathrm{TEM}}}{E}, \text{ years} \tag{1.38}$$

1.7. ESTIMATION OF THE PAYBACK PERIOD OF TEM AT ITS CREATION IN THE CITY OF IRPIN

To calculate the payback period of the TEM of the city of Irpin, the copyright software “Thermal Energy Market” [24] was used. In the first place, it is necessary to determine the overall benefit from the creation of TEM in its operation in one calendar year. Since the essence of the model is to determine the difference in the economic performance of the city’s district heating system in case of monopoly and competition, it is necessary to build an existing city heat supply system.

The existing Irpin heating system is presented in Figure 1.5.

Figure 1.5. Existing heat supply system of the city of Irpin in the software “Thermal Energy Market”

Analyzing the constructed scheme it can be determined that at present there are 4 large non-interconnected systems of heating networks. The total length of the thermal networks of the existing system, according to the calculation results, is approximately 19 km. The main technical characteristics of the existing system are presented in Table 1.4.

Table 1.4. Main technical characteristics of the existing heat supply system in the city of Irpin

Characteristics of the heat supply system	Value
Total length of heating networks	18.896 km
Annual thermal energy consumption in the heat supply system	42137 Gcal
Annual thermal energy production by sources of heat generation	48065 Gcal
Losses of thermal energy in networks for a year	5928 Gcal
Relative losses in heat networks	12.33%

There is no centralized hot water supply in the Irpin heating system. The graph of consumption and heat energy production for heating by months in the city of Irpin is presented in Figure 1.6.

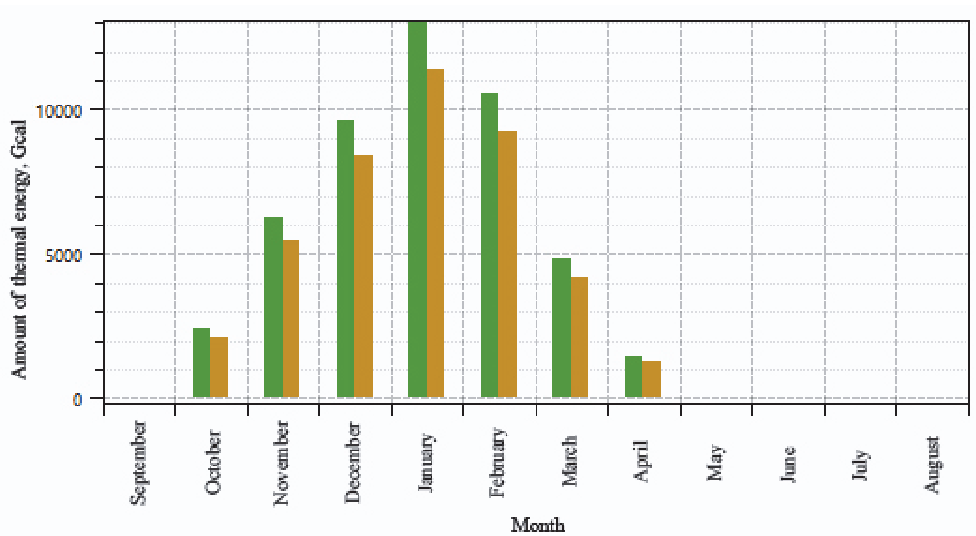

Figure 1.6. The schedule of consumption and heat energy production for heating by months in the city of Irpin (green – production value, orange – the value of consumption)

Based on the determined state of the Irpin heating system, a connected system of heat networks and producers (independent and main) was designed. The newly designed system forms the basis for functioning of the heat energy market in the city. The design of the new system is presented in Figure 1.7.

Figure 1.7. Designed heat supply system of the city of Irpin on the basis of the existing "Thermal Energy Market" software to ensure the functioning of the TEM

The main technical characteristics of the system for the Thermal Energy Market are presented in Table 1.5.

Table 1.5. Basic technical characteristics of the heating system in the city of Irpin during the operation of the TEM

Characteristics of the heat supply system	Value
Total length of thermal networks	33.661 km
Length of newly built thermal networks	14.765 km
Annual thermal energy consumption in the heat supply system	42137 Gcal
Annual thermal energy production by sources of heat generation	53107 Gcal
Losses of thermal energy in networks for a year	10970 Gcal
Relative losses in heat networks	20.66%

When creating a system for the Thermal Energy Market, due to the construction of new thermal networks, we see an increase in absolute and relative losses almost doubled in relation to the monopoly situation in the city. The graph of consumption and heat energy production for heating by months in the city of Irpin during the operation of the TEM is presented in Figure 1.8.

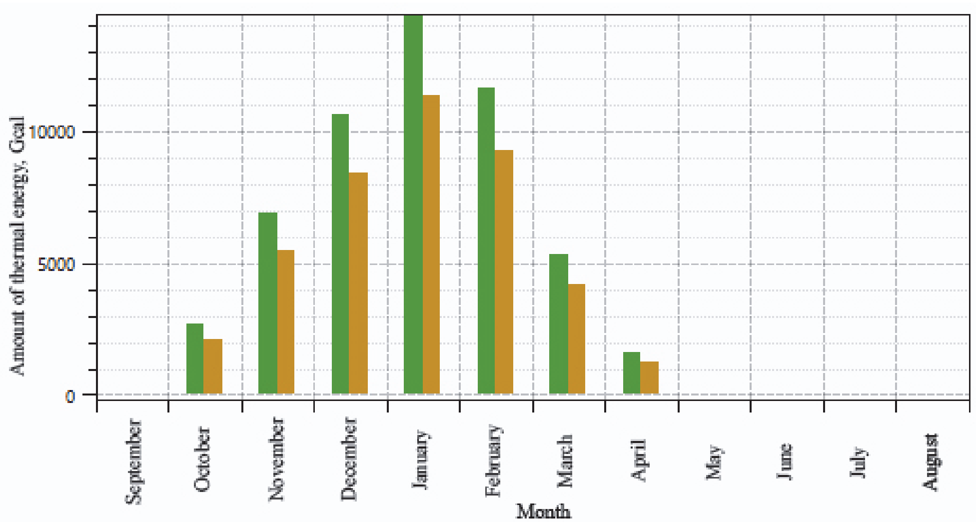

Figure 1.8. The schedule of consumption and heat energy production for heating by months in the city of Irpin in the functioning of the TEM (green – the value of production, orange – the value of consumption)

The model defines 1.7 independent manufacturers, which connect their heat generating facilities to the integrated heat network of the city. Each of the producers has its own resources, on the basis of which it introduces its entrepreneurial activity in the production of thermal energy. Each of the manufacturers determines their capital costs for the construction of facilities and operating costs for the production of heat energy. Based on these indicators, the manufacturer forecasts his profit for the season, taking into account his allowable rate of return. Thus, the estimated tariff is calculated based on the amount of heat energy that a producer can sell for a year, which in turn is determined depending on the market share coefficient existing on the heat energy market at present. The optimal market share is determined by the model. Dependence of the absolute efficiency of the market of thermal energy on the coefficient of market share is presented in Figure 1.9.

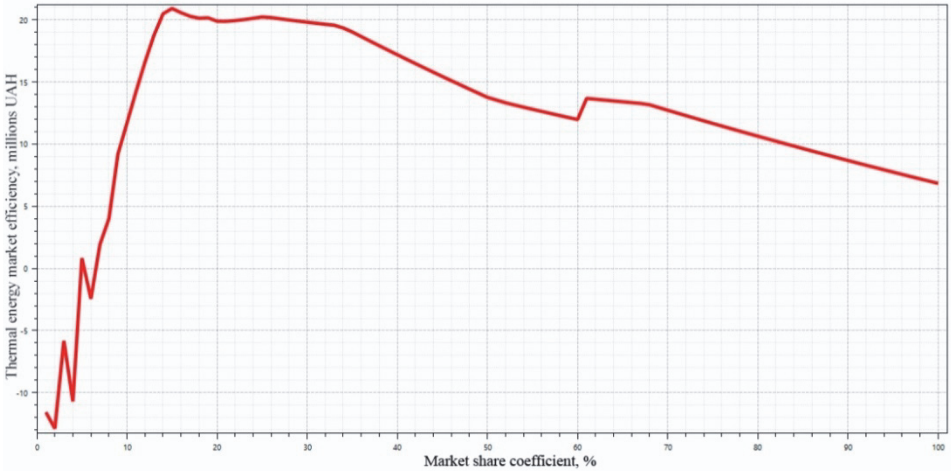

Figure 1.9. Graph of the dependence of the absolute efficiency of the Thermal Energy Market on the market share factor

Consequently, the optimal factor of market share on the basis of performed calculations is 0.15. Characteristics of heat energy producers in the functioning of TEM with a coefficient of market share of 0.15 is presented in Table 1.6.

Table 1.6. Characteristics of heat energy producers at TEM in the city of Irpin

Producer's name	**Number of objects of heat generation**	**Type of energy source**	**Forecasted tariff, UAH/Gcal**	**Forecaste *d* rate of return, %**	**Annual limit of thermal energy production, Gcal**
Main producer	23	Natural gas	1608.77	3	53107
Independent producer No. 1	3	Biomass (wood chips)	1124.94	35	7927
Independent producer No. 2	2	Biomass (seed pellets)	1356.54	32	7927
Independent producer No. 3	2	Biomass (wood)	1281.12	40	7927
Independent producer No. 4	3	Biomass (straw pellets)	1366.58	36	7927
Independent producer No. 5	1	Biomass (wood pellets)	1006.5	33	7927
Independent producer No. 6	2	Peat (pellets)	1257.41	34	7927
Independent producer No. 7	2	Energy of environment	886.73	30	7927

On the basis of the submitted applications of producers, which contain the amount of heat energy and the price for it, for which producers are ready to sell it, an auction is conducted, where manufacturers are identified who will produce and sell heat energy at the price indicated in the application. The results of the auction are presented in Tables 1.7 and 1.8.

Table 1.7. Results of the auction on the market of thermal energy, Gcal (for the heating season)

No.	Producer's name	October	November	December	January	February	March	April	Total
1.	Producer No. 7	398.3	1035.6	1593.2	2111.5	1752.5	796.6	239.0	7927
2.	Producer No. 5	398.3	1035.6	1593.2	2015.5	1752.5	796.6	239.0	7927
3.	Producer No. 1	398.3	1035.6	1593.2	2063.5	1752.5	796.6	239.0	7927
4.	Producer No. 6	398.3	1035.6	1593.2	2111.5	1752.5	796.6	239.0	7927
5.	Producer No. 3	398.3	1035.6	1593.2	2111.5	1752.5	796.6	239.0	7927
6.	Producer No. 2	398.3	1035.6	1593.2	2111.5	1752.5	796.6	239.0	7927
7.	Producer No. 4	265.5	690.4	1062.1	1814.1	1168.4	531.1	159.3	5691
8.	Main producer	0	0	0	0	0	0	0	0

Table 1.8. Financial results of auctioning in the heat energy market (during the heating season)

No.	Producer's name	Revenue, UAH	Costs, UAH	Profit, UAH	Deviation, UAH	Profitability, %
1.	Producer No. 7	7 028 836	3 141 885	3 886 950	0	55.3
2.	Producer No. 5	7 881 634	6 828 732	1 052 902	0	13.36
3.	Producer No. 1	8 863 099	6 708 699	2 154 400	0	24.31
4.	Producer No. 6	9 967 122	8 718 730	1 248 392	0	12.53
5.	Producer No. 3	10 155 112	9 201 221	954 891	0	9.39
6.	Producer No. 2	10 752 899	8 655 560	2 097 339	0	19.5
7.	Producer No. 4	7 777 272	6 936 985	840 287	–1 370 651	10.8
8.	Main producer	0	6 222 469	–6 222 469	–6 344 735	0

As a result of the auction conducted, we have results in terms of the financial performance of each of the producers, as well as the aggregate values that characterize the efficiency of the heat energy market. In Table 1.9 shows the results of the imitation modeling of the heat energy market in the city of Irpin.

Table 1.9. Expected results of the work of RTU in the city of Irpin (during the heating season)

	When functioning TEM without compensation	**When functioning TEM with compensation**	**In the absence of TEM**
Cost of consumed heat energy, UAH	62 425 801	68 648 270	77 325 682
Average tariff for the consumer, UAH/Gcal	1175.47	1292.63	1608.77
Absolute benefit for consumers, UAH	14 899 880	8 677 411	–
Absolute benefit for producers, UAH	6 011 645	12 234 161	–
Absolute efficiency of TEM	20 911 573	20 911 573	–
Relative benefit for consumers, %	19.27	11.22	–
Relative benefit for producers, %	7.77	15.82	–
Relative efficiency of TEM, %	27.04	27.04	–

According to formula (1.4), the sum of capital costs for the creation of the heat energy market in Irpin city according to the existing technical means is calculated:

$$C_{\Sigma}^{\mathrm{TEM}} = C_{\Sigma}^{\mathrm{P}} + C_{\Sigma}^{\mathrm{HSO}} + C_{\Sigma}^{\mathrm{C}} + C_{\Sigma}^{\mathrm{SC}} = 20 + 90 + 20 + 10 = 140 \text{ UAH million} \quad (1.39)$$

According to the determined results of the functioning of TEM in Irpin, a simple pay-back period is determined by the formula (1.38):

$$T^{s} = \frac{C_{\Sigma}^{\mathrm{TEM}}}{E} = \frac{140\,000\,000}{20\,911\,573} \approx 6.7 \text{ years} \quad (1.40)$$

The discounted payback period of TEM in the city of Irpin is calculated according to the formulas (1.36) and (1.37) under the condition i = 14%. The calculation results for each year are presented in Table 1.10. The graph of dependence NPV from the year presented in Figure 1.10.

Table 1.10. Calculation of the discounted payback period of RTE in the city of Irpin

Year	NPV (i), UAH million
0	–140.00
1	–119.09
2	–100.74
3	–84.65
4	–70.54
5	–58.16
6	–47.30
7	–37.77
8	–29.41
9	–22.08
10	–15.65
11	–10.01
12	–5.06
13	–0.72
14	3.08

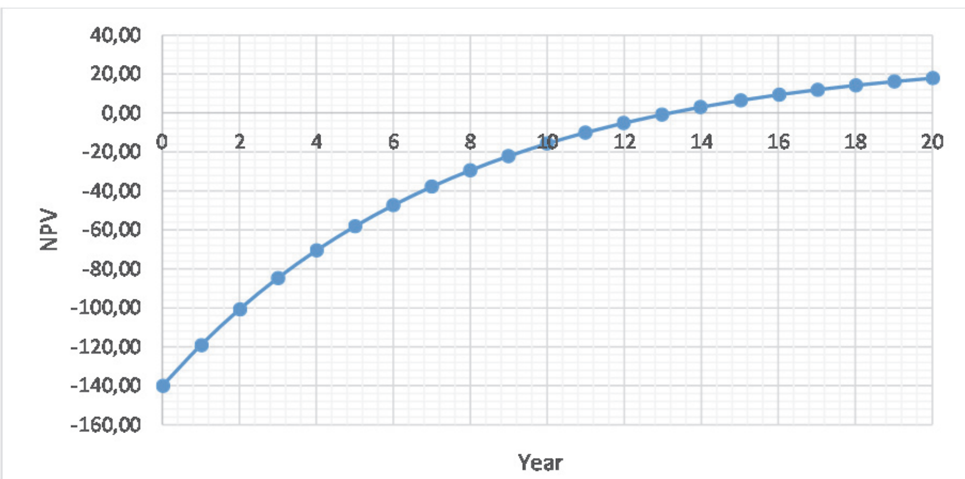

Figure 1.10. The graph of NPV dependence on the year

Thus, the discounted payback period of RTE in the city of Irpin is:

$$T = (14-1) + \frac{0.72}{3.08-(-0.72)} \approx 13.2 \text{ years} \tag{1.41}$$

1.8. CONCLUSIONS

Consequently, the Thermal Energy Market is a set of economic relations between market participants that may or may not be present, depending on the level of localization of the district heating system, where the heat energy and related products are in the form of goods (for which there is demand and supply) and services without which the functioning of the market is impossible.

In this paper the main structural schemes of relations between the entities of the Thermal Energy Market were defined and appropriate models of the Thermal Energy Market were proposed, depending on the level of localization of the heat supply system.

Efficient use of local resources as heat production is an important aspect in the operation of the Thermal Energy Market from the point of view of the state policy in the field of energy. When creating the Thermal Energy Market, the analysis of the energy potential of resources is fundamental, since this particular information provides the use of an objective indicator of market share as a constraint in combination with the characteristics of the local heat energy market, such as the amount of heat energy consumption and the number of producers.

In this work a list of necessary technical means for the creation of the market of thermal energy was determined. Without the provision of the market for thermal energy by these means, its functioning is impossible, therefore the classification is given regarding the areas of responsibility for the creation of TEM: the zone of producers, the district heat supply organization, the zone of consumers, the zone of state authorities. The calculation of capital expenditures according to the classification of areas of responsibility for the creation of TEM is given.

In this paper an analysis of the conditions for functioning of the heat energy market for the city of Irpin was conducted. According to the results of the simulation of the interaction of 8 producers with different technologies of heat energy production on the market with consumption volume of 42 thousand Gcal, the coefficient of market share according to certain conditions in the heat energy market is optimized, which equals 0.15.

In the software "Thermal Energy Market" it is determined that with an optimal coefficient of market share, which is 0.15, at the tariff of the main producer at 1608.77 UAH/Gcal, the average consumer tariff will be about 20% lower in the functioning of the thermal market of energy is 1292.63 UAH/Gcal. According to the results of the model, the relative efficiency of the heat energy market in Irpin city at the given conditions amounted to 27.04%.

On the basis of the calculated amount of capital expenditures for the creation of TEM in the city of Irpin, the simple payback period of TEM is 6.7 years, and the discounted payback period is 13.2 years at a discount rate of 14%. The sources of funding for the creation of TEM were not identified in the work.

The following parameters may influence the payback period of the Thermal Energy Market: the number of independent producers, the volume of heat energy consumption, losses in heat networks, capital expenditures on the creation of the TEM, the discount rate, the market share coefficient, the rules for determining the market share factor and the efficiency of the TEM. From this, it is important to determine the parameters that most affect the results of the model.

The Thermal Energy Market, besides economic indicators, can have an impact on such parameters as the ecological situation in the region, from the point of view of the use of local resources for their disposal, harmful emissions (for example, if there was a source of energy in the form of stone or brown coal) and reliability of heat supply in the system. All these indicators can be expressed in a monetary equivalent in one way or another and have an impact on the overall payback period of a local project to create TEM.

This model can be used as a tool for strategic planning of district heating systems of existing cities as well as projected cities to ensure the maximum efficiency of such systems, where the final price and quality of heat energy are the key factors for consumers.

REFERENCES

[1] Deshko V.I., Zamulko V.I., Karpenko D.S., *Estimation of efficiency of functioning of the local market of thermal energy*, “Problems of General Energy” 2017, 3 (50), pp. 41–49.

[2] Karpenko D.S., Deshko V.I., *Construction of an effective model of the Thermal Energy Market in the realities of Ukraine*, “Power Engineering and Electrification” 2016.

[3] About heat supply//Law of Ukraine dated 02.06.2005 No. 2633-IV with current editing from 01.01.2016, <http://zakon3.rada.gov.ua/laws/show/2633-15/page>.

[4] Semenov V.G., *Assessment of the possibility of competition in heat supply systems*, <www.rosteplo.ru/Tech_stat/stat_shablon.php?id=316>.

[5] Lyulchak Z.S., Khtey N.I., Akimova L.M., *Principles of the formation of competitive relations in the regional Thermal Energy Markets of the district heating system*, Bulletin Publishing House of the Lviv Polytechnic National University, No. 623.

[6] Geletukha G.G., *Status and prospects of bioenergy development in Ukraine. Prospects for implementing a competitive heat energy market*, <http://uabio.org/img/files/Events/pdf/b4e-conf-geletukha-20-09-2016-ua.pdf>.

[7] Shevtsov A.I., Barannik V.O., Zemlyanii M.G., Ryuazova T.V., *The state and prospects of reforming the heat supply system in Ukraine*. *Analytical report.*

[8] Geletukha G.G., Zhelyezna T.A., Bashtovy A.I., *Analysis of the models of functioning of the district heating system in the countries of the European Union*, Part 1, “Industrial Heat Engineering” 2016, Vol. 38, No. 4, pp. 63–70.

[9] Geletukha G.G., Zhelezna T.A., Bashtovy A.I., *Analysis of the models of functioning of the district heating system in the countries of the European Union*, Part 1, “Industrial Heat Engineering” 2016, Vol. 38, pp. 78–85.

[10] Zyabkin A.C., *The market of thermal energy and its specificity in the classical and modern concepts of market relations*, Business Education Right, History of Volgograud Institute of Business, 2011, No. 3 (16).

[11] Geletukha G.G., Zhelyezna T.A., Bashtovy A.I., *Analysis of tariff setting in the district heating system of the countries of the European Union*, “Analytical Note of the Bioenergy Association of Ukraine” 2016, No. 14, <http://www.uabio.org/img/files/docs/position-paper-uabio-14-ua.pdf>.

[12] Brich V., Fedirko M., Yanik I., *Organizational and economic prerequisites for reengineering of business processes in the market of municipal heat and power engineering in Ukraine*, “Herald of TNEU” 2016, No. 2, pp. 7–19.

[13] Semenov V.G., *Poland’s experience in heat supply is a lesson for Russia*, “Heat Supply News” 2002, No. 9 (25), pp. 8–15.

[14] Gavrikova A.O., *Critical analysis of the functioning model of the energy market of Ukraine*, <vestnik.kpi.kharkov.ua/files/vestnik/2011/39/2_39_2011.pdf>.

[15] Demina O.V., *Thermal Energy Markets: Trends in Spatial Organization*, “Spatial Economy” 2016, No. 4, pp. 33–60.

[16] Papushkin V.N., *Radius of heat supply. Well forgotten old*, “News of Heat Supply” 2010, No. 9 (25), pp. 44–49.

[17] Papushkin V.N., Polyantsev S.O., Shcherbakov A.P., Khrapkov A.A., *Method of calculating the radius of effective heat supply for heat supply schemes*, <http://www.rosteplo.ru/Npb_files/npb_shablon.php?id=1601>.

[18] Dolmatov I.A., Panova M., Drobysh I., *Analysis of possible consequences and problems of implementation of the new model of the Thermal Energy Market*, “Energoryunok” 2015, No. 3 (128), pp. 57–66.

[19] Bashmakov I.A., Papushkin V.N., *Problems of heat supply and the need to develop programs for the development, modernization and rehabilitation of heat supply systems*, “S.O.K. Magazine” 2005, 4.

[20] Malafeev V.A., *On the question of a single buyer in heat supply*, NP “Russian Heat Supply”.

[21] Pindic R.S., Rubinfeld D.L., *Microeconomics*, 2001.

[22] Deshko V.I., Karpenko D.S., *Method of optimization of expenses of objects of heat generation of enterprises in the local market of thermal energy*, Materials of the X scientific and technical conference of the Institute of Energy Saving and Energy Management “Energy. Ecology. Man”, pp. 191–194.

[23] Akulich I.L., *Mathematical programming in examples and tasks: Tutorial*, 3rd ed., Publishing House Lan, 2011, p. 352.

[24] Deshko V.I., Karpenko D.S., *Simulation and optimization of the heat energy market*, Materials of the VIII international scientific and practical conference “Integrated quality assurance of technological processes and systems”, Vol. 2, pp. 231–232.

[25] Shubin E.P., *Materials, methods of the device and calculation of heat insulation of pipelines*, Gosenergoizdat, 1948, p. 151.

OPTIMIZATION OF CENTRALIZED HEAT SUPPLY OF BUILDINGS IN CONDITIONS OF PROGRAM SUPPLY OF HEAT

Anatoliy M. Pavlenko, Hanna V. Koshlak, Jerzy Z. Piotrowski

Department of Building Physics and Renewable Energy
Kielce University of Technology

In Ukraine, the district heating system serving greater part heat consumers. Compared with decentralized heat supply they have several advantages. First is the possibility of burning low-grade local types of fuel with high efficiency, the use of secondary energy sources, reduction of CO_2 emissions they have infrastructure for maintenance service of heat generating equipment and a number of other advantages.

However, currently the district heating system is in crisis situation. High heat tariffs lead to disconnection part of consumers and their transition to individual heating systems and hot water supply. The reason is the crisis situation a number of factors: political, financial, economic and technical. In this work we will focus more on technical issues is improving the operating characteristics of district heating systems.

The existing district heating system designed and built in the time of “cheap” energy carriers. Therefore, a number of strategic design decisions that were laid in them now were energy intensive and require of modernization measures. These energy-intensive solutions include low thermal resistance building envelopes heated buildings, thermal insulation of pipelines, lack of means metering of heat energy, lack of means regulation of supply of heat for heating and hot water supply in individual thermal points of buildings, lack of tanks-accumulators at central heating points, the use of hydraulic elevator for connecting heating systems to heating systems, lack of means recycling exhaust air heat and many others.

Overall strategy adopted decisions was aimed at stabilizing the temperature control of heated buildings. Much of this was justified by the lack of reliable engineering tools (eg pumps and regulators) to control the thermal and hydraulic regime consumer of heat. In fact, management carried out only at the source of heat by using the heating temperature schedule.

It is known that the application of local and individual management tools supply of heat economy of energy resources can be up to 25% of annual costs. Why, now, when there is equipment for program supply of heat, regulators with weather correction and other technical means, there are only isolated cases of automation of supply of heat to consumers? In most cases, the main reason is the lack counters of heat of consumers. However, lack of counters of heat only pushes the problem into an impasse for making not interested in saving energy as heat producers and its consumers, who pay for the “square meter”. Therefore, if we are really committed to saving energy carriers alternative account of heat in the future there is not.

The next question that arises immediately after installation of meters heat – how to get the maximum savings of heat with minimum capital loss? First – insulation of external building envelopes, replacement windows. Second – upgrading heating systems and thermal unit. Third – modernization of the district heating system.

The main difficulty modernization of centralized heat supply is that this is a system in which many different interrelated elements, each of which has its own heat engineering characteristics. For example disconnection from one building heating network will not lead to a proportional reduction in costs coolant source of heat, as a result of hydraulic dis-regulation of this coolant immediately re-distributed between the neighboring houses. If they do not have the automation means the increase in loss heat carrier will increase the heating and saved the heat be released into the environment through ventilation overheated rooms.

There are many schemes of automation individual and central heat stations, heating devices and heating risers. At various times by various authors examined the individual elements of the system. Separately, especially the formation of microclimate of premises [1–3], thermal and hydraulic of the heating system modes [4, 5] and heating devices with temperature regulators [6, 7], individual and central heat points [8, 9], thermal network [10, 11] and characteristics work heat generating equipment [12, 13]. However, ignoring features of the system generally leads to a lack of a strategic plan for the modernization of the district heating system to reduce energy savings in the future.

Therefore this work is an attempt to find strategic approaches to modernize the district heating system by considering it as a system rather than a set of individual elements. To do this we will need a mathematical model which should be combined thermal regimes of buildings, hydraulic and thermal modes of of the heating system, the work of means of automatic regulation, heating networks and heat source.

2.1. FEATURES OF MODELING OF INDIVIDUAL ELEMENTS OF THE HEATING SYSTEM

As we consider the system whose main purpose is to create a microclimate of premises – a necessary condition for this mathematical model is calculation of thermal sensation human in the room. To assess the level of comfort microclimate international standard ISO [14] recommends the use of index PMV (Probable Value of Thermal Comfort).

Index PMV is a parameter that predicts the thermal sensation large group of people under the 6-point scale: +3 – hot; +2 – warmth; +1 – barely warmth; 0 – comfortable; –1 – barely cool; –2 – cool; –3 – coldly. The index value PMV within ±2 corresponds of acceptable parameters microclimate in the premises. The methodology for its calculation takes into account the impact of a number of microclimate premises for thermal feelings of a person. Chief among these is the internal air temperature and medium-radiation temperature surfaces in the premises.

When considering transient thermal processes in the premises of buildings necessary to determine the temperature on the surface and inside the various building designs at any given time. Generally, most building envelopes is multilayered. Moreover, the thermophysical characteristics of various layers differ significantly. Load-bearing structures typically have significant mass and high thermal conductivity. Thermal insulation layers, light and contrast are small value of coefficient of thermal conductivity. Solution of these problems requires consideration of different thermal and physical characteristics materials and their relative position to calculate the unsteady temperature. Problems of this type are referred to problems of nonlinear thermal conductivity.

The methods of problem solving nonlinear thermal conductivity can be divided into analytical and digital. To include analytical method Laplace integral transformations and variational methods linearization. Analytical study of these problems encountering significant difficulties. For the simplest cases known to only a few analytical solutions [15] because in practice used mainly close (digital) decision [16].

To find the temperature distribution within a multilayer enclosure used Fourier heat conduction equation. For *i*-layer:

$$\frac{\partial t_{i(x,\tau)}}{\partial \tau} = \frac{\lambda_i}{c_i p_i}\frac{\partial^2 t_{i(x,\tau)}}{\partial x_i^2} + \frac{q_{v(x,\tau)}}{c_i p_i} \tag{2.1}$$

where: $t_{i(x,\tau)}$ – temperature of thickness *i*-th layer walls, which depends on the spatial coordinates x and time τ; λ_i, c_i, ρ_i – under thermal conductivity, heat capacity and density *i*-th layer this design; $q_{v(x,\tau)}$ – specific volumetric sources or sinks heat, W/m^3. Conditions of contact between the layers can be considered ideal. Boundary conditions usually apply 3rd kind.

To solve the problems of non-stationary nonlinear heat conductivity needed a method that would have minimal restrictions and the optimal balance between the possibility of expansion complexity formulation of the problem and its solution. An important condition is independent of time and coordinate steps between them and on the of thermophysical characteristics of the material within the specified accuracy range calculation.

The features determining the medium-radiation temperature (t_R) on the premises are unknown coefficients mutually radiation of various designs together. So apply the exact formula [17] can not:

$$t_{R1} = \sum \varphi_{1-j} t_j \tag{2.2}$$

where: φ_{1-j} – the coefficient radiation from the surface 1 to all other surfaces (j) at the premises; t_j – temperature j-th surfaces at the premises, °C.

Using the approximate formula:

$$t_{R1} = \frac{\sum F_j t_j}{\sum F_j} \tag{2.3}$$

where F_j is the surface area of j-th design at the premises, leads to the fact that the amount of radiation heat flow is significantly different from zero. It is therefore necessary to improve the methodology for calculating the average-radiation temperature premises.

The calculation of the heating system must take into account the transport delay, joining various heating devices and pipes, correctly calculate the temperature regime in the return pipeline heating system. In addition, the heating system must work correctly in terms of quantity and quality of regulation.

Regulation of supply heat for heating Individual Heat Points (IHP) can obtain savings of thermal energy as a result of consideration of the thermal domestic, insolation (with the façade in regulation) and reduce the quantity of infiltrated air. According to literary data such savings can range from 10% to 15% of annual cost of heat for heating [18, 19]. In addition, much of central heat points has no means to control the temperature of the coolant in the of quarterly heat networks. In this case, you can also get additional savings of heat during the "fracture" heating schedule (1–11% in Ukraine) by controlling the thermal mode of buildings in IHP.

Analysis of the work known technological schemes of regulation of supply of heat to the subscriber inputs [20–23] shows that management process to supply of heat in all schemes usually associated with a change (decrease) loss of heat carrier in heat network. That is, the heat savings achieved through the use of quantitative methods of regulation that has significant shortcomings.

The work of heating network affect all its subscribers. In quantitative regulation mode, ie by changing the heat consumption may be dis-regulating heat network and subscribers. By individual consumers will come more amount of coolant than necessary, and others less. This is the hydraulic dis-regulation in heating network. To assess the hydraulic dis-regulation of individual subscribers if you disable one or more of them used the method of hydraulic characteristics [24]. Changing the flow rate leads to a change in thermal conditions and heating systems as a result of hydraulic dis-regulation occurs thermal dis-regulation.

The calculation results show that the total cost of coolant in the heat supplying system little changed when disconnecting the 30% of consumers [25]. With increasing pressure losses in pipelines of thermal network compared with heating system, value hydraulic dis-regulation increases and the efficiency of known schemes ITP reduced. To eliminate hydraulic dis-regulation of Europe's leading producers of automation recommend installing a pressure regulator in each ITP. The disadvantage of this solution is the high cost of automation. For example, the cost of a pressure regulator with a nominal diameter of 50 mm is an average of 2600 euros. A system heat supply from HEC can be connected to more than one hundred homes.

Getting substantial savings heat by reducing heat consumption in heat network is possible only in the automation of most of the customers in need of significant investment. This is one of the main reasons that the known as regulatory scheme tempering heat ITP are not widely spread.

On the other hand, if automate the supply of heat to most ITP without the use of pressure regulators – creating favorable conditions for the "avalanche" closing regulators due to redistribution of coolant between subscribers heating network. This phenomenon may cause a sharp change in heat consumption to the heat source and emergency situations.

An analysis of the shortcomings of existing schemes regulation in ITP points to necessity of application of automated thermal point scheme, which would give the opportunity to receive economic effect without affecting the hydraulic regime of thermal networks. That is required for this scheme "quality" of regulation. In them heat savings achieved through coolant return with a high temperature to a source of heat. This allows you to get real economic effect even with automation just one unit in thermal heat network.

In the presence of heat network CHP with exchangers enabled by two-step mixed or sequential scheme part of heat saved can be used to heat water for hot water supply. Generally, lower heat load to the second degree of heat exchangers CHP helps stabilize the thermal and hydraulic regimes magistral heating network. It creates favorable conditions for saving thermal energy and to save energy for pumping coolant.

Availability in boiler house of boilers with developed heating surfaces require maintenance coolant temperature in the return pipeline heating network not lower 60–70°C, which is provided recirculation pumps [26]. Increasing the temperature of the coolant in the return pipe heating network at work regulators in ITP can reduce the amount of coolant passing through the circulation pumps. This allows you to get additional economic effect due to decrease electricity consumption.

For HEC increase temperature of coolant has a negative effect, since it leads to a decrease in the efficiency electric power output. Therefore, the coolant temperature in the return pipe should not exceed the calculated values (according to the heating schedule) [27].

2.2. MATHEMATICAL MODEL

2.2.1. Assessment of comfort microclimate

Index PMV can be determined knowing the level of physical activity, type of clothing, air temperature, medium radiation temperature, air mobility and the partial pressure of water vapor. The value of this index is calculated based on the conditions of the heat balance on the surface of the human body. At this a person is in a state of thermal equilibrium with the surrounding environment.

The value of the index PMV finds the formula:

$$\text{PMV} = \left(0.303\ell^{-0.036q_{on}} + 0.028\right)\left\{q_{met} - q_{duf} - q_n - q_{dux}^B - q_{dux}^T - q_o^r - q_o^k\right\} \quad (2.4)$$

where: q_{on} – specific energy of metabolism, W/m^2; q_{met} – specific metabolic heat release, W/m^2; q_{duf} – heat loss due to water vapor diffusion through human skin, W/m^2; q_n – heat loss through sweating, W/m^2; q_{dux}^B, q_{dux}^T – specific heat loss during respiration, under “hidden” and “obvious” component, W/m^2; q_o^r, q_o^k – specific heat loss through clothing, respectively due to the thermal radiation and due to convection, W/m^2.

In the case $q_{met} = q_{duf} + q_n + q_{dux}^B + q_{dux}^T + q_o^r + q_o^k$ index PMV = 0 – man is in a state of thermal comfort. If $q_{met} > q_{duf} + q_n + q_{dux}^B + q_{dux}^T + q_o^r + q_o^k$ – index PMV > 0 – the human body is overheating and she feels uncomfortable. If $q_{met} < q_{duf} + q_n + q_{dux}^B + q_{dux}^T + q_o^r + q_o^k$ – index PMV < 0 – felt of cold discomfort.

According to European standard norms for comfortable conditions area index values must be within PMV = ±0.5, and for acceptable conditions – PMV = ±2.

Expand the value of specific heat flow:

$$q_{met} = q_{on}\left(1-\eta\right) \tag{2.5}$$

$$q_{duf} = 3.05\cdot 10^{-3}\left(5733-6.99q_{on}\left(1-\eta\right)-P_B\right) \tag{2.6}$$

$$q_P = 0.42\left(q_{on}\left(1-\eta\right)-58.15\right) \tag{2.7}$$

$$q_{dux}^{B} = 1.72\cdot 10^{-5}\left(5867-P_W\right)q_{OP} \tag{2.8}$$

$$q_{dux}^{T} = 0.0014q_{OP}\left(34-t_{In}\right) \tag{2.9}$$

$$q_O^R = 3.96f_{clo}\left[\left(\frac{t_{O+273}}{100}\right)^4-\left(\frac{t_R+273}{100}\right)^4\right] \tag{2.10}$$

$$q_O^C = \alpha_K f_{clo}\left(t_O - t_{In}\right) \tag{2.11}$$

where: η – efficiency work done by man; P_W – the partial pressure of water vapor in the air, P; t_{In} – the internal temperature of the air in the room, °C; f_{clo} – the relative area of clothing; t_O – the surface temperature of clothing, °C; t_R – medium radiation room temperature, °C; α_C – convective heat transfer coefficient at the surface of clothes, W/(m^2°C).

Given the values q_O^R, q_O^C temperature on the outer surface clothing found from the heat balance equation:

$$t_O = 35.7-0.0276q_{on}\left(1-\eta\right)-0.155I_{clo}f_{clo}\left\{3.96\left[\left(\frac{t_O+273}{100}\right)^4-\left(\frac{t_R+273}{100}\right)^4\right]+\alpha_C\left(t_O-t_{In}\right)\right\} \tag{2.12}$$

where f_{clo} is heat transfer resistance clothes, clo.

This transcendental equation in which the desired temperature clothing used as one of the variables. These equations can be solved by method successive approximations. Convective heat transfer coefficient are finding by known dependencies:

$$\alpha_C = \max \begin{cases} 2.38\sqrt[4]{t_O - t_{In}} \\ 12.1\sqrt{V_\Pi} \end{cases} \tag{2.13}$$

where V_Π is the mobility of air in the room, m/s.

The value of the ratio $f_{clo} = \dfrac{F_o}{F_m}$ find the formula:

– for $I_{clo} \leq 0.5clo$

$$f_{clo} = 1 + 0.2I_{clo} \tag{2.14a}$$

– for $I_{clo} > 0.5clo$

$$f_{clo} = 1.05 + 0.1I_{clo} \tag{2.14b}$$

Index PMV corresponds to stationary conditions, but it can be used for small changes of one or more variables.

Limitations. Recommended domain of definition each of the six independent parameters that are included in calculation PMV: q_{on} = 46÷232 W/m^2; I_{clo} = 0÷2 clo; t_{In} = 10÷30°C; t_R = 10÷40°C; V_Π = 0÷1 m/s; P_W = 0÷2700 P.

2.2.2. Transient thermal processes in multilayer building envelope

Consider stratified squamous wall Figure 2.1. Each layer has thermophysical properties (density, thermal conductivity, heat capacity, etc.). To find the temperature distribution inside the walls divide it parallel planes into several calculated layers, using step Δx_i. Moreover coordinate step Δx_i may be different for different of structural layers of wall. Numeration of calculation of layers can be carried on the inner surface design (i = 1) to the outside (i = n). We assume that within a single layer of thermophysical characteristics wall of material at a given time constant.

Assume that the mass array, limited step $\pm\Delta x$ concentrated in the plane of this layer. Then, for the i-th the inner layer (i = 2÷(n – 1)) in the middle of material can add the following heat balance equation:

$$c_i m_i \frac{dt_i}{d\tau} = \frac{F\left(t_{i-1} - t_i\right)}{\dfrac{\Delta x_{i-1}}{\lambda_{i-1}} + \dfrac{\Delta x_i}{\lambda_i}} - \frac{F\left(t_i - t_{i+1}\right)}{\dfrac{\Delta x_i}{\lambda_i} + \dfrac{\Delta x_{i+1}}{\lambda_{i+1}}} + q_{V(i)} \cdot F \cdot 2 \cdot \Delta x_i \tag{2.15}$$

where: c_i – specific heat i-th layer of material enclosure, J/(kg·°C); m_i – weight material i-th heat accumulating layer, kg; t_1, t_2, …, t_i – temperature corresponding layer enclosure, °C; λ_i – thermal conductivity i-th layer of material, W/(m°C); F – the surface area of design, m^2; $q_{V(i)}$ – specific volume source of heat energy, W/m^3.

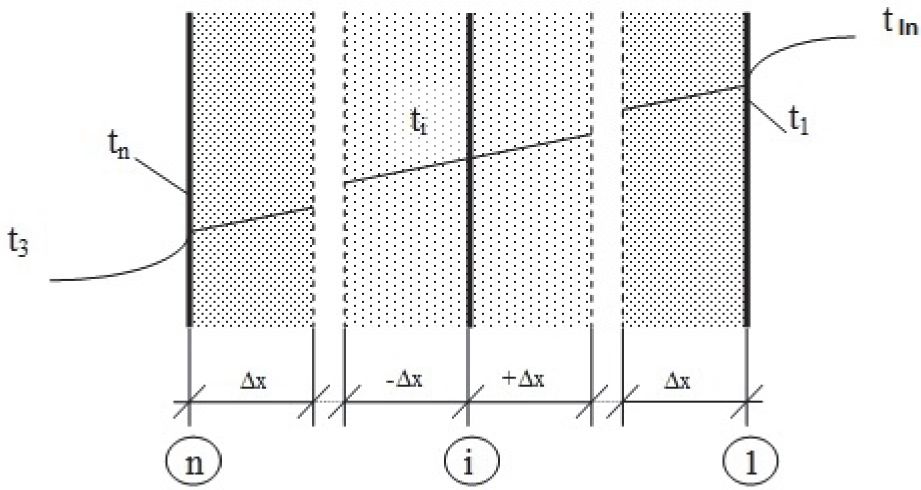

Figure 2.1. The scheme of distribution of the external enclosure of a number of calculated layers with step Δx_i

Near the inner surface of asking the boundary conditions of the third kind with the distribution of heat flow in convection and radiation components. Then the heat balance equation for the outer layer (i = 1) will have the following form:

$$c_1 m_1 \frac{dt_1}{d\tau} = \alpha_{In}^{C} F\left(t_{In} - t_1\right) + \alpha_{In}^{R} F\left(t_R - t_1\right) - \frac{F\left(t_1 - t_2\right)}{\dfrac{\Delta x_1}{\lambda_1} + \dfrac{\Delta x_2}{\lambda_2}} + q_{V(1)} \cdot F \cdot \Delta x_1 \tag{2.16}$$

where: α_{In}^{C} – convective heat transfer coefficient at the inner surface, W/m^2°C; α_{In}^{R} – coefficient of radiant heat transfer at the inner surface, W/m^2°C; t_{In} – internal air temperature, °C; t_R – medium radiation temperature in the room, °C.

For the latter (outer) layer of material:

$$c_n m_n \frac{dt_n}{d\tau} = \frac{F\left(t_{n-1} - t_n\right)}{\dfrac{\Delta x_{n-1}}{\lambda_{n-1}} + \dfrac{\Delta x_n}{\lambda_n}} - \alpha_{OUT} F\left(t_n - t_{AMB}\right) + q_{V(i)} \cdot F \cdot \Delta x_n \tag{2.17}$$

where: α_{OUT} – heat transfer coefficient near the outer surface of the enclosure, W/m^2 °C; t_{AMB} – ambient temperature, °C.

Whereas, for the boundary layers of material weight $m_i = \Delta x_i \cdot \rho_i \cdot F$, and for the inner layers $m_i = 2 \cdot \Delta x_i \cdot \rho_i \cdot F$, obtain a system of n equations:

$$c_1 \Delta x_1 \rho_1 \frac{dt_1}{d\tau} = \alpha_{In}^{C}\left(t_{In} - t_1\right) + \alpha_{In}^{R}\left(t_R - t_1\right) - \frac{\left(t_1 - t_2\right)}{\dfrac{\Delta x_1}{\lambda_1} + \dfrac{\Delta x_2}{\lambda_2}} + q_{V(1)} \cdot \Delta x_1$$

$$2 c_i \Delta x_i \rho_i \frac{dt_i}{d\tau} = \frac{\left(t_{i-1} - t_i\right)}{\dfrac{\Delta x_{i-1}}{\lambda_{i-1}} + \dfrac{\Delta x_i}{\lambda_i}} - \frac{\left(t_i - t_{i+1}\right)}{\dfrac{\Delta x_i}{\lambda_i} + \dfrac{\Delta x_{i+1}}{\lambda_{i+1}}} + q_{V(i)} \cdot 2 \cdot \Delta x_i \qquad (2.18)$$

$$c_n \Delta x_n \rho_n \frac{dt_n}{d\tau} = \frac{\left(t_{n-1} - t_n\right)}{\dfrac{\Delta x_{n-1}}{\lambda_{n-1}} + \dfrac{\Delta x_n}{\lambda_n}} - \alpha_{OUT}\left(t_n - t_{AMB}\right) + q_{V(i)} \cdot \Delta x_n$$

the corresponding number of unknown temperatures.

The resulting system of differential equations is easily solved by digital methods, for example by a method Runge-Kutta 4th order [28]. An important feature of the proposed mathematical model is that all of its thermophysical characteristics (α_{In}, α_{OUT}, λ_i, c_i, ρ_i, $q_{V(i)}$, Δx_i) can also be defined as a function of time and coordinates $\boldsymbol{X}$. In addition, its feature is the ability partitioning design a desired number of layers of different thickness. This allows you to use the proposed mathematical model to determine the temperature regimes multilayer enclosing structures (under ideal thermal contact between layers).

Inside the building envelope also play an important role in the formation dynamic microclimate premises. For the mathematical description their thermal modes use the mathematical model presented above with some modifications. Consider the symmetric problem with boundary conditions of the 3rd kind near the outer surface and the absence of heat flow in the center of this design. Applying a similar breakdown construction on a number calculated of layers may have different thermophysical characteristics, the system of equations would look like this:

$$c_1 \Delta x_1 \rho_1 \frac{dt_1}{d\tau} = \alpha_{In}^C \left(t_{In} - t_1 \right) + \alpha_{In}^R \left(t_R - t_1 \right) - \frac{\left(t_1 - t_2 \right)}{\dfrac{\Delta x_1}{\lambda_1} + \dfrac{\Delta x_2}{\lambda_2}} + q_{V(1)} \cdot \Delta x_1$$

$$2c_i \Delta x_i \rho_i \frac{dt_i}{d\tau} = \frac{\left(t_{i-1} - t_i \right)}{\dfrac{\Delta x_{i-1}}{\lambda_{i-1}} + \dfrac{\Delta x_i}{\lambda_i}} - \frac{\left(t_i - t_{i+1} \right)}{\dfrac{\Delta x_i}{\lambda_i} + \dfrac{\Delta x_{i+1}}{\lambda_{i+1}}} + q_{V(i)} \cdot 2 \cdot \Delta x_i \tag{2.19}$$

$$c_n \Delta x_n \rho_n \frac{dt_n}{d\tau} = \frac{\left(t_{n-1} - t_n \right)}{\dfrac{\Delta x_{n-1}}{\lambda_{n-1}} + \dfrac{\Delta x_n}{\lambda_n}} + q_{V(i)} \cdot \Delta x_n$$

To calculate the temperature on the inner surface of the small heat capacity enclosing structures (windows, exterior doors, etc.) write the equation their heat balance excluding accumulation of heat:

$$\alpha_{In}^C F_{MC} \left(t_{In} - t_{MC} \right) + \alpha_{In}^R F_{MC} \left(t_R - t_{MC} \right) = \frac{F_{MC}}{R_{MC}} \left(t_{MC} - t_{AMB} \right) \tag{2.20}$$

where: F_{MC} – area of small heat capacity of designs, m^2; R_{MC} – heat transfer resistance design without considering heat transfer at its inner surface, m^2°C/W; t_{MC} – the temperature on the inner surface, °C.

After the reduction in the area from the equation (2.20) can determine the temperature on the inner surface small heat capacity of designs:

$$t_{MK} = \frac{\alpha_{In}^C t_{In} + \alpha_{In}^R t_R + t_{AMB} / R_{MK}}{\alpha_{In}^C + \alpha_{In}^R + 1/R_{MK}} \tag{2.21}$$

2.2.3. The internal environment of the building and heating system

To find the air temperature of the internal environment of the building use heat balance equation:

$$\begin{aligned} c_A m_A \frac{dt_{B(\tau)}}{d\tau} = {} & \alpha_2^C F_2 \left(t_{W(\tau)} - t_{B(\tau)} \right) - \sum \alpha_B^K F_{3K} \left(t_{B(\tau)} - t_{3K(0,\tau)} \right) - \\ & - \sum \alpha_B^K F_{BK} \left(t_{B(\tau)} - t_{BK(\delta/2,\tau)} \right) - c_A G_{inf} \left(t_{B(\tau)} - t_{3(\tau)} \right) - \\ & - \sum \alpha_B^K F_{MC} \left(t_{B(\tau)} - t_{MK(\tau)} \right) + Q_{BT} \end{aligned} \tag{2.22}$$

where: c_A – the heat capacity of air, J/(kg°C); m_A – mass air or equivalent for the environment, kg; α_2^C – convective heat transfer coefficient near the heating elements, W/(m^2°C); F_2 – area of heat exchange surface of the heating system, m^2; t_{HS} – temperature heat exchange surface of the heating system, °C; G_{inf} – loss infiltration air, kg/s; Q_{BT} – domestic and technological thermal flow, W.

Sign amount of equation (2.22) points to the addition of heat flow from enclosing structures with different thermophysical characteristics.

Heat exchange radiation occurs almost instantaneously, so the equation of thermal balance of radiation components of heat flow to the internal environment of the heated building is stationary character:

$$a_2^R F_2 \left(t_{HS} - t_R\right) - \sum a_{In}^R F_{3K} \left(t_R - t_{3K(0,\tau)}\right) - \sum a_{In}^R F_{BK} \left(t_R - t_{BK(\delta/2,\tau)}\right) - \\ - \sum a_{In}^R F_{MK} \left(t_R - t_{MK}\right) = 0 \quad (2.23)$$

From the equation (2.23) can be defined medium-radiation temperature of heating buildings:

$$t_R = \frac{\alpha_2^R F_2 t_{HS} + \sum \alpha_{In}^R F_{3K}\, t_{3K(0,\tau)} + \sum \alpha_{In}^R F_{BK} t_{BK(\delta/2,\tau)} + \sum \alpha_{In}^R F_{MK} t_{MK}}{\alpha_2^R F_2 + \sum \alpha_{In}^R F_{3K} + \sum \alpha_{In}^R F_{BK} + \sum \alpha_{In}^R F_{MK}} \quad (2.24)$$

With the use of standard “water tube” systems heating formula (2.24) allows to determine heat flows to within 1÷2%.

For description transient thermal processes in the heating system will replace it equivalent for heat dissipation to the heating unit. Then design scheme 2-pipe heating system takes the form – Figure 2.2.

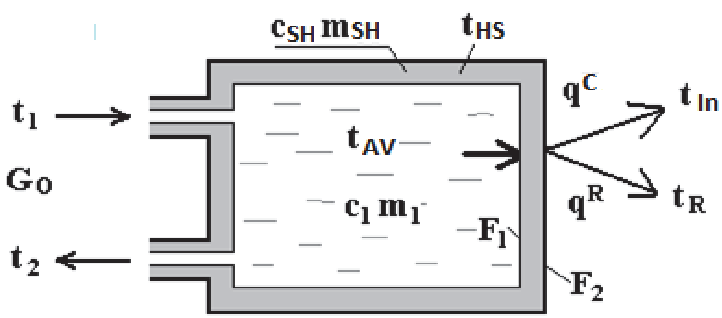

Figure 2.2. Estimated scheme “water tube” heating system

Accordance with the [29, 30] can apply the mathematical model of the “water tube” of the heating system:

$$\begin{cases} c_1 m_1 \dfrac{dt_{2(\tau)}}{d\tau} = \left(c_1 G + \alpha_1 F_1\right)\left(t_{2(\infty)} - t_{2(\tau)}\right) \\ c_1 m_1 \dfrac{dt_{AV(\tau)}}{d\tau} = c_1 G\left(t_1 - t_{2(\tau)}\right) - \alpha_1 F_1\left(t_{AV(\tau)} - t_{HS(\tau)}\right) \\ c_{SH} m_{SH} \dfrac{dt_{HS(\tau)}}{d\tau} = \alpha_1 F_1\left(t_{AV(\tau)} - t_{HS(\tau)}\right) - \alpha_2^{K} F_2\left(t_{HS(\tau)} - t_{In(\tau)}\right) - \alpha_2^{R} F_2\left(t_{HS(\tau)} - t_R\right) \end{cases} \tag{2.25}$$

where: c_1 – heat capacity of water, J/(kg°C); m_1 – mass of water in the heating system, kg; t_2 – the coolant temperature in the return pipeline of the heating system, °C; G – heat consumption in the heating system, kg/s; α_1 – heat transfer coefficient between the coolant and wall equivalent to the heat transfer heating device, W/(m^2°C); F_1 – area of internal heat transfer surface, m^2; t_{AV} – the average temperature of the coolant in the heating system, °C; c_{SH} – the average the heat capacity of the heating system elements, J/(kg°C); m_{SH} – mass of the heating system elements, kg.

To determine the temperature in the return pipe heating system in stationary conditions can apply the following formula:

$$t_{2(\infty)} = t_{HS} + \left(t_1 - t_{HS}\right)\ell^{-\frac{\alpha_1 F_1}{c_1 G}} \tag{2.26}$$

Current GOS [31] provides for installation in heating systems individual means tempering heat regulation – of thermostats. We assume that each heating device is equipped with an automatic temperature controller direct action. Each thermostat consists of a valve and thermostatic head.

For a description heating system with radiator thermostats must combine their thermal and hydraulic regime Figure 2.3. The total loss of pressure in the automated heating system will consist of a loss of pressure on the thermostatic valve and pressure loss in pipelines and heating devices:

$$\Delta P_{PL} = \Delta P_{TV} + \Delta P_{SH} \tag{2.27}$$

where: ΔP_{TV} – loss of pressure in thermostatic valve, bar; ΔP_{SH} – loss of pressure in the heating system, bar.

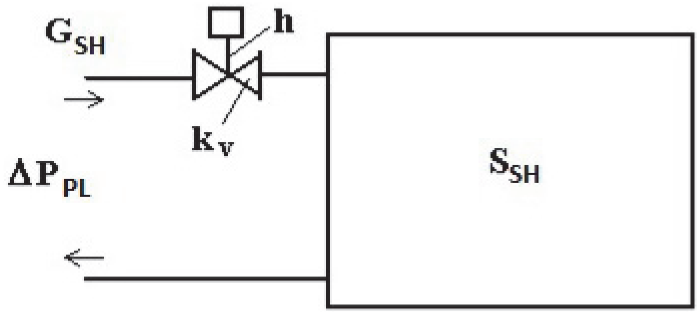

Figure 2.3. Estimated scheme of the heating system with individual thermostats

Considering that a heating system 2-pipe – all valves connected in parallel. Using the method of hydraulic characteristics equation (2.27) can be written as:

$$\Delta P_{PL} = \left(\frac{1}{(Nk_V)^2} + S_{SH} \right) G_{SH}^2 \tag{2.28}$$

where: N – the total number of thermostatic valves, units; k_V – coefficient of bandwidth valve, $(m^3/h)/bar^{0.5}$; S_{SH} – hydraulic characteristics of the heating system, $bar/(m^3/h)^2$; G_{SH} – heat consumption in the heating system, m^3/h.

From formula (2.28) can be find heat consumption in the heating system:

$$G_{SH} = \sqrt{\frac{\Delta P_{PL}}{\frac{1}{(Nk_V)^2} + S_{SH}}} \tag{2.29}$$

The relationship between move of valve stem and it coefficient bandwidth called of costly characteristic of the valve. There are three main types of characteristics: linear, quadratic and straight-percentage. Each type characteristics corresponding to his of profiling plates valve. For radiator thermoregulators used primarily logarithmic characteristic. Coefficient of bandwidth valve with logarithmic characteristic can be defined by the formula:

$$k_V = (k_{VO})^h (k_{VC})^{1-h} \tag{2.30}$$

where: k_{VO} – coefficient of bandwidth valve in open position, $(m^3/h)/bar^{0.5}$; k_{VC} – also in the closed position, $(m^3/h)/bar^{0.5}$; h – the relative position of the valve stem.

Coefficient of bandwidth valve in the open state depends on the a standard size of the valve is determined by hydraulic calculation of the heating system. Coefficient of bandwidth valve in the closed position can be taken as standard leakage $k_{VC} = 0.0005\ k_{VO}$.

Hydraulic resistance the valve is defined as stem position (h). The maximum position stem ($h_{\max} \le 1$) is set at previous setting valve (installation). Other provisions stem depends on the air temperature in the room. Excluding the friction in the valve stem faucet stem its provisions can describe linear dependence the type of:

$$h_{(\infty)} = h_{\max}\ , \text{ if } \quad t_{In} < t_{\min}$$

$$h_{(\infty)} = \frac{t_{\max} - t_{In}}{t_{\max} - t_{\min}}\ , \text{ if } \quad t_{\min} \le t_{In} \le t_{\max} \tag{2.31}$$

$$h_{(\infty)} = 0\ , \text{ if } \quad t_{In} > t_{\max}$$

where: $h_{(\infty)}$ – stem position after transitional processes; $t_{\max}$, $t_{\min}$ – in accordance with the maximum and minimum air temperature at which the valve stem reaches extreme positions, °C.

Maximum and minimum air temperature is set by turning the thermostatic valve head. For fully open the valve in ideal conditions $t_{\max} - t_{\min} = 2$ K. In case preset, this temperature difference is decreases.

Friction stem thermostatic valve in the faucet stem leads to the appearance a temperature hysteresis. This negative phenomenon reduces energy-efficient effect of the use valves. If the value hysteresis does not exceed 0.4°C (eg thermostats for Danfoss company) – in this problem we can ignore it.

Other important factor is time the transition process in the head thermostatic valve. For thermoregulators Danfoss company is this period $\tau_K = 12 \div 15$ min. Given the transition processes in thermostatic head valve stem position can be described by the formula:

$$h_{(\tau)} = h_{(\infty)} + \left(h_{(0)} - h_{(\infty)}\right)\ell^{-\frac{\tau}{\tau_K}} \tag{2.32}$$

The system of equations (2.25)–(2.32) unites thermal and hydraulic regime of the heating system in transition processes and take into account the work of individual thermostatic valves. The resulting system of equations of heat hydraulic balance can be solved, if you set the corresponding initial conditions.

2.2.4. Mathematical modeling automated thermal point

Mathematical model of regulation heat tempering in individual thermal point depends on its circuit. In this paper we consider one of the most common schemes regulating with a pump in the circuit of heating system, return valve on the mixing pipeline and 2-way valve on the return pipeline of thermal network Figure 2.4. There are several modifications of this scheme (with a pump on the return pipeline with 2-way valve to the feeding pipeline, etc.) that are individual features of operational nature. However, for this study, these differences can not be considered fundamental.

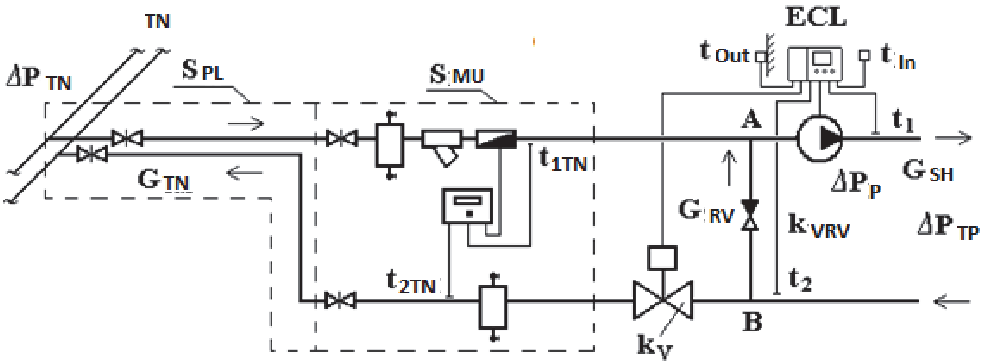

Figure 2.4. Principle scheme automation of thermal units

Mathematical model of thermal hydraulic modes automated thermal units (Figure 2.4). Consists of several equations. Let point tapping tees mixing pipeline with return valve in the feeding pipeline (A) and reverse pipeline (B).

Total hydraulic characteristics of all elements of the thermal network to the characteristic points AB:

$$S_{\Sigma} = S_{PL} + S_{MU} + \frac{1}{k_V^2} \tag{2.33}$$

where: S_{PL} – hydraulic characteristics of supplying and reverse pipelines of heat network from heat point to tapping tees in thermal chamber; S_{MU} – hydraulic characteristic elements of the thermal unit to control valve (eliminator, metering unit); k_V – coefficient of permeability 2-way valve of temperature controller, $(m^3/h)/bar^{0.5}$.

Coefficient of permeability two-way valve controller determined by one of disposables characteristics:

$$k_V = (k_{VO})^h (k_{VC})^{1-h} \text{ – straight-percent}$$

$$k_V = k_{VC} + (k_{VO} - k_{VC}) h^2 \text{ – the quadratic}$$

$$k_V = k_{VC} + (k_{VO} - k_{VC}) h \text{ – linear (recommended [22])} \tag{2.34}$$

where: k_V – coefficient of permeability 2-way valve of controller, $(m^3/h)/bar^{0.5}$; k_{VC} – coefficient of permeability 2-way valve of controller in the closed position, $(m^3/h)/bar^{0.5}$; k_{VO} – coefficient of permeability 2-way valve of controller in the open position, $(m^3/h)/bar^{0.5}$; h – relative position of the rod of two-way valve controller.

For a given differential pressure in thermal chamber (ΔP_{TN}) and a known differential pressure between the points A and B (ΔP_{AB}) heat consumption of heating network can be calculated by the formula:

$$G_{TN} = \sqrt{\frac{\Delta P_{TN} - \Delta P_{AB}}{S_\Sigma}} \tag{2.35}$$

The loss of coolant through the return valve find the formula:

$$G_{RV} = k_{V3K} \sqrt{|\Delta P_{AB}|} \tag{2.36}$$

Small loss of pressure on the tees mixing pipeline can be neglected. Then the pressure loss on the jumper will be equal pressure losses on the return valve. For return valve opening pressure at point A shall be lower than the pressure at point B, so the pressure drop in the return valve:

$$\Delta P_{RV} = -\Delta P_{AB} \tag{2.37}$$

Next two ways of calculating the coefficient the permeability return valve:

- if the differential pressure sufficient for its opening $\Delta P_{RV} > \Delta P_{V0}$ then determine coefficient of permeability for the approximation formula:

$$k_{V3K} = k_{V0}\left(1 - \ell^{-20(\Delta P_{RV} - \Delta P_{V0})}\right) \tag{2.38}$$

- in another case ($\Delta P_{RV} \leq \Delta P_{K0}$) $k_{V3K} = 0$ movement of coolant on mixing pipeline is missing.

Given the mixing heat consumption in the heating system:

$$G_{SH} = G_{TN} + G_{RV} \tag{2.39}$$

The differential pressure generated by the circulating pump find to approximating formula:

$$\Delta P_P = A + BG_{SH} - CG_{SH}^2 \tag{2.40}$$

where the coefficients A, B and C are approximation coefficients, which are determined based on the working passport characteristics of the a standard size pump.

The new value differential pressure in points A-B:

$$\Delta P_{AB} = S_{SH} G_{SH}^2 - \Delta P_P \tag{2.41}$$

where S_{SH} is hydraulic characteristics of the heating system.

For thermal balance determines the temperature in the supplying pipeline heating system:

$$t_1 = \frac{t_{1TN} \cdot G_{TN} + t_2 \cdot G_{RV}}{G_{SH}} \tag{2.42}$$

where t_{1TN} is the temperature in the supplying pipeline of thermal network, °C.

Since the convergence of the system of equations (2.35)–(2.41) relatively slow, it is desirable to perform the calculation method of secant. The initial value of differential pressure at characteristic points AB, can be set ΔP_{AB} = 0. The calculation is performed until it is provided with the necessary accuracy of determination differential pressure ΔP_{AB}.

The valve controls the electronic unit executed based microcontroller. With it set by law of regulation. In controller of this type most common of proportional-integral law regulation (PI).

Position of the rod 2-way controller within the limits h = 0÷1 determined by the formula:

$$h_{(\infty)} = \frac{1}{X_P}\left(t_1^C - t_{1SH} + \frac{1}{Z_i}\int_{\tau=0}^{\tau}\left(t_1^C - t_{1SH}\right)d\tau\right) \tag{2.43}$$

where: X_P – zone of proportionality, °C; t_1^C – corrected of calculated the temperature in the supplying pipeline heating system, °C; Z_i – constant of integration sec. In controller *f.* Danfoss zone of proportional can be set within the limits 1÷250°C, constant of integration –5÷999 sec.

Corrected the calculated temperature in the supplying pipeline heating system is determined by the formula:

$$t_1^C = t_1^P + 0.1K_t\left(t_{In}^{PR} - t_{In}\right) \tag{2.44}$$

where: K_t – coefficient of influence of temperature of internal air; t_{In}^{PR} – program set value to temperature of internal air, °C. This coefficient may have the value 1÷99.

Calculated temperature in the heating pipeline the supplying will be set linearized dependence parameters which determine the formula:

$$t_1^C = t_{InC} + \left(t_{HD} - t_{InC}\right)\overline{Q}^{0.8} + \left(t_{1O}^C - t_{HD}\right)\overline{Q} \tag{2.45}$$

where: t_{InC} – calculated temperature of internal air of heated premises, °C; t_{HD} – average temperature of heating devices, °C; t_{1O}^C – the calculated coolant temperature in the supplying pipeline heating system, °C; $\overline{Q}$ – the relative loss of heat at different outdoor temperatures.

The relative cost of heat for heating is calculated by the formula:

$$\overline{Q} = \frac{t_{InC} - t_{OUT}}{t_{InC} - t_{OUTC}} \tag{2.46}$$

where t_{OUTC} is calculated temperature of outdoor air, °C.

In controller with weather correction type ECL Comfort 200 time constant performing mechanism of valve can be set within 5–250 s. Thus, for most executive mechanisms of when changing position of the rod from one extreme position to another is τ_K = 30÷300 s. Given the work actuating mechanism the position valve stem can be described by the formula:

$$h_{(\tau)} = h_{(\infty)} + \left(h_{(0)} - h_{(\infty)}\right)\frac{\tau}{\tau_K} \tag{2.47}$$

where $h_{(0)}$ is the average starting position of the valve rod.

2.2.5. Modelling of heating network

In general form, the two-pipe heating network can be represented as a scheme Figure 2.5. One of the subscribers is equipped with automatic thermal units. It is necessary to determine the change in differential pressure at the point of joining a subscriber to the heating network in the event of changes in the costs of coolant through its ITP. You must also determine what impact the will create regulation a thermal units this consumer on network hydraulic regime as a whole.

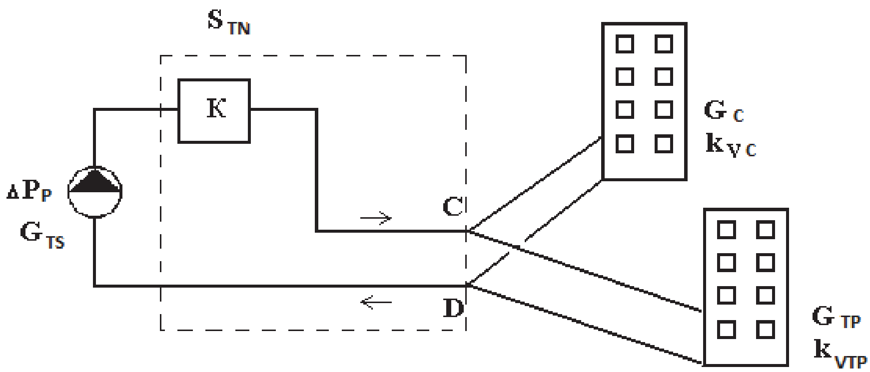

Figure 2.5. Scheme of two-pipe heating network

Differential pressure in point's accession automated thermal units to heat network (*C-D*):

$$\Delta P_{CD} = \frac{G_{TS}^2}{k_{VCD}^2} \tag{2.48}$$

where: G_{TS} – loss heat carrier on the heat source, m^3/h; k_{VCD} – the coefficient of permeability networks between points *C-D*, (m/h)/bar$^{0.5}$.

The loss coolant on the sources of heat:

$$G_{TS} = \sqrt{\frac{\Delta P_P}{S_{TN} + \frac{1}{k_{VCD}^2}}} \tag{2.49}$$

where: ΔP_P – differential pressure network pumps, bar; S_{TN} – hydraulic characteristics of the thermal network, bar/(m^3/h)^2.

Differential pressure network pumps can be determined using the approximation formula:

$$\Delta P_P = A + BG_{TS} - CG_{TS}^2 \tag{2.50}$$

where A, B, C are approximation coefficients calculated for the known working characteristics of network pumps.

The hydraulic characteristics of thermal network (S_{TN}) determined through the loss of pressure on the the relevant sections of heating network at the calculated loss of coolant.

The coefficient of permeability of areas C-D is the sum of the coefficients of permeability all subscribers:

$$k_{VCD} = k_{VTP} + k_{VC} \tag{2.51}$$

where: k_{VTP} – coefficient permeability of subscriber with automated thermal point, $(m^3/h)/bar^{0.5}$; k_{VC} – coefficient of permeability is not automated thermal points other consumers, $(m^3/h)/bar^{0.5}$.

The coefficient of permeability subscriber with automatic thermal point can determine at any time by the formula:

$$k_{VTP} = \frac{1}{\sqrt{S_\Sigma}} \tag{2.52}$$

where S_Σ is determined by the formula (2.33).

The coefficient of permeability not automated thermal point other consumers is constant, which is determined for calculation mode of heating network of the formula:

$$k_{VC} = \frac{G_C}{\sqrt{\Delta P_{CD}^C}} \tag{2.53}$$

where: G_C – the calculated loss of coolant not automated part of customer, m^3/h; ΔP_{CD}^C – pressure differential between points C-D in a calculated mode, bar.

In the proposed mathematical model compiled computer program AVTCO.

2.3. INITIAL DATA FOR MATHEMATICAL MODELING OF THERMAL AND HYDRAULIC PROCESSES OF THE SYSTEM HEAT SUPPLYING

The research performed on the example heat supply academic building No. 9 Poltava National Technical Yuri Kondratyuk University.

Parameters of microclimate and human: specific energy of metabolism q_{on} = 70 W/m^2, heat insulating properties of clothing 0.7 clo, the efficiency of the of the work performed $\eta = 0$, relative humidity of air $\varphi = 60\%$, mobility of air in the room $V_{\Pi} = 0.2$ m/s. The calculated temperature of internal air 18°C.

Thermophysical parameters of the building and its enclosing structures, area of the building in the plan 1170 m^2; volume for external measurement 9711 m^3; area of windows 150.8 m^2; their resistance to heat transfer 0.455 m^2°C/W; area of external doors 9 m^2; their resistance to heat transfer 0.455 m^2°C/W; area of outer walls 1031.2 m^2; wall material – bricks density 1800 kg/m^3, its thermal conductivity 0.71 W/(m°C), thickness 1.08 m, the overall resistance to heat transfer 1.68 m^2°C/W. Area of garret overlapping 1170 m^2; the composition of enclosure: board of pine of thickness 50 mm, density 500 kg/m^3, heat capacity 2300 J/kg°C, thermal conductivity 0.18 W/m°C; the gravel keramzite of thickness 200 mm, density 400 kg/m^3, thermal conductivity 0.14 W/m°C, heat capacity 840 J/kg°C. Thermophysical characteristics of materials taken from the GOS [32] the parameter B.

Inner wall of brick of thickness 640 mm, the total area 2056.9 m^2. Inner wall of brick of thickness 250 mm, with an area of 310 m^2. Area of intermediate floor 2340 m^2; area of a floor 1st floor 1170 m^2.

The mass of air in the building 7144 kg, mass environment inside buildings (desks, chairs, cabinets, tables and other furniture) 3883 kg. We consider them evenly distributed over the volume of the building. The total mass of air with furniture 7144 + 3883 = 11027 kg.

Estimated air exchange during working hours made one fold (1.984 kg/s), and outside working hours – 0.38 aliquot (0.754 kg/s). Domestic heat-income during working hours 23 W/m^2 heated area, and 1 W/m^2 outside working hours.

The heating system of the building has the following thermophysical characteristics: mass of water 1589 kg; mass of steel pipelines 1565 kg; weight of cast iron radiators 5551 kg; heat capacity of steel 460 J/(kg°C); heat capacity of cast iron 540 J/(kg°C); area of of the inner surface of pipelines and radiators 55.88 + 106.45 = 162.33 m^2; area of of the outer surface of pipelines 67.12 m^2; external surface area of radiators 193.55 m^2; total 67.12 + 193.55 = 260.67 m^2; the average coefficient mutual shading sections of radiators $\varphi = 0.65$, and for heating systems in general $\varphi = 0.7$; the calculated loss of heat carrier $G_C = 1.456$ kg/s. The calculated parameters heat carrier of heating system 95–70°C. The mass of walls (of pipelines and heating devices), of heating system 1565 + 5551 = 7116 kg, the average heat capacity of wall 522 J/kg°C, heat capacity of water 4187 J/kg°C. The coefficient of heat transfer from heat carrier to the inner surface of pipelines and heating devices (sectional radiators M-140) approximated dependence:

$$\alpha_1 = 15.88\left|t_{AV} - t_{HS}\right|^{0.25} + 41.81\left|t_{AV} - t_{HS}\right|^{0.30} \qquad (2.54)$$

Coefficient of convective $\left(\alpha_2^C\right)$ and radiation $\left(\alpha_2^R\right)$ heat transfer at the outer surface of the water pipe of heating system approximated equations:

$$\alpha_2^C = 1.66\left(t_{HS} - t_{In}\right)^{0.33} \tag{2.55}$$

$$\alpha_2^R = 4.9\varphi\left(0.81 + 0.005\left(t_{HS} - t_R\right)\right) \tag{2.56}$$

For selection radiator thermostats applied the theory of authorities [21]. Based on the setting workspace regulator in the optimal mode accept the authority of valves at level $\boldsymbol{a}^* = 0.3$. The internal authority of valve RTD-N 15 $a_B = 1 - \frac{k_v^2}{k_{vs}^2} = 1 - \frac{0.6^2}{0.9^2} = 0.56.$

Its external authority $a_3 = \frac{a^*}{a_B} = \frac{0.3}{0.56} = 0.54.$ Thus, the loss of pressure thermostatic valves should not be less than 54% of the differential pressure at the outlet of the heat point. If the differential pressure creates of pump of 20 kP, the pressure loss on the valve will amount to 10.8 kP, and the heating system 9.2 kP. The calculated thermal power of heating system, 152407 W. The average thermal power of the heating device 1800 W, their amount $\boldsymbol{N} = 85$ units. The average permeability thermostatic valves $k_V = 0.188$, which roughly corresponds to the level configuration 4 ($k_V = 0.2$). By using preset perform hydraulic linkage heating system. In real conditions, these actions are accompanied by changing the position of valve stem.

The coefficient of permeability valve in the open position is selected when it calculation. The coefficient of permeability valve in the closed position can be taken as standard leakage $k_{VC} = 0.0005 \cdot 0.9$. Equation (2.30) can determine the position of the rod preset valve in the open state:

$$0.188 = (0.6)^h(0.0005 \cdot 0.9)^{1-h} \tag{2.57}$$

from where the initial position of the rod $h = 0.839$. Therefore, real zone proportional valve will be reduced – $Xp = 0.839 \cdot 2 = 1.678$°C. The minimum temperature at which the valve starts to close specified at level +18°C. Considering Xp the valve fully closes at a temperature 18 + 1.678 = 19.678°C.

Initial data for thermal point. The calculated temperature in the supplying pipeline of thermal network 115°C. Temperature mode of heating system 95–70°C. The estimated coefficient mixing:

$$u = \frac{t_{1TN} - t_{1SH}}{t_{1SH} - t_{2SH}} = \frac{115 - 95}{95 - 70} = 0.8 \tag{2.58}$$

Estimated loss of heat carrier in the heating system 2.376 m^3/h. Estimated loss heat carrier in heat network, m^3/h:

$$G_{TN} = \frac{G_{SH}}{1+u} = \frac{2.376}{1+0.8} = 1.32 \qquad (2.59)$$

The estimated differential pressure in heat chamber of thermal network 0.49 bar. Calculated pressure loss on the pipelines of thermal network 0.05 bar. Calculated pressure loss on metering unit 0.15 bar. Calculated pressure loss in the heating system 0.092 bar. Calculated pressure loss in the radiator thermostats 0.022 bar.

The valve temperature controller in ITP elect its permeability

$$k_{V2K} = \frac{G_{2K}}{\sqrt{\Delta P_{2K}}} = \frac{1.32}{\sqrt{0.49-0.15-0.05}} = 2.45 \qquad (2.60)$$

Applied the saddle control valve VS2 with a coefficient of permeability 2.5 with a nominal diameter of 20 mm. The valve has a linear expenditure characteristic (the real characteristic of valve is combined linear-linear). With the constant pressure in the heat chamber authority of valve is high enough $a = (0.49 - 0.2)/0.49 = 0.59$.

Return valve select on its permeability in mode the full recycling heat carrier in the heating system:

$$k_{VRV} = \frac{G_{RV}}{\sqrt{\Delta P_{RV}}} = \frac{2.376}{\sqrt{0.05}} = 10.6 \qquad (2.61)$$

Applied of return valve with a coefficient of permeability of 12 and nominal diameter of 25 mm.

The pump is select on spending 2.376 m^3/h and pressure loss $0.05+0.092+0.022=$ 0.164 bar or 1.64 mm.w.c. According the catalog [33] choose the pump with wet rotor Wilo-Star-RS 30/4 that operates at top speed. The characteristic point of its hydraulic characteristics H_1 = 3.5 mm.w.c., G_1 = 0.7 m^3/h; H_2 = 2.0 mm.w.c., G_2 = 2.0 m^3/h; H_3 = 0.9 mm.w.c., G_3 = 3.0 m^3/h. Approximation coefficients: $A = 0.434$, $B = -0.1217$, $C = -0.002341$.

For work automatic regulator program delivery of heat in ITP asked the following parameters: zone of proportional 3; constant of integration 120 s; coefficient of influence of temperature indoor air 99.

Initial data for the description of heat network with a source of heat: the calculated loss heat carrier in the heat source 132 m^3/h, the loss of pressure in areas of heating main from network pumps to points *C-D* 3 bar, calculated differential pressure of network pumps 3 + 0.49 = 3.49 bar. Console pumps Wilo-VeroNorm-NP 100/315V with the diameter of of the work wheel 326.7 mm on revs 1450 re/min. The characteristic point of its hydraulic characteristics H_1 = 37 mm.w.c., G_1 = 1 m^3/h, H_2 = 36 mm.w.c., G_2 = 150 m^3/h, H_3 = 28.5 mm.w.c., G_3 = 250 m^3/h. Approximation coefficients: $A = 3.7$, $B = 3.47 \cdot 10^{-3}$, $C = 2.74 \cdot 10^{-5}$.

2.4. THE RESULTS OF MATHEMATICAL EXPERIMENTS AND THEIR ANALYSIS

2.4.1. The research cooling mode

The period of cooling housings is the main source of energy saving in conditions program tempering of heat. The longer this period the lower the temperature of the internal environment of premises by greater economic effect can be achieved.

Consider the process of cooling housings academic building No. 9 Poltava National Technical Yuri Kondratyuk University at various outdoor temperatures – Figure 2.6.

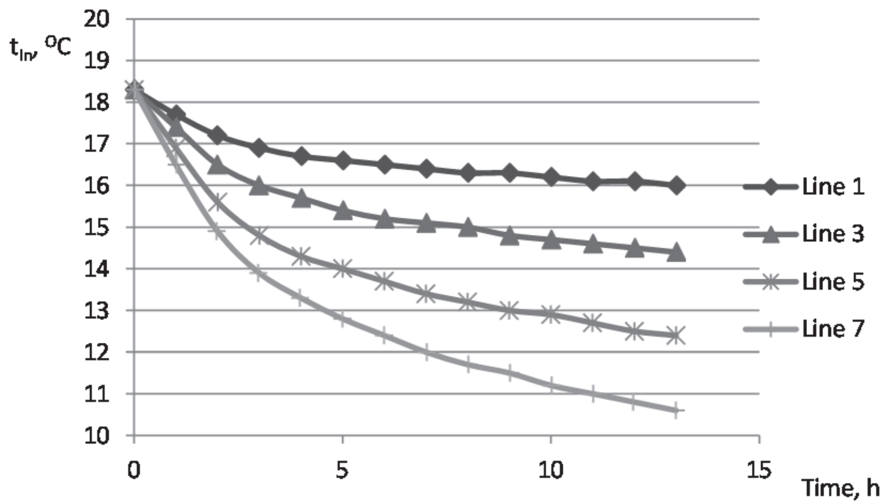

Figure 2.6. The cooling of internal air of buildings in mode night temperature decrease in working days at different outdoor temperatures; line 1: t_3 = +8°C; line 3: t_3 = 0°C; line 5: t_3 = –5°C; line 7: t_3 = –20°C

Investigation of the process cooling the heated premises brick building with massive building envelope indicates the two modes with different speed transient thermal processes. The rapid decrease air temperature characteristic of irregular temperature regime [34]. During this mode is observed intensive cooling of heating system, air environment in building and the directions heat flows may vary. The duration of this regime does not depend on outside air temperature and of the building is approximately 3 hours.

After completion of the irregular temperature regime cooling process significantly slows down heat flow directions remain unchanged, and the building becomes regular cooling mode. During regular regime cooling rate room is determined by heat exchange processes in internal and external enclosure. Comparison of cooling rates between these two modes shows that the rates of cooling indoor air during irregular regime about 4.5 times the speed of cooling in the regular mode.

Another important aspect is the much dependence "depth" of cooling on outside air temperature. Low speed transient processes, especially at relatively high outdoor temperatures, a factor which significantly limits the energy saving when program tempering of heat. So to improve the energy saving effect is necessary to reduce heat accumulating capacity of massive building envelope.

2.4.2. Determining necessary supply of area of a surface of heating system for work of program regulation

The duration of daily internal air of cooling buildings is limited to duration of the period heating housings before beginning work. To make heating housings before beginning work is needed additional thermal power of heating system. In the conditions of district heating is not possible to use higher settings coolant (increase loss, raise the temperature in supplying pipeline district heating system). Therefore, the main means of increasing the the thermal power of heating system is to increase the area of heat exchange surface.

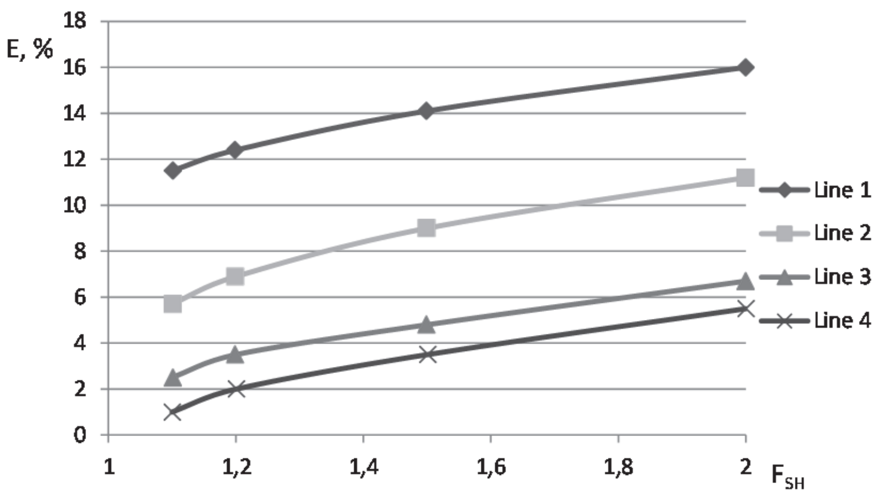

Figure 2.7. The dependence of relative energy saving effect (E) of the software controlling the increase in area of a surface of heating system (F_{HS}) at different outdoor temperatures; line 1: +8°C; line 2: 0°C; line 3: –10°C; line 4: –20°C

The results of modeling of the influence increasing area of a surface of heating system (F_{HS}) on the energy-saving effect at program lowering the temperature inside air in heated premises shown in Figure 2.7. Energy saving effect (E) defined relative to the calculated loss heat building for the relevant temperatures of external air.

As seen from Figure 2.7, energy-saving effect of night low temperature internal air housings increases with area of heat exchange surface of heating system. At increase outside air temperature the share saved of heat is increasing, but the thermal power of heating system decreases. For eliminate the effect of variable outside air temperature calculated average annual energy saving effect (E_p) – Figure 2.8.

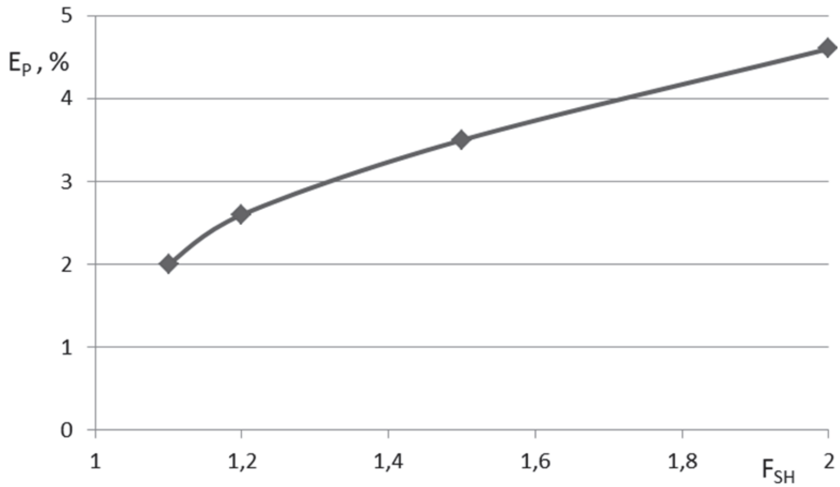

Figure 2.8. The average annual energy saving effect of the program regulating by increasing the area of a surface of heating system

The results show that increasing area of a surface the heating system (in this case of radiator) leads to a steady increase in average annual energy saving effect. On the other hand it will increase the cost of the heating system.

The relatively low value of economy of power resources (2÷5%) related primarily to the short duration of cooling regime of rooms and a large duration of the period heating housings before beginning work. The reason for this is the large heat accumulating capacity of massive building envelope.

Results of the study heating of housings before beginning work, Figure 2.9 demonstrates the:

- its relatively large duration 6÷14 hours,
- inversely-proportional dependence on the area heat exchange surface of heating system,
- depending on the outside temperature.

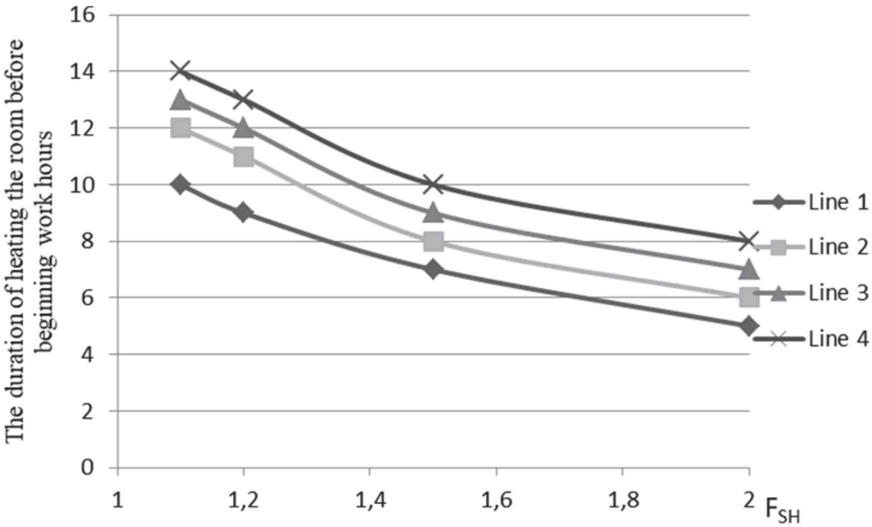

Figure 2.9. The duration of the heating room before starting work at different outdoor temperatures; line 1: $t_3 = +8°C$; line 2: $t_3 = 0°C$; line 3: $t_3 = –10°C$; line 4: $t_3 = –20°C$

The calculations show that the duration of heating the room before starting work during the heating period should changed with changes in outside air temperature. In particular, for this building period the heating premises before starting work is necessary to increase by 1 hour every 10°C of temperature decrease the outside air.

The modern weather-dependent of controls tempering heat such functions are not.

Knowing the cooling period (Figure 2.10) can determine the theoretical average annual energy saving effect, %:

$$E_{TES} = \frac{100}{N_O}\frac{\tau_O}{24}\sum\left(1-\frac{t_{In}^N - t_3}{t_{In}^D - t_3}\right)\frac{t_{In}^D - t_{OUT}}{t_{In}^D - t_{OUTC}}N_{t_{OUT}} \quad (2.62)$$

where: N_O – duration of heating period, hour; τ_O – duration of cooling, hour; t_{In}^N – "night" internal air temperature, °C; t_{In}^D– "day" internal air temperature, °C; $N_{t_{OUT}}$ – duration of period "standing" outside air temperature, hour; t_{OUTC} – calculated temperature of outdoor air, °C; t_{OUT} – outdoor air temperature, °C.

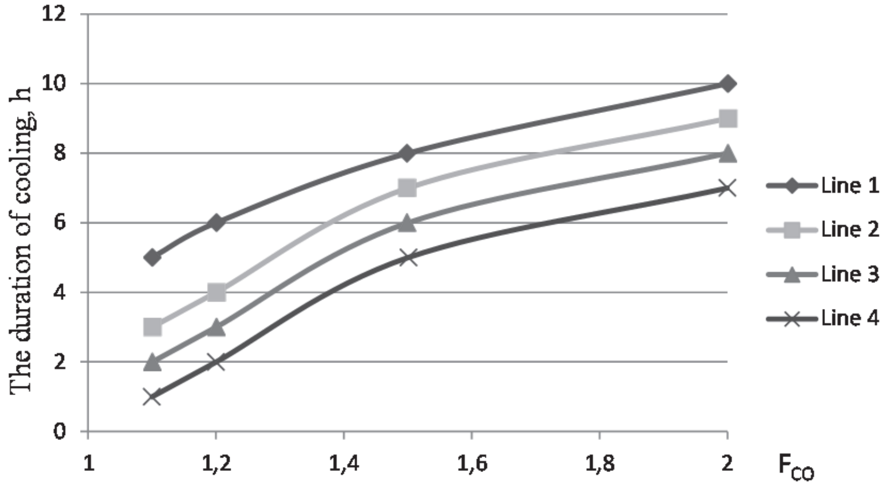

Figure 2.10. The duration period of cooling at different outdoor temperatures; line 1: $t_3 = +8°C$; line 2: $t_3 = 0°C$; line 3: $t_3 = –10°C$; line 4: $t_3 = –20°C$

Comparing the experimental values of energy saving effect (Figure 2.8) to the theoretical (Figure 2.11) can determine the effectiveness of the program tempering heat in this building – Figure 2.12.

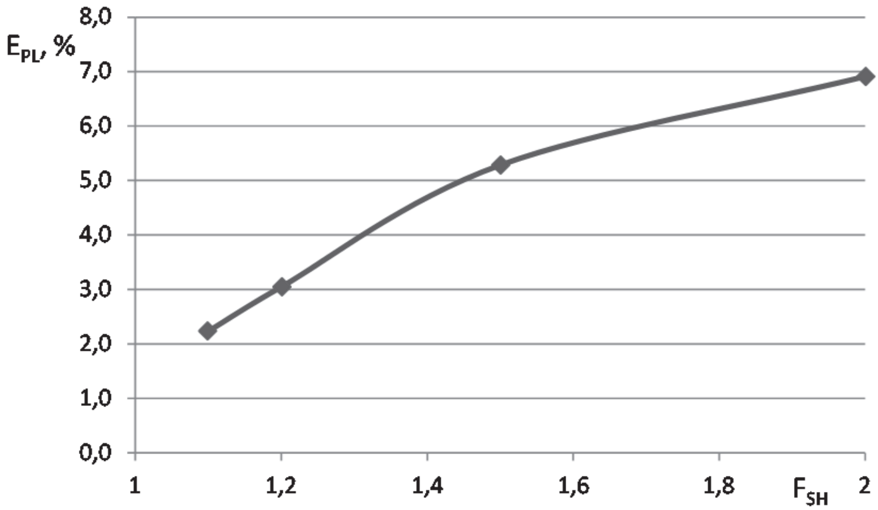

Figure 2.11. The theoretical annual energy saving effect from program tempering of heat

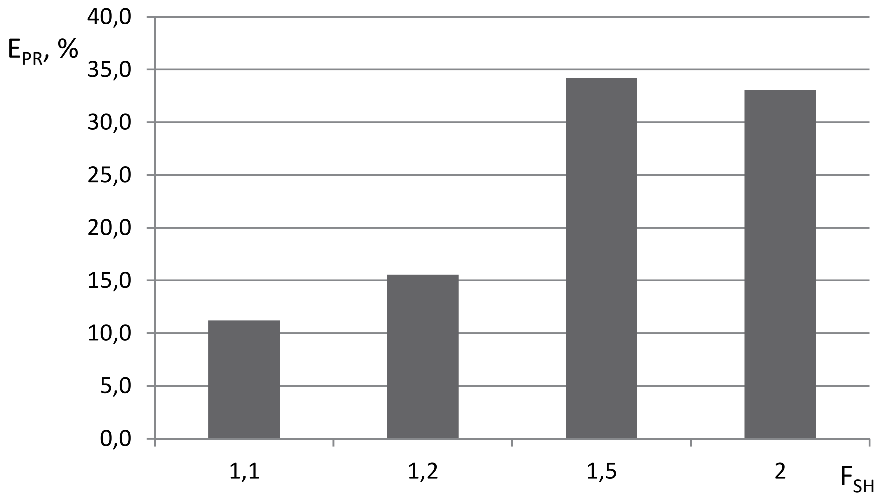

Figure 2.12. The efficiency of program tempering of heat

For efficiency calculations program tempering of heat in nonisolated buildings with massive enclosing at best 34%. However, to obtain it necessary to increase the area of heat exchange surface of heating system at least 1.5 times. A further increase in the area of heating system leads to the need to combat excessive heating housings during working hours and efficiency of this energy-saving measure decreases.

2.4.3. Thermal and hydraulic mode of heating system at program tempering heat

Increasing the area of a surface of heating system will increase its the thermal power and reduce the temperature in the supplying and the return pipeline heating system. In addition, the reduced heat consumption in heating network and its temperature in the return pipeline. By means of system heat balance equation can calculate the thermophysical characteristics of heating system while increasing its surface area.

The results of calculation the thermal power of heating system on condition fixed costs heat carrier shown in Figure 2.13. Obviously, the thermal power of heating system increased is not proportional to the increase area of surface heating devices. Especially small effect is observed at high calculation parameters heat carrier in heat network.

When using automated ITP is also possible the increase of power of heating system due to reduction in the mixing. In this case, the coolant temperature in the supplying the pipeline is maintained equal to the calculated, and the loss heat carrier are reduced. The results of calculation the work of heating system at a constant temperature heat carrier in the supplying the pipeline shown in Figure 2.14.

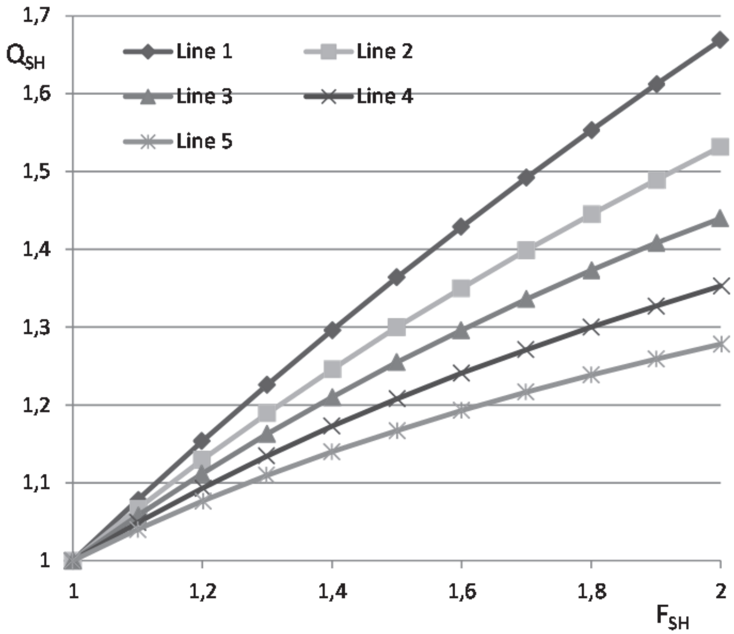

Figure 2.13. Increasing the the thermal power of heating system with constant heat consumption; line 1: 95–70°C; line 2: 105–70°C; line 3: 115–70°C; line 4: 130–70°C; line 5: 150–70°C

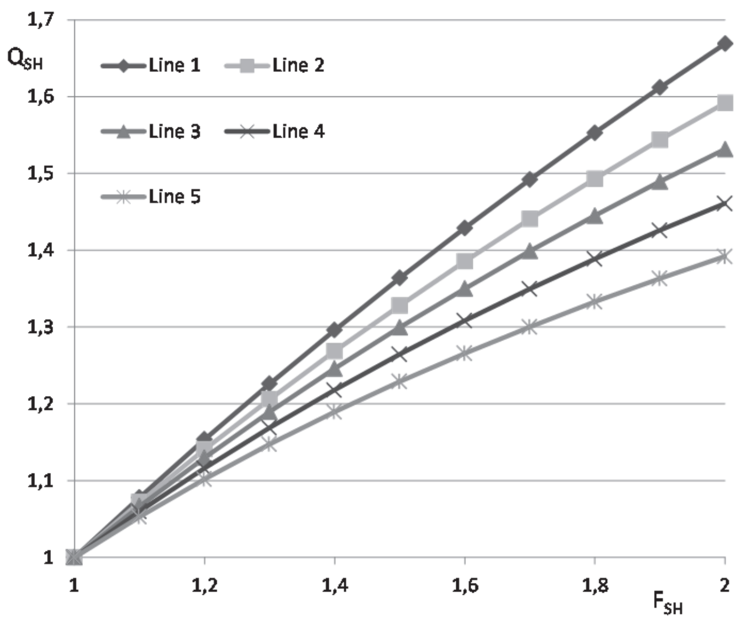

Figure 2.14. Increasing the the thermal power of heating system while reducing the coefficient mixing; line 1: 95–70°C; line 2: 105–70°C; line 3: 115–70°C; line 4: 130–70°C; line 5: 150–70°C

Comparison of results of calculation Figures 2.13 and 2.14 shows significant advantage regulating in mode of heating housings before beginning work on maintaining maximum design temperature heat carrier in the supplying the pipeline of heating system. Besides increasing the the thermal power of heating system, this method can reduce the temperature of heat carrier in the return pipe heating network (Figure 2.15) and the loss of heat carrier in the heating system (Figure 2.16).

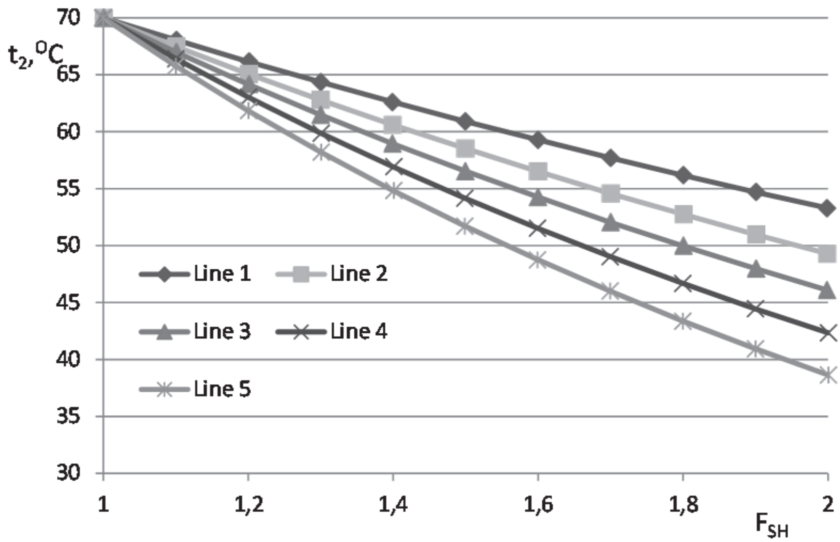

Figure 2.15. The temperature in the return pipeline of heating system with decreasing the coefficient mixing; line 1: 95–70°C; line 2: 105–70°C; line 3: 115–70°C; line 4: 130–70°C; line 5: 150–70°C

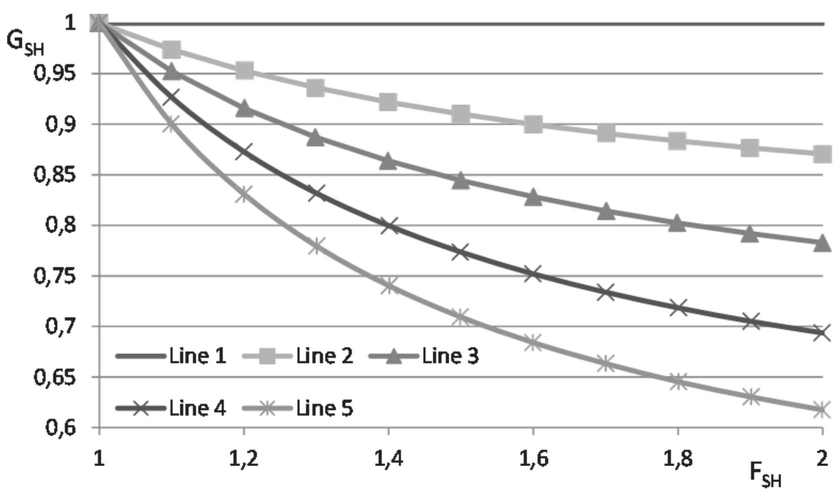

Figure 2.16. The loss heat carrier in the heating system while reducing the coefficient mixing; line 1: 95–70°C; line 2: 105–70°C; line 3: 115–70°C; line 4: 130–70°C; line 5: 150–70°C

Figures 2.13–2.16 built for regime of heating housings before beginning work. In the period operating mode of the heat power of heating system is gradually approaching its calculated thermal capacity. This is achieved by the work of the regulator in ITP, which reduces the supply of heat carrier heating network and increases the coefficient mixing. For the calculation of this mode, the relative thermal power of heating system can be taken $Q_{SH} = 1$. Results of calculation of the temperature heat carrier in the supplying and return pipelines of heating system for the "working" regime of heating system shown in Figure 2.17.

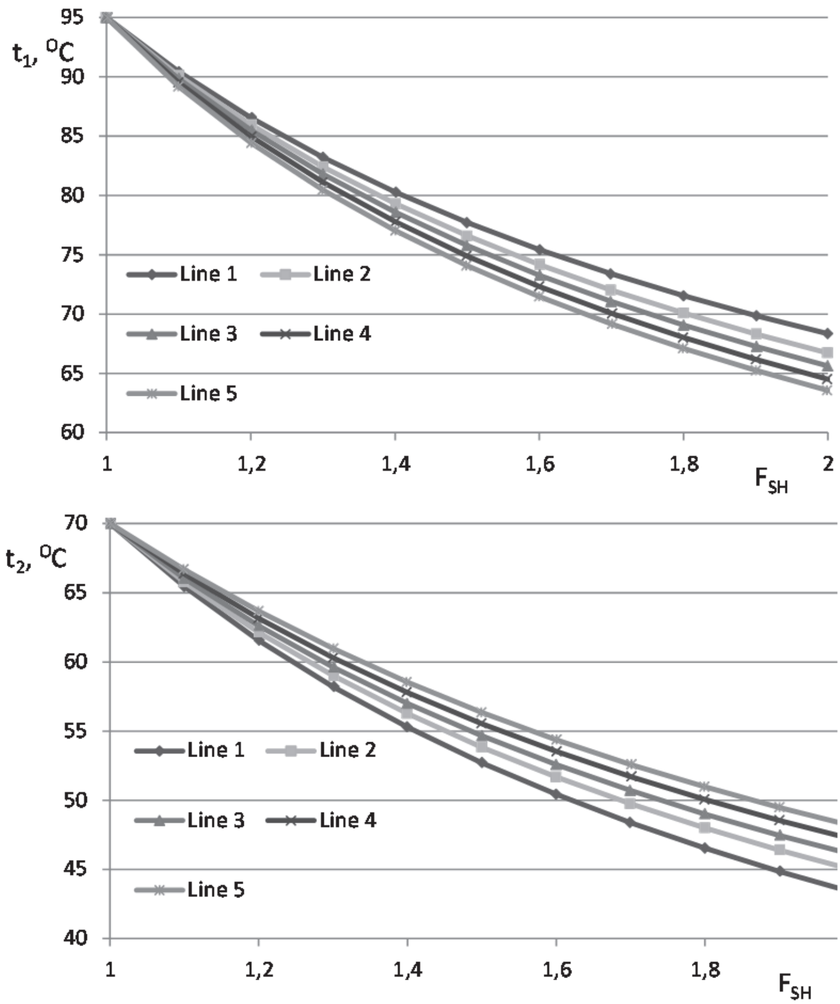

Figure 2.17. The temperature of heat carrier in the supplying (t_1) and return (t_2) pipeline of heating system during working hours; line 1: 95–70°C; line 2: 105–70°C; line 3: 115–70°C; line 4: 130–70°C; line 5: 150–70°C

In the operating mode of loss heat carrier and its temperature in the return pipeline heating network decreases – Figure 2.17. When used dependent scheme in ITP temperature decrease in the return pipe of heating system will result in a similar temperature decrease in the return pipe heating network. If the source of heat is HEC – this has positive impact on the efficiency of producing electrical energy. Moreover, reducing the temperature in the return pipe of heating system can reduce heat loss in heat networks in the environment. The negative aspect of this regulation is hydraulic dis-regulating in heating network.

Increase area heat exchange surface of heating system is additional capital cost. However, it is important not just to increase the number heating devices but also to find out which devices are more economical in conditions transient thermal processes.

2.4.4. The research of work of the various systems of heating in a mode of heating the room before starting work

Ratio radiation and convective component of heat flow from heating appliances of heating system significant effect on microclimate of premises and the thermal sensation of people. It is known that increasing the infrared component of the heat flow increases the comfort level in the room. However, increasing the convective component leads to a reduction in heat loss through the exterior envelope of the building. For various heating devices convective component of heat flow is: flat panel warming – 50÷55%, two-column of cast iron radiators 55÷60%, aluminum, bi-metal and steel radiators 60÷65%, convectors with casing of approximately 95%.

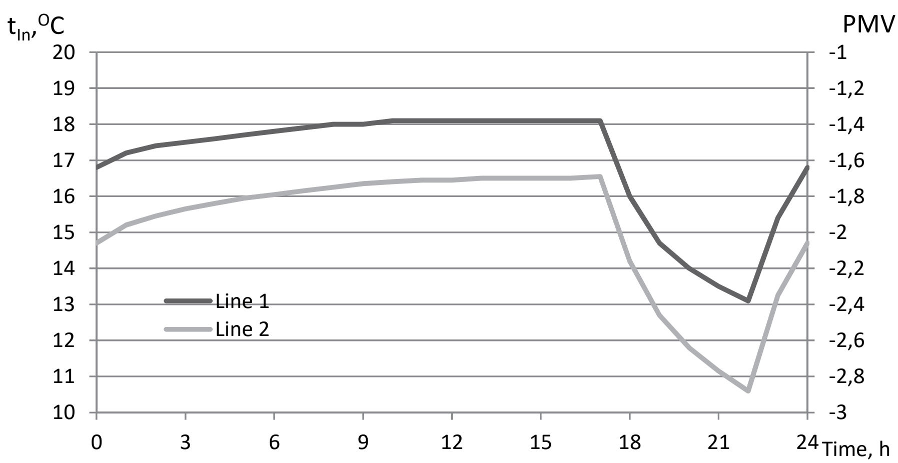

Figure 2.18. The thermal mode and thermal sensation at program tempering of heat; line 1 – internal air temperature, °C; line 2 – index of comfort (PMV)

Results of calculation of temperature regime room at night lowering the air temperature is shown in Figure 2.18. Heating devices – sectional cast iron radiators. The calculation performed at the outdoor temperature –23°C (calculated temperature). The calculation results for the heater in similar conditions shown in Figure 2.19.

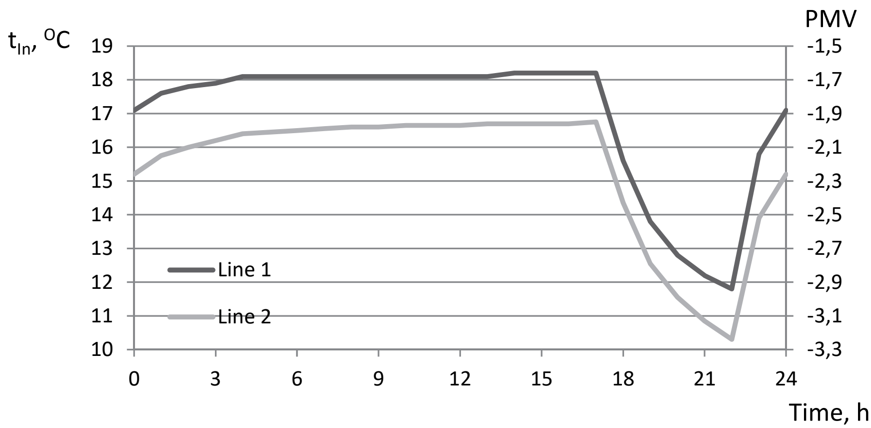

Figure 2.19. The thermal mode and thermal sensation at program tempering of heat; line 1 – internal air temperature, °C; line 2 – index of comfort (PMV)

For evaluation impact of the type of heating devices on the room temperature we held digital experiment. Imitation application of various heating devices was achieved by changing the ratio between the convective and radiation component of heat flow from the heating system. The calculations made for different temperatures of external air. The calculation results are shown in Figure 2.20.

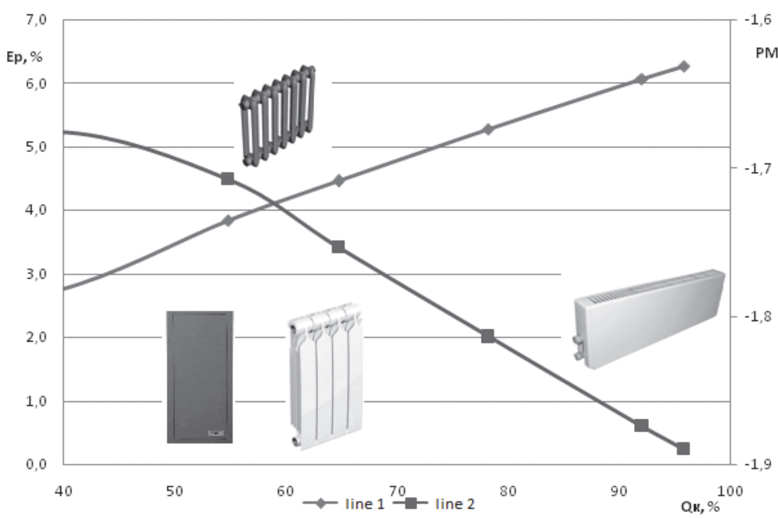

Figure 2.20. Effect of different heating devices; line 1 – annual energy saving effect, %; line 2 – index of comfort (PMV)

Analysis of the results indicates the expediency of application convectors for office type housings. Thus there is a maximum energy saving effect at allowable of microclimate parameters. In residential buildings where the priority highest level of comfort, should be used bimetal radiators.

2.4.5. The research of work radiator thermostats in conjunction with automated ITP

It is known that the scheme of regulation in ITP with reverse valve on the mixing pipeline is sensitive to changes in pressure in heat network [22]. Because from the heat network is recommended to install the valve – pressure stabilizer. Also in [21] observed necessity of application of pump with adjustable number rotations for optimum the work of the scheme. However, issues of interaction of hydraulic conditions in ITP with work of radiator thermostats in literary sources highlighted enough. In order to determine this issue a number of digital experiments. The results of research influence the position of rod radiator thermostat (h_r) and 2-way valve in ITP (h_{ITP}) on the relative heat dissipation of heating system shown in Figure 2.21.

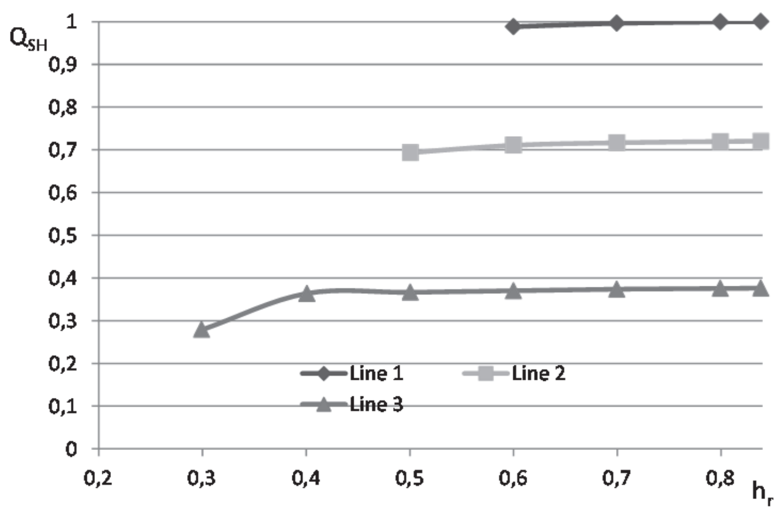

Figure 2.21. The relative thermal power of heating system at closing radiator thermostats (h_r) and the initial position of the rod regulator in the ITP; line 1: $h_{\mathrm{ITP}} = 1$; line 2: $h_{\mathrm{ITP}} = 0.5$; line 3: $h_{\mathrm{ITP}} = 0.2$

The calculation results show that at a certain point to automation in ITP “did not notice” closing radiator thermostats. Thermal power of heating system practically does not changes. Closing the radiator thermostats lower left border causes oscillatory process valve in ITP.

So we can conclude the following. Achieving stable operation of the said regulation in ITP is possible only with fixed costs heat carrier in the heating system. This can be achieved in two ways:

a) the use of heating systems with constant loss heat carriers;
b) stabilized differential pressure at the outlet of the heat point by setting the relief valve between the supplying and return pipelines heating system.

In the first case, you can use 3-way thermostats with bypass of heat carrier outside of the heating device or use of fan coil units or electric heaters. In the second – should be set quite expensive pressure regulator at the outlet of the heat point.

Recommended to install pump with adjustable the number of rotations ensures a constant differential pressure but does not provide fixed costs heat carrier in the heating system. Therefore its use in this scheme can not be considered justified. In any case, the work of individual means of regulating leads to disruption of the temperature regime of thermal point and temperature controller must immediately respond by reducing loss heat carrier with heating network.

2.5. CONCLUSIONS

1. One of the ways to improve the energy-saving effect of the program regulation is to reduce of heat accumulating capacity of the building envelope.
2. Application program tempering of heat in district heating systems needs to increase heat transfer area of heating system by about 50%. Smaller values of excess space (when installing radiator thermostats recommended 15%) do not give a significant energy saving effect. The increase in area of a surface of heating system more than 50% (recommended SBN) does not increase energy saving effect through the emergence of overheating the room before starting work during working hours.
3. In calculating the automatic of heating systems should focus on the maximum temperature heat carrier in the supplying pipeline. The temperature in the return pipeline and the loss of heat carrier should be calculated taking into account the additional increase in the area of the heating system and temperature schedule of heat source.
4. To improve the efficiency program tempering of heat in office premises is better to use heaters. For residential housings better suited sectional radiators.
5. Work radiator thermostats is able to break the hydraulic regime node mixing of coolant in the ITP. For the avoidance this phenomenon expenses coolant through the circulation pump should be permanent.

REFERENCES

[1] Markus T.A., Morris E.N., *Buildings, climate and energy*, ed. by N.V. Kobyshevoj, L: Gidrometeoizdat, 1985, p. 541.

[2] Bonhidi L., *The thermal indoor climate*, ed. by V.M. Beljaeva, V.I. Prohorova and A.L. Naumova, M: Strojizdat, 1981, p. 248.

[3] Gubernskij U.D., Lickevich V.K., *Housing for man*, M: Strojizdat, 1991, p. 227.

[4] Bogoslovskij V.N., Skanavi A.N., *Heating*, M: Strojizdat, 1991, p. 735.

[5] Tihomirov K.V., Sergeenko E.S., *Heat engineering. Heat and gas supply and ventilation*, M: Strojizdat, 1991, p. 480.

[6] Pyrkov V.V., *The hydraulic regulation of heating and cooling systems: theory and practice*, K: II DP "Taki spravi", 2005, p. 304.

[7] *Recommendations for use of bimetallic sectional radiators* "Armat bimetal", M: OOO Vitaterm, 2004, p. 36.

[8] Zinger N.M., Bestolchenko V.G., Zhidkov A.A., *Improving the efficiency of heat points*, M: Strojizdat, 1990, p. 188.

[9] Manjuk V.I., Kaplinskij J.I., Hizh E.B., Manjuk A.I., *Handbook of adjustment and operation of the water heating networks*, M: Strojizdat, 1982, p. 217.

[10] Sokolov E.A., *Thermofication and heat networks: textbook for high schools*, 7th ed, M: publishing house MEI, 2001, p. 472.

[11] Varfolomeev U.M., Kokorin O.J., *Heating and heating networks: the textbook*, M: INFRA-M, 2006, p. 480.

[12] Shhegolev M.M., Gusev U.L., Ivanova M.S., *Boiler systems*, M: Strojizdat, 1972, p. 384 .

[13] Deljagin G.N., Lebedev V.I., Permjakov B.A., Havanov P.A., *Heat-generating installations: textbook for universities*, 2nd ed., Revised and Additional, M: OOO ID "Bastet", 2010, p. 624.

[14] ISO 7730:2005(E) Ergonomics of the thermal environment – Analytical determination and interpretation of thermal comfort using calculation of the PMV and PPD indices and local thermal comfort criteria. Geneva: ISO, 2005, p. 52.

[15] Martinson L.K., Malov U.I., *Differential equations of mathematical physics*, Publisher MSTU. N.E. Bauman, Moscow 2002, p. 368.

[16] Kuznecov G.V., Sheremet M.A., *Difference methods for solving the thermal conductivity: textbook*, TPU, Tomsk 2007, p. 172.

[17] Bogoslovskij V.N., *The building of thermal physics (thermophysical basics of heating, ventilation and air conditioning): textbook for universities*, 2nd ed., rev. and add. M: Vyssh. shkola, 1982, p. 415.

[18] Skanavi A.N., Mahov L.M., *Heating*, M: ASV, 2002, p. 576.

[19] Vitalev V.P., Nikolaev V.B., Seldin N.N., *Operation of heating units and heat consumption systems: textbook*, M: Strojizdat, 1988, p. 623.

[20] *The use of automation Danfoss, in thermal point of district heating systems of buildings: handbook*, M: OOO "Danfoss", 2013, p. 62.

[21] Pyrkov V.V., *Modern heating point. Automation and regulation*, K: II DP "Taki spravi", 2008, p. 252.

[22] Pokotilov V.V., *Control valves automated heating and cooling systems*, Herz Armaturen, Vienna 2010, p. 176.

[23] Chistovich S.A., *Automatic control of heat consumption in heat supply systems and heating systems*, L: Strojizdat, 1975, p. 160.

[24] Stroj A.F., Skalskij V.L., *Calculation and designing of heating networks*, K: Budivelnik, 1981, p. 144.

[25] Kutnyi B.A., *Automated elevator heating point for district heating systems. Materials 1st Intern. scientific-prakt. konf. Collection of scientific papers Transportuvannja, kontrol jakosti ta oblik energonosiïv*, State University "Lviv Polytechnic", Lviv 1998, pp. 20–26.

[26] SNiP II-35-76 Boiler systems. Reissued with changes. Ukrarhbudinform, Kyiv 2006, p. 43.

[27] On approval of rules of technical operation of thermal equipment and networks: Ministry of Fuel and Energy of Ukraine, No. 71, 14.02.2007 with changes No. 183 from 27.03.2015.

[28] Demidovich B.P., Maron I.A., Shuvalova E.Z., *Numerical methods of analysis*, M: Fizmatgiz, 1963, p. 400.

[29] Kutnyi B.A. *Unsteady thermal mode of heating system of the building in conditions quantitative regulations. Collection of scientific papers (galuzeve mashinobuduvannja, budivnictvo)*, Poltava National Technical Yuri Kondratyuk University, PoltNTU, Poltava 2004, Issue 14, pp. 113–116.

[30] Kutnyi B.A., *The heat mode of heating system the building in conditions of quantity and quality regulation. Collection of scientific papers (galuzeve mashinobuduvannja, budivnictvo)*, Poltava National Technical Yuri Kondratyuk University, PoltNTU, Poltava 2005, Issue 15, pp. 177–181.

[31] SBN B.2.5-67:2013. Heating, ventilation and air conditioning, K: Ukrarhbudinform, 2013, p. 141.

[32] SBN B.2.6-31:2006 Thermal insulation of buildings. K: Ukraine Ministry of Construction, 2006, p. 70.

[33] Wilo catalog on equipment for the buildings and structures 2013/2014. Pumps, pumping stations and accessories for heating systems, air conditioning, refrigeration, 2013, p. 679.

[34] Stroj A.F., *Thermal management of buildings and structures*, K.: Vishha shk., 1993, p. 155.

Chapter 3

ENERGY SAVINGS IN HEAT SUPPLY SYSTEMS USING SOLAR ENERGY

Viktoriia V. Dubrovska, Victor I. Shklyar

National Technical University of Ukraine "Igor Sikorsky Kyiv Polytechnic Institute"
Institute of Energy Saving and Energy Management

3.1. ENERGY SAVINGS IN HEAT SUPPLY SYSTEMS USING SOLAR ENERGY

Today, more and more attention has been paid to providing humanity with energy. About 90% of currently used energy resources are non-renewable (coal, oil, natural gas, uranium, etc.) energy sources due to their high energy potential, relative availability and feasibility of production.

Considering the technical possibilities of organic fuel extraction and the rate of their expenditure due to the increased energy consumption, the estimation of organic fuel reserves on the planet shows their limited availability. Especially it concerns oil, gas, high-quality coal, which are valuable chemical raw material and burning them as fuel is irrational and wasteful. The main reasons for the deterioration in the use of energy are the decline in industrial production, wear of energy-consuming and energy-generating equipment, that has reached 63–75%.

The share of energy resources in the production cost structure is constantly rising. Their share in expenses for the payment of utility bills reaches from 40% to 70% in different regions.

Combustion of large amounts of fuel in traditional power plants negatively affects the environment: pollution, changes in gas composition of the atmosphere, warming of water bodies, increase of radioactivity in Thermal power plant zones, general change in the thermal balance of the planet.

Due to increased negative impact on the environment, special attention is paid to energy that would cause the least harm to the environment. More and more scientists agree with the opinion that the future lies in alternative energy sources development, elaboration of the latest technologies, implementation of energy-efficient and energy-saving systems.

An effective energy program of the state should be aimed at reducing the use of fossil fuels while preserving the quality of existing production processes.

One of the rational ways to solve the problems of energy saving considering environmental requirements in the energy sector is introduction of alternative heat supply systems based on the integrated use of traditional and renewable environmentally friendly energy sources.

Application of solar energy for the heat supply of municipal and industrial facilities occupies an important place in the development of renewable energy in Ukraine. It is provided by the availability of a resource and technological base; climatic conditions (Figure 3.1) that allow the use of solar installations in any region of the country [1]; the experience in running a sufficient number of operating solar installations that have rather favorable payback periods.

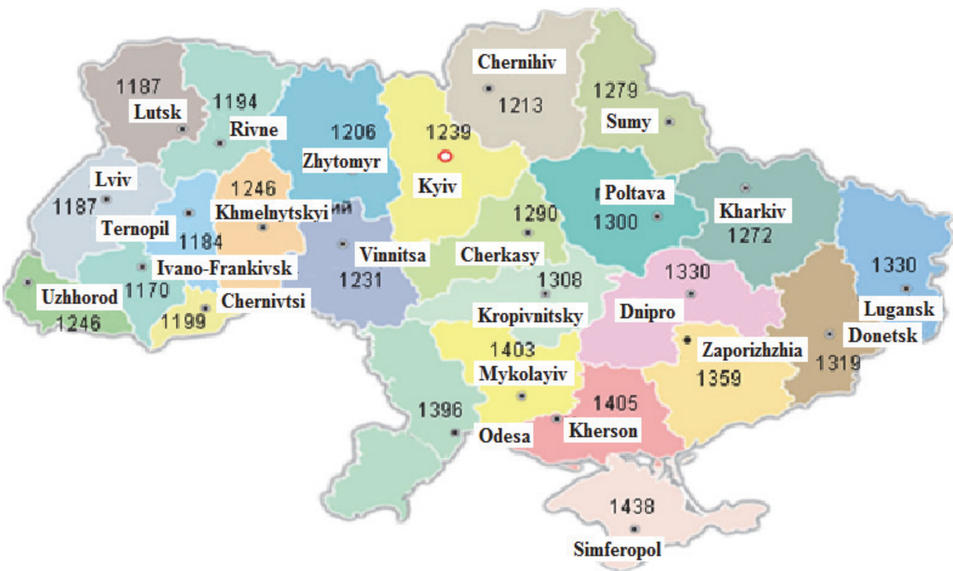

Figure 3.1. The income of solar energy on the territory of Ukraine, kW·h/m^2

The main reasons that restrain the implementation of alternative heat supply systems are high level of initial capital expenditures, daily and seasonal unevenness in energy production, and strict dependence on climatic conditions.

In order to intensify the introduction of alternative heat supply systems, it is necessary to improve their profitability by increasing the rate of substitution of organic fuel with renewable energy sources. However, this task cannot be solved only by singe renewable energy source (“mono-source”), because of cyclical change in its natural properties throughout the year, season and day.

3.1.1. Solar heat supply systems

The solar energy incoming on the territory of Ukraine enables its application in heat supply systems.

Solar heat supply systems can be classified into:

– active solar heating systems, in which are used active-type installations based on solar collectors with heat transfer agent circulation;
– passive solar heating systems, in which various structural elements and materials are used as heat receivers;
– combined solar heating systems.

With the help of modern solar collector devices (solar installations) it becomes possible to use an essential part of solar energy for the production of hot water, as well as for the use of heat in the heating system.

The main element of the active solar heating system is the solar collector (SC), in which solar energy is captured, transformed into heat and the heat transfer agent heats up. The two most common types of solar collectors are flat (Flat-Plate Solar Collector – FPSC) and glass tubular evacuated (Evacuated Solar Collector – ESC).

Increasingly, in solar Hot Water Supply (HWS) systems, vacuum solar collectors are used that perceive direct and diffused solar radiation. Due to the cylindrical shape of the tubes from which the vacuum collectors are assembled, they absorb more solar radiation, and the use of heat pipes in them enhances their efficiency and makes it possible to use the collector at low outside air temperatures (down to –35°C).

Solar HWS systems have an additional source of heat (for example, an electric heater) for providing consumers with stable supply of hot water in the absence of solar radiation.

An important indicator in determining the efficiency of solar collector is calculation of the rate of hot water supply load, which is provided by solar energy (fuel substitution rate). The substitution rate can be determined by three methods: N.V. Kharchenko [2], J. Duffy [3] and RETScreen [4].

When designing heat supply systems using solar energy it is necessary to proceed from the fact that it is economically feasible to cover only a certain share f_{year} of annual heat load Q_{load}^{year} by solar energy, and the other part, that is to say, $(1-f_{year})Q_{load}^{year}$ should be provided by an additional source of energy. The value f_{year} depends on the characteristics of the solar system and the climatic data, as well as on the cost of the system and fuel, but usually it does not exceed 0.5, and for seasonal installations it can reach 0.75 or more [5].

The degree of heat load replacement for a certain period can be determined from the equation [2]:

$$f = \frac{W}{Q_{load}} \tag{3.1}$$

where: W – heat production by a solar installation for a certain period; Q_{load} – total load of heating and hot water supply for a certain period.

Annual heat production W_{year}, kWh/year, in a solar installation is defined as the total amount of thermal energy produced in each j-th month:

$$W^{year} = \sum_{j}^{n} W_j^{\mathrm{M}} = \sum_{j=1}^{12} 10^{-3} \cdot z_j \cdot \sum_{i} q_i^K \cdot A \tag{3.2}$$

where: W_j^M, kWh/month – amount of heat generated by the solar water heater; z_j – number of days in the j-th month; A – area, m^2, of the installed solar collectors; $\sum_i q_i^K$ – sum of daily values of specific energy of radiation for j-th month.

The specific heat flow q_{Ki}, W·h/m^2, which is efficiently used in the hot water supply system every hour under real conditions of cloudiness and heat loss, is determined by the formula [2]:

$$q_i^K = q_i' \cdot \eta_K \cdot \eta_3 = q_i \cdot \eta_{\mathrm{O}} \cdot \eta_K \cdot \eta_1 \cdot \eta_2 \cdot \eta_3 \tag{3.3}$$

where: η_1 – coefficient that considers the degree atmospheric transparency, its value ranges from 0.8 in industrial areas to 1 in the resort zone. For mountain resorts $\eta_1 = 1.1$; η_2 – coefficient that considers losses caused by the non-stationary heat exchange under variable cloudiness. It is recommended to assign: $\eta_2 = 0.9$; η_3 – coefficient that considers loss of heat from solar collector to consumer. The value of this coefficient is assigned 0.85 for centralized hot water supply systems, and 0.98 for local water heaters; η_K – coefficient of solar collector efficiency, which depends on its design.

The data on dependence $\eta_K = f\,(t_K - t_O)$ must be reported by the solar collector manufacturer, where t_K is the temperature water heated in the collector, and t_O is the temperature of the air surrounding the collector [6]. In the absence of these data, it is recommended to use graphs [7] or in the range of temperature differences of 20–55°C:

– for a flat polished (selective) collector is defined from the dependence:

$$\eta_K = 0.82 - 0.005\ (t_K - t_O);$$

– for flat unpolished collector:

$$\eta_K = 0.8 - 0.0067\ (t_K - t_O);$$

– for vacuum collector:

$$\eta_K = 0.73 - 0.0025\ (t_K - t_O)$$

The temperature t_K is determined by the project and is usually assigned at 55°C.

η_O – the coefficient that considers the real conditions of cloudiness, which can be calculated by the formula:

$$\eta_O = \frac{\sum H_P}{\sum (H_B + H_D)} \tag{3.4}$$

where: $\sum H_P$ – total energy of direct and diffused solar radiation falling on a horizontal surface in a settlement per day in real conditions of cloudiness. The value $\sum H_P$ is given in climatological reference books [6, 8]; H_B and H_D – specific heat fluxes, W/m^2, of direct and diffused solar radiation, falling on a horizontal surface at latitude of a settlement with a cloudless sky [9].

The specific heat flux q'_i, W·h/m^2, received per 1 m^2 of the inclined surface of the solar collector for the *i*-th hour in real conditions of cloudiness and heat loss, is determined by the equation:

$$q'_i = q_i \cdot \eta_O \cdot \eta_1 \tag{3.5}$$

The value of the specific thermal energy q_i, W·h/ m^2, received per 1 m^2 of the inclined surface of the solar collector for the *i*-th hour on a cloudless day, is determined by the formula [5]:

$$q_i = H_B \frac{\cos(\varphi - s)\cos\delta\cos\omega + \sin(\varphi - s)\sin\delta}{\cos\varphi\cos\delta\cos\omega + \sin\varphi\sin\delta} + H_D = H_B \cdot R_B + H_D \tag{3.6}$$

where: φ – latitude of the area; ω – hour angle; R_B – coefficient of converting direct solar radiation to an inclined surface with a southern orientation; s – surface inclination angle of the solar collector to the horizon [1].

The useful energy according to the method [3], derived from the collector at the present moment of time, is the difference in the amount of solar energy absorbed by the collector plate and the amount of energy lost to the environment and is determined from the equation:

$$Q_K = AF_R\left[I_T\left(\tau\alpha\right)_n - U_L\left(t_l^{in} - t_{env}\right)\right] \tag{3.7}$$

where: A – area of the solar collector, m^2; F_R – coefficient of heat withdrawal from the collector; I_T – flux density of total solar radiation in the collector plane, W/m^2; τ – bandwidth of transparent coatings related to solar radiation; α – absorption capacity of the collector plate related to the solar radiation; $(\tau\alpha)_n$ – optical efficiency of the solar collector, determined from research with incoming solar radiation normally to the surface of the collector; U_L – total coefficient of heat loss of the collector, W/(m^2·°C); t_l^{in} – the temperature of the liquid at the inlet to the collector, °C; t_{env} – temperature of the environment, °C.

The dependence of the coefficient f on X and Y by the method [3] can be defined by the equation:

$$f = 1.029Y - 0.065X - 0.245Y^2 + 0.0018X^2 + 0.0215Y^3 \tag{3.8}$$

where: $0 < Y < 3$ and $0 < X < 18$.

Dimensionless complexes X and Y are determined from the equations:

$$X = \frac{A\,F_R\,U_L\,\dfrac{F_R'}{F_R}\left(100 - \overline{t}_{inv}\right)\Delta\theta}{Q_{load}^M} \tag{3.9}$$

$$Y = \frac{A\,F_R\left(\tau\alpha\right)_n\left(\dfrac{F_R'}{F_R}\right)\dfrac{\left(\overline{\tau\alpha}\right)}{\left(\tau\alpha\right)_n}\overline{H}_T\,z_j}{Q_{load}^M} \tag{3.10}$$

where: $\Delta\theta$ – number of seconds per month; 100 – basic temperature, °C; $\overline{t}_{inv}$ – average monthly temperature of the environment, °C; Q_{load}^M – monthly heat load for heat supply, J/month; $\overline{H}_T$ – average monthly income of the total solar radiation per day on the inclined surface of the collector, J/(m^2·day):

$$\overline{H}_T = 3.6\cdot10^3\sum_i q_i' \tag{3.11}$$

z_j – number of days in a month; $\left(\overline{\tau\alpha}\right)$ – average monthly optical efficiency of the solar collector (the absorption capacity is given); F_R' – effective coefficient of heat transfer, which allows to calculate the characteristics of the collector, taking into account the influence of the intermediate heat exchanger; $\frac{F_R'}{F_R}$ – adjustment coefficient that considers the effect of heat exchanger. It takes a value from 0 to 1 and characterizes the decrease in the collector useful energy due to the application of a two-circuit heat transfer scheme with an intermediate heat exchanger; $\frac{\left(\overline{\tau\alpha}\right)}{\left(\tau\alpha\right)_n}$ – coefficient that takes into account the orientation of the collector surface. If the inclination angle of the SC to the horizon is in the interval between (φ – 15°, φ + 15°) and its orientation differs from southern no more than by 15°, then the coefficient $\frac{\left(\overline{\tau\alpha}\right)}{\left(\tau\alpha\right)_n}$ for all months of the heating season equals 0.96 for collectors with single glass or 0.94 – with double glass. For a more precise definition of this coefficient method [4] is used.

Values $F_R\left(\overline{\tau\alpha}\right), F_R\,U_L$ are the characteristics of a SC and are provided by manufacturers.

If the thermal load consists only of the load on the HWS, then the applied method should be corrected by the introduction of adjustment coefficients.

$$\frac{X_{CK}}{X} = \frac{11.6 + 1.18 \cdot t_{HW} + 3.86 \cdot t_{CW} - 2.32 \cdot t_{inv}}{100 - t_{inv}} \tag{3.12}$$

where: t_{HW} – the temperature of hot water, is taken 55°C [10]; t_{CW} = 15°C – the temperature of cold water in summer and t_{CW} = 5°C in winter.

Calculation of the hot water supply solar systems with different collectors, determination of the degree of substitution and fuel economy and the payback period can be performed in the software environment RETScreen.

In this work, calculations of the degree of fuel substitution by the above-mentioned methods for the solar hot water supply system in Kyiv were carried out. Were studies three variants of solar system: with flat-polished; flat unpolished and vacuums collectors, which had approximately the same area of 5.5 m^2 and were installed on the southern side of the building with a sloped roof. The angle of inclination of the collectors was 45°. The system is designed to provide hot water to 4 people living in the house.

The calculations took into account the solar radiation for a given area and the accumulator tank with a volume of 0.35 m^3 [11].

Total solar radiation on a horizontal surface has different values and depends on the method of its definition (Table 3.1).

Table 3.1. Total solar radiation on a horizontal surface, J/m^2 h

	Months of the year												
	I	II	III	IV	V	VI	VII	VIII	IX	X	XI	XII	
1 [1]	1.07	1.87	2.95	3.96	5.25	5.22	5.25	4.67	3.12	1.94	1.02	0.86	3.1
2 [4]	0.84	1.55	2.58	3.73	5.26	5.71	5.46	4.69	3.23	1.86	0.81	0.57	3.03
3 [12]	2.48	4.00	6.28	8.74	10.65	11.53	11.08	9.53	7.27	4.86	2.95	2.09	6.79
4 [13]	1.58	3	4.21	6.33	7.74	8.31	7.97	6.61	5.05	3.42	1.9	1.24	4.78
5 [13]	1.54	3	4.31	6.53	8.09	8.71	8.34	6.83	5.27	3.56	1.99	1.29	4.96

As we see from Table 3.1, the difference between average statistic values and actual solar radiation income may reach more than 50%.

The efficiency of the solar collector depends on its design.

By the method of Kharchenko it is determined from equation (3.2), taking into account t_O – the average daily temperature of the air that surrounds the collector:

$$t_O = t_{AVE} + 0.3 \cdot A_t \tag{3.13}$$

where: t_{AVE} and A_t – average daily air temperature and the maximum amplitude of daily temperature fluctuations of the calculated month, are taken according to norms [6].

It is seen from equations (3.12) and (13.13) that the substitution coefficient of the Duffy method depends on the values of X and Y, which consider the characteristics of the collector $F_R\left(\overline{\tau\alpha}\right), F_R\,U_L$.

The dimensionless complex Y can be interpreted as the ratio of the amount of energy absorbed by the collector during the month to the full month's thermal load, and X as the ratio of the monthly heat loss of the collector at baseline temperature to the full month's thermal load.

By Duffy's method, the collector efficiency is determined from the equation:

$$\eta = \frac{Q_K}{I_T A} = F_R(\tau\alpha)_n - \frac{F_R U_L}{I_T}\left(t_l^{in} - t_{env}\right) \tag{3.14}$$

Comparison of the formulas for determining the efficiency of the collectors shows that according to the method [3] its value depends not only on the temperature of the environment and characteristics $F_R\left(\overline{\tau\alpha}\right), F_R\, U_L$, but also on the density of the total solar radiation in the plane of the collector. And using the method [2], the coefficient before the difference in temperature has a constant value in the range of changing from 0°C to 50°C.

From the software database of RETSrreen4 [4] were defined intervals for $F_R'\left(\overline{\tau\alpha}\right), F_R'\, U_L$ values for the different types of collectors shown in Table 3.2 and Figure 3.2.

Table 3.2. Values for different types of collectors

Type of collector	$F_R\left(\overline{\tau\alpha}\right)$	$F_R U_L$
Vacuum	0.84–1.92	0.35–0.59
Polished	3.67–8.21	0.54–0.78
Unpolished	12.36–21.31	0.76–0.87

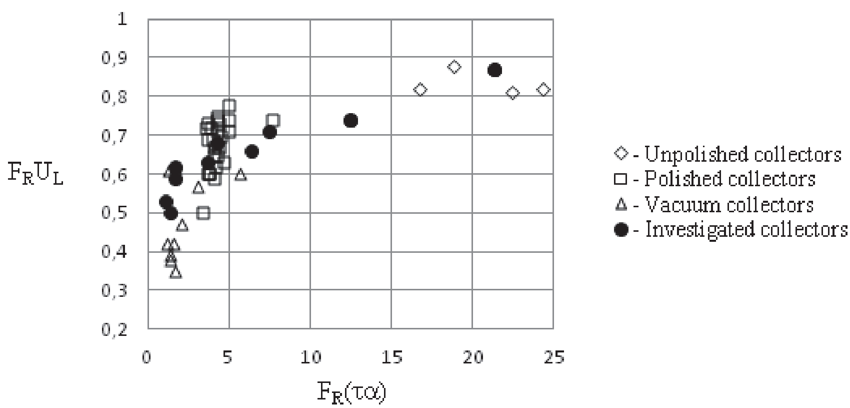

Figure 3.2. Dependence of $F_R\left(\overline{\tau\alpha}\right)$ on $F_R\left(\overline{\tau\alpha}\right)$ for different types of collectors

In order to compare the collectors of different types by method [1], was determined their area, that was compared with the area of collectors in RETScreen program. Areas of the investigated collectors are presented in Table 3.3. For visibility, values of their $F_R\left(\overline{\tau\alpha}\right)$ and $F_R\left(\overline{\tau\alpha}\right)$ are shown in Figure 3.2.

Table 3.3. Characteristics of the investigated collectors [4]

Type of collector		Kyiv	Chernihiv	Odessa	Simferopol
Vacuum	A, m^2	4.25	4.28	3.8	3.52
	$F_R U_L$	0.62	0.53	0.5	0.59
	$F_R\left(\tau\alpha\right)_n$	1.65	1.03	1.38	1.63
Polished	A, m^2	4.22	4.38	3.86	3.45
	$F_R U_L$	0.68	0.71	0.66	0.63
	$F_R\left(\tau\alpha\right)_n$	4.22	7.45	6.37	3.67
Unpolished	A, m^2	4.3	4.3	3.85	3.45
	$F_R U_L$	0.74	0.74	0.87	0.87
	$F_R\left(\tau\alpha\right)_n$	12.38	12.38	21.31	21.31

In calculations according to the method [1], were taken $\eta_1 = 0.9$; $\eta_2 = 0.9$ and $\eta_3 = 0.98$. Calculations of the annual degree of fuel substitution using solar collectors of different types for Ukrainian cities are shown in Figures 3.3 and 3.4.

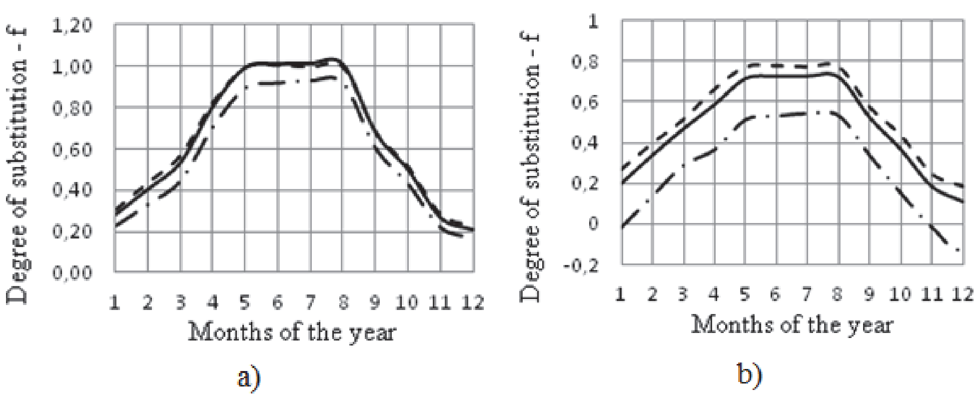

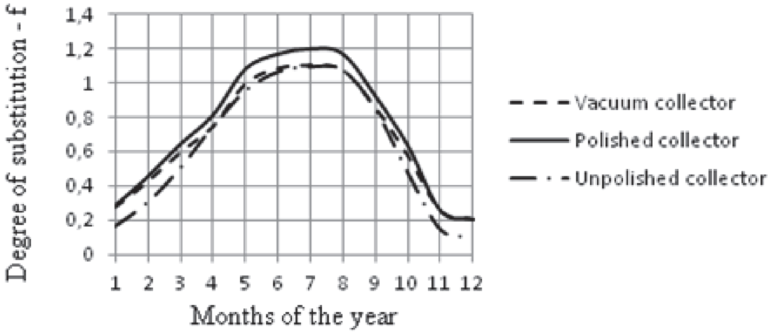

c)

Figure 3.3. Results of calculating by different methods the degree of substitution during the year for Kyiv using collectors: a) method N.V. Kharchenko [2], b) method J. Duffy [3], c) method RETScreen

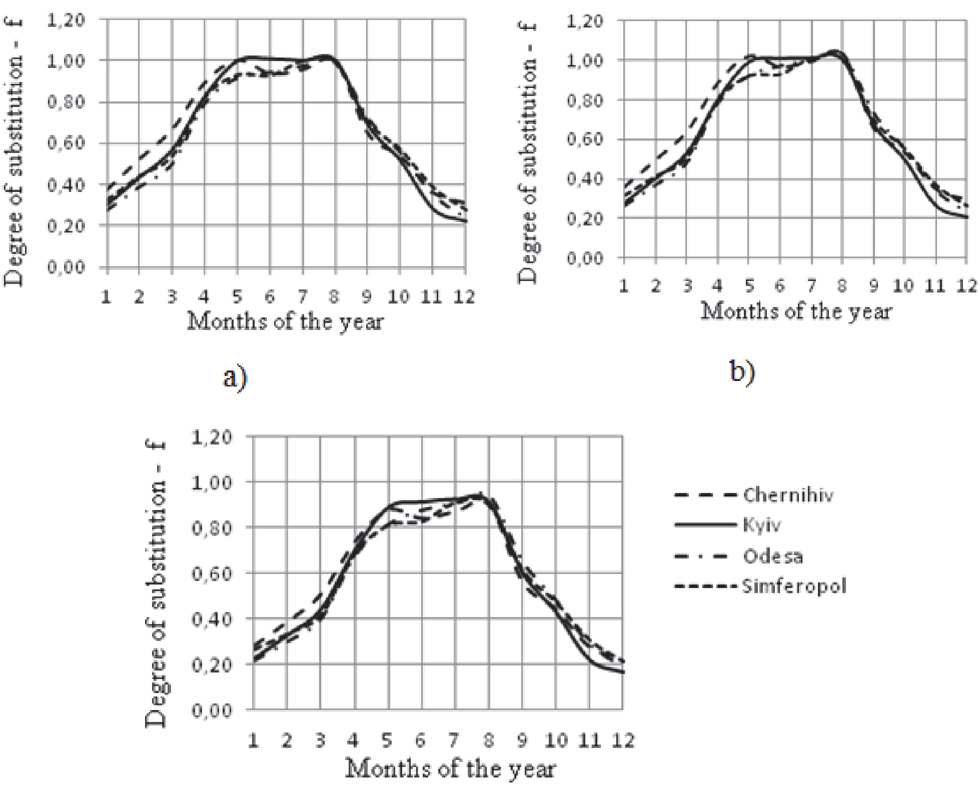

Figure 3.4. Results of calculating the degree of substitution during the year according to Kharchenko's methodology for Ukrainian cities: a) vacuum collector, b) polished collector, c) unpolished collector

From Figure 3.3 can be seen that the above methods of determining the degree of substitution present different results for the used collectors. The largest value of the degree of substitution is received by RETScreen, and the smallest by Duffy.

It should be noted that for calculations by Duffy's method for solar system with unpolished collector, the value of f acquires negative values, which is explained by imperfection of the dependence (3.8) for determination of small values of f at small Y and large X.

In Figure 3.3 and Figure 3.4 the calculated degree of substitution takes the value of more than 1, which is explained by the area of the selected collectors by the program RETScreen for comparative analysis of the use of various methods. In practice, the collector's area is selected considering the required water needs, possible area for its installation and the planned degree of substitution of heat.

The calculation of annual degree of substitution by Kharchenko's method, with taking into account the area of the investigated collectors for different cities of Ukraine, is given in the Table 3.4.

Table 3.4. Annual value of the degree of substitution calculated by Kharchenko's method for different cities of Ukraine

City	Type of collector		
	Vacuum	Polished	Unpolished
Chernihiv	0.682	0.688	0.58
Kyiv	0.653	0.642	0.566
Odessa	0.639	0.636	0.564
Simferopol	0.661	0.647	0.564

Reduction of the annual consumption of traditional fuel B, kg/year (m^3/year), using solar collectors, are found from the equation:

$$B = \frac{\sum_{1}^{n} \left(f_i \cdot \left(Q_{load}^{M} \right)_j \right)}{Q_l^W \cdot \eta_{HG}} \qquad (3.15)$$

where: Q_l^W – lower heating value of fuel (mass or volume); η_{HG} – coefficient of efficiency of the heat generator (boiler).

Annual values of the degree of substitution and the saving of organic fuel (natural gas) consumption with efficiency of the boiler 0.8 for Kyiv are displayed in Table 3.5.

Table 3.5. The value of the degree of substitution and cost savings of fossil fuels

Type of collector	Kharchenko		Duffy		RETScreen	
	f	B, m^3	f	B, m^3	f	B, m^3
Vacuum	0.653	375	0.533	306	0.66	379
Polished	0.642	368	0.472	271	0.72	413
Unpolished	0.566	325	0.38	218	0.6	344

Analysis of the analytical research shows that the use of solar water supply system with a solar collector area of 4.2 m^2 for a private house in Kyiv makes it possible to save on average from 200 m^3 to 420 m^3 of natural gas of architectural and constructive solutions of the building.

3.1.2. Passive solar heat supply systems

Passive are called those solar heating systems, in which the building itself or its separate enclosing structures serve as an element that perceives solar radiation and transforms it into heat. In passive solar systems the use of solar energy is carried out solely at the expense.

There are many advantages of including a solar heating system to the building design, the equipment for receiving heat from the Sun:

- is environmentally friendly, doesn't pollute the environment and doesn't produce greenhouse gases;
- helps to save energy resources of the Earth;
- stable in its cost;
- protects against inflation and political/economic risks that may occur when using other types of fuel.

For the heating of buildings, the following types of passive systems are used:

- with direct capture of solar radiation, that enters through a building or a greenhouse adjacent to the southern wall (winter garden, greenhouse);
- with the indirect capture of solar radiation, that is, with a heat accumulating wall, located behind the glazing of the southern facade;
- with a circuit of convective air circulation and a pebble heat accumulator.

In systems with direct heat supply the sun's rays penetrate into the heated room through the window apertures and heat up the building structures that become receivers and accumulators of heat. In such systems temperature of the room and objects surface change almost simultaneously with the change in solar radiation entering the room. Such systems are especially useful when the cycle of the heat demand coincides with the cycle of incoming solar radiation alteration. For example, such systems can be used for offices where heating is necessary during the day, but not at night.

In systems with indirect capture the solar radiation does not directly penetrate into the room, but is absorbed by a heat-receiver (protected by a translucent construction), combined with external enclosing structures, that usually are heat accumulators. Accumulated heat in accumulators (building constructions) is transferred by air to the room [5].

For design of passive solar heating system are taken into account the most general limits imposed on the system by such factors as the geographic location of the building and its purpose, size of the building, the permissible cost, necessary materials, etc. As a rule, a sketch study of several variants of the solar system is being carried out, ending with a choice of the prevailing option. After this, a detailed project is being developed and a decision is made regarding the location, size of the rooms, orientation of the building, choice of materials and the specification of all sizes.

To reduce the fuel consumption for heating, it is expedient to use a passive solar system with a Trombe wall (Figure 3.5) [14].

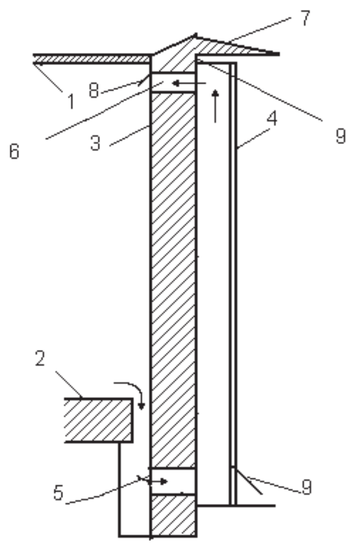

Figure 3.5. Trombe passive heating system: 1 – ceiling of the room, 2 – floor, 3 – wall made of concrete or other material, 4 – a double-glazed surface, 5 – inlet of cold air, 6 – outlet of the warm air to the room, 7 – cover from the summer sunrays, 8 – valve, 9 – ventilation valve

The heat of solar radiation that enters into the room through the glazing by a unit of the outer absorbing surface of the heat sink wall of the PSH system during each estimated month, MJ/m^2 [15]:

$$q_{ABS} = K_W \cdot K_G \cdot \beta_{SD} \cdot [(\tau\alpha)_s P_s f_s K_{\mathrm{INS}} S' + (\tau\alpha)_d P_d f_d K_{\mathrm{CL}} D + r(\tau\alpha)_r P_r f_r (S' + D)] \tag{3.16}$$

where: K_W – coefficient that considers the influence of window frames ($K_W = 0.9 – 0.97$), with smaller values for wooden frames, and larger for metal ones; K_G – coefficient that considers the glass pollution: $K_G = 0.9^n$, where: n – number of layers of glazing, accepted $K_G = 0.81$; β_{SD} – thermal transmission coefficient of sunshade devices, accepted $\beta_{SD} = 1$ [15]; $(\tau\alpha)_s = 0.834$, $(\tau\alpha)_d = 0.834$, $(\tau\alpha)_r = 0.834$ – given absorption capacity for direct, diffuse and reflected radiation, respectively. Calculated according to the method [15] with the average monthly angle of direct solar radiation. $P_s = 3.58$, $P_d = 0.276$, $P_r = 0.724$ – coefficients of the position of translucent surface for direct, diffused, reflected solar radiation; f_s, f_d, f_r, – coefficients of conversion of solar radiation passing through a translucent surface on its heat-receiving surface. For the Trombe wall are equal to 1; K_{INS} – coefficient of insolation of direct radiation system. Values K_{INS} are taken from the appendix [15]; S', D – monthly amount of direct and diffuse solar radiation falling on a horizontal surface, respectively, MJ/m^2. Found from the appendix [8, 16]; $K_{\mathrm{CL}} = 0.29$ – coefficient of irradiation of the diffused radiation system if shading elements are present; $r = 0.25$ – coefficient of reflection from the ground.

Calculation of the solar radiation heat that enters the Trombe wall in different cities of Ukraine is shown in Figure 3.6.

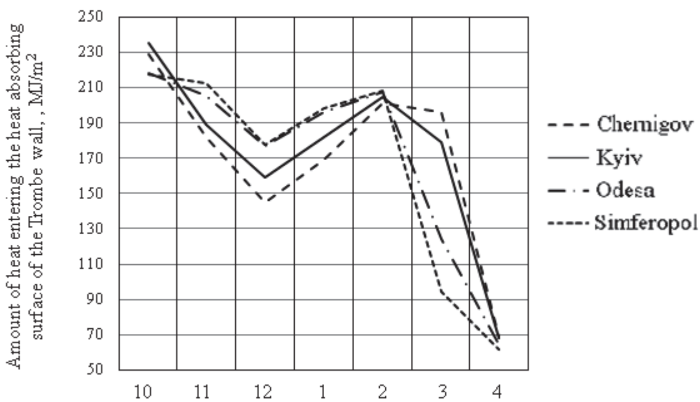

Figure 3.6. The amount of heat entering the heat absorbing surface of the Trombe wall during the heating season in the cities of Ukraine

The efficiency coefficient η indicates which part of the solar radiation heat, absorbed by the PSH system, is spent on heating the room.

For the heating system of the Trombe wall, the efficiency coefficient is:

$$\eta = \eta_0 + \Delta\eta \tag{3.17}$$

where: η_0 – coefficient of heat transfer efficiency in the absence of natural air circulation through the openings between the space behind the glazing (space limited by glazing and heat-absorbing wall) and the room; $\Delta\eta$ – increase in the efficiency of heat transfer of solar radiation in the presence of natural circulation.

The value η_0 is determined by the formula:

$$\eta_0 = \frac{R_n + R_H}{R_n + R_0^B} \tag{3.18}$$

where: R_H = 0.075 m^2K/W – heat transfer resistance on the outer surface of the receiver wall; R_0^B – heat transfer resistance of the heat-receiving wall, $m^2 \cdot K/W$. It depends on thermal conductivity of material and thickness of layers of the heat-receiving wall, and is determined by the appendix [17]. R_n = 0.415 $m^2 \cdot K/W$ – heat transfer resistance from the air behind the translucent coating to the outside air without taking into account the air permeability.

The value $\Delta\eta$ is calculated by the formula:

$$\Delta\eta = f_C \cdot c \cdot \left(1 - g \cdot e^{\left(-d \cdot R_T^B\right)}\right) \tag{3.19}$$

where: f_c = 0.067 – coefficient characterizing the circulation of air. It depends on the area of the circulation holes per 1 m of width of the heat-receiving wall, and on the vertical distance between the input and output axes [15]; c, d, g – coefficients for different materials of the heat-receiving wall, are given in Table 3.6.

Table 3.6. The values of the coefficients in the equation $\Delta\eta = f_C \cdot c \cdot \left(1 - g \cdot e^{\left(-d \cdot R_T^B\right)}\right)$

Material	**Coefficient *S*,** $\frac{\mathbf{W}}{(\mathbf{m^2K})}$	$c \cdot 10^2$	*g*	*d*
Cellular concrete $\gamma = 600\frac{\text{kg}}{\text{m}^3}$	3.36	$0.405\left(\frac{q_{ABS}}{m} + 1.57\right)\left(\overline{t_n} + 24.6\right)$	0.636	1.3
Claydite concrete $\gamma = 1200\frac{\text{kg}}{\text{m}^3}$	6.36	$0.436\left(\frac{q_{ABS}}{m} + 1.83\right)\left(\overline{t_n} + 18.1\right)$	0.691	1.66
Brick $\gamma = 1800\frac{\text{kg}}{\text{m}^3}$	9.2	$0.544\left(\frac{q_{ABS}}{m} + 2.26\right)\left(\overline{t_n} + 13\right)$	0.699	1.57

To achieve the maximum efficiency of using a passive heating system, an optimum relation was found between the geometric characteristics of the Trombe wall: thickness of the air layer between the glazing and the heat absorbing wall and the thickness of the massive wall for three wall materials: cellular concrete, brick and claydite concrete.

The calculations were carried out in EnergyPlus software package [18] that allows to use climatic data of Ukrainian cities. The IWEC (International Weatherfor Energy Calculations) program file contains typical weather files that are suitable for application in modeling energy processes.

As a model, was studied a residential building with the area of 150 m^2 with passive heating system such as Trombe wall with natural air circulation. The heat-storing wall of 17.5 m^2 is painted in black. At the top and bottom of the wall there are five circular openings, the area of which is 0.15 m^2. As an external glazing there is used a single-chamber or double-chamber windows. The thickness of the air layer between the glass wall and the heat absorbing surface varied from 0.013 m to 0.08 m. The wall had a southern orientation and a sunshade canopy, the length of which was 0.75 m, to reduce overheating in summer.

The effectiveness of the Trombe wall was estimated by the amount of minimum possible energy consumption per unit of the building area, which ensues from the thermal balance.

The consumption of thermal energy for heating without a Trombe wall for Kyiv is 59.7 kWh/m^2.

Calculations were made taking into account the amount of solar radiation received during the day for each month of the heating season in Kyiv.

Modeling results of determining the heat consumption for heating, depending on the geometrical characteristics of the Trombe wall: thickness of the air layer between the glazing and the heat absorbing wall and the thickness of the massive wall for different wall materials, depending on the location [19].

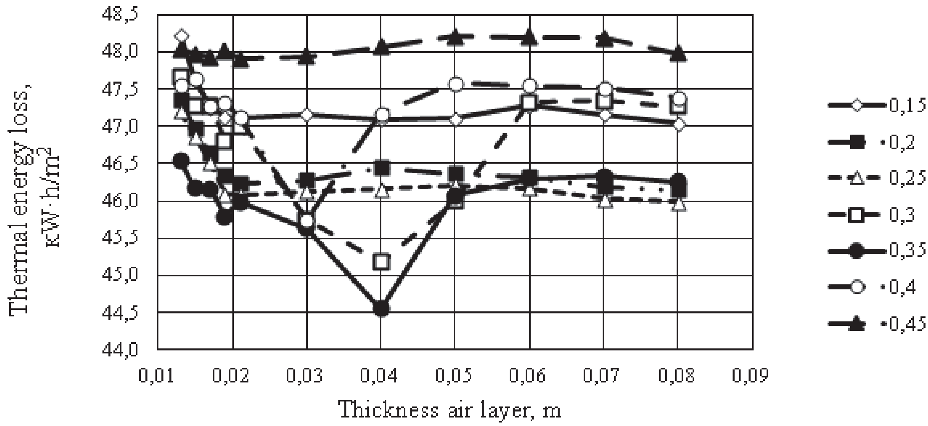

Figure 3.7. Dependence of thermal energy loss from 1 m^2 per year on the thickness of the claydite concrete wall and air layer for Kyiv

Based on the results of simulation, were determined the optimal parameters of the Trombe wall for Kyiv (Table 3.7).

Table 3.7. Optimal parameters of the Trombe wall for Kyiv

	Type of wall material		
	cellular concrete	**brick**	**claydite concrete**
Wall thickness, m	0.4	0.4	0.35
Thickness of the air layer, m	0.03	0.03	0.04
Heat consumption for heating, kWh/m^2	48.4	46.1	44.8

The efficiency coefficient η = 0.352 at optimal parameters of the Trombe wall of claydite concrete.

Calculations of the efficiency coefficient of solar radiation heat transmission of the Trombe wall during heating season for Ukrainian cities are shown in Figure 3.8.

Figure 3.8. Dependence of the efficiency coefficient of solar radiation heat transfer

The tendency of decrease in solar heat transfer efficiency in April and March persists in all cities, due to small solar radiation absorption capacity of the Trombe wall.

Consequently, the efficiency of heat accumulating surface depends on the characteristics, the composition of the wall, the natural air circulation and the climatic conditions of each city, namely the external air temperature and the amount of solar radiation heat mentioned above, which falls on the heat absorbing surface. The coefficient shows how efficiently and when the wall would work under identical parameters in different cities of Ukraine.

The amount of solar radiation entering the room is equal to

$$Q_{ENT} = A_W \cdot q_{ABS} \cdot \eta \tag{3.20}$$

where: A_W – the area of the absorbing surface of the PSH system, m^2:

$$A_W = h \cdot l \tag{3.21}$$

where: h – height of the Trombe wall, 3.5 m; l – length of the wall, 5 m.

So,

$$A_W = 3.5 \cdot 5 = 17.5 \text{ m}^2$$

The amount of heat entering the room in January:

$$Q_{ENT} = 17.5 \cdot 179.87 \cdot 0.352 = 1109.5 \text{ MJ}$$

After calculating Q_{ENT} of each month of the heating period for the selected cities of Ukraine were received the results shown in Figure 3.9.

The results showed that in the coolest winter period, amount of incoming heat from solar radiation is larger in the southern part of the country than in the northern and central regions.

Figure 3.9. Dependence of the amount of heat from solar radiation entering the room monthly during the heating season

The total heat loss of the room is calculated in the absence of solar radiation:

$$Q_{HL} = 86.4 \cdot 10^{-3} \cdot m \cdot \left(\sum_i \frac{A_i}{R_{oi}} + 0.28 M_{inf} \right) \cdot \left(t_r - t_{env} \right) \qquad (3.22)$$

where: m – number of calendar days in a month; A_i – area of protective structures, m^2; R_{oi} – heat transfer resistance of protective structures, (m^2·K)/W; M_{inf} – the amount of external air that is infiltrated into the room; t_r – estimated room temperature, °C; t_{env} – estimated outside air temperature, °C.

To calculate the component $\sum_i \frac{A_i}{R_{oi}}$, we specify the composition of the enclosing structures such as roof, floor, exterior walls, entrance doors, windows, and their area [17].

The values Q_{HL} for each month of the heating period for Ukrainian cities are shown in Figure 3.10.

Using values Q_{ENT} and Q_{HL} can be found the heating coefficient of the room:

$$K_H = \frac{Q_{ENT}}{Q_{HL}} \qquad (3.23)$$

After calculating the heating coefficient for each month of the heating period, the received results for selected cities of Ukraine are shown in Figure 3.10.

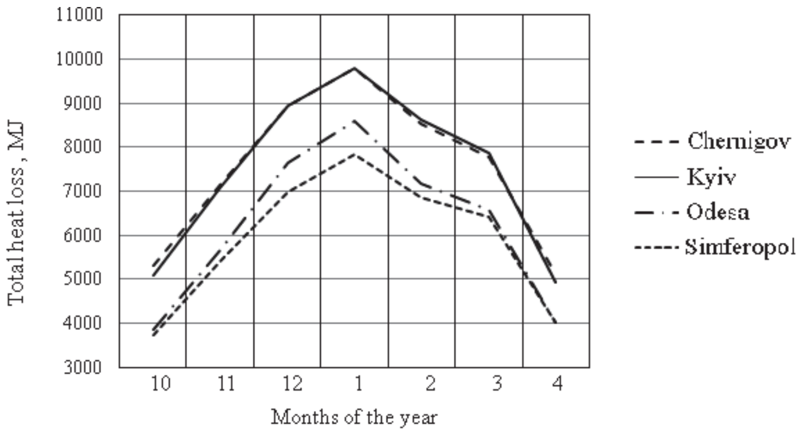

Figure 3.10. Dependence of the total heat loss of the building from the months of heating period

Figure 3.11. Dependence of the heating coefficient on the months of the heating season

By the value of C_{OP} for PSH systems are determined the monthly coefficients of substituting by heat of solar radiation the heat consumption for heating f (Figure 3.11), where after the substitution coefficient of the system during the heating period is derived from the equation:

$$f_{year} = \frac{\sum_{k=1}^{6}\left(f_k \cdot Q_{HL.k}\right)}{\sum_{k=1}^{6} Q_{HL.k}} \tag{3.24}$$

where k is month index of the heating period.

The effectiveness of PSH during the day for each month of the heating season in Kyiv is shown in Figure 3.12, and the monthly substitution coefficients of PSH for the heating period for different cities of Ukraine are shown in Figure 3.13.

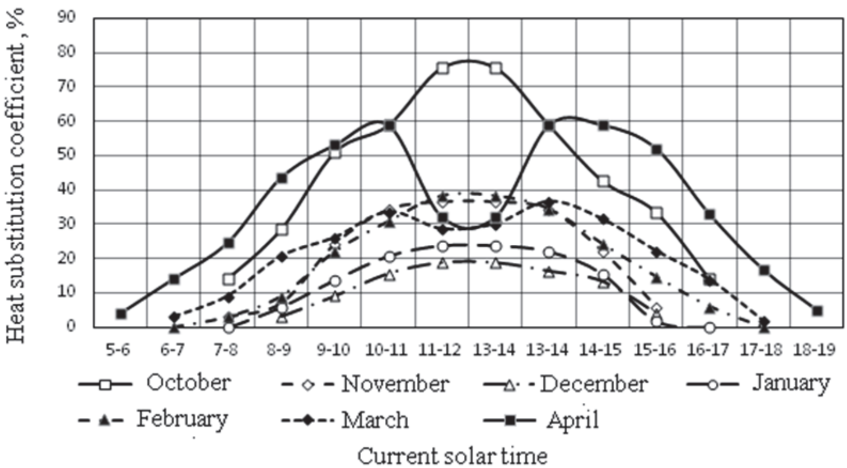

Figure 3.12. Dependence of the heat substitution coefficient from the current solar time in Kyiv

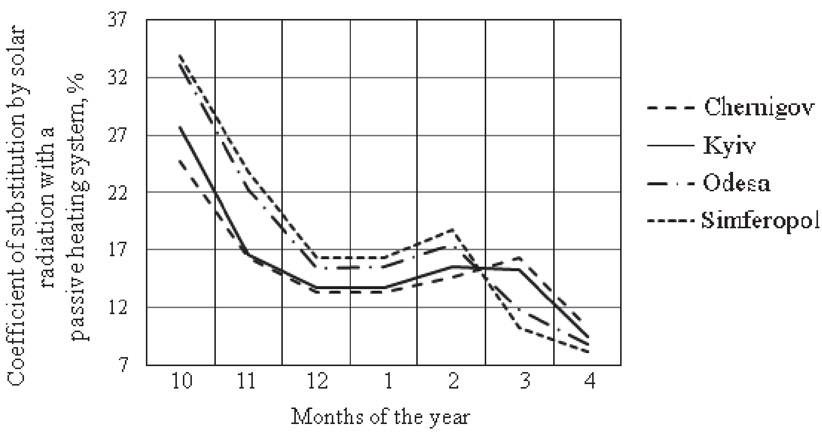

Figure 3.13. Dependence of the coefficient of substitution by solar radiation with a passive heating system

The results of calculating the average parameters during the heating season are shown in Table 3.8.

Table 3.8. The amount of solar radiation heat, total heat loss of the building, heating coefficient, coefficient of substitution of heat consumption for heating and fuel economy for different cities of Ukraine

City	q_{ABS}	η	Q_{ENT}	Q_{HL}	K_H	f	B
			MJ/m²			%	m³
Chernihiv	169.1	0.440	1301.3	10273	0.13	14.3	261
Kyiv	182.3	0.442	1409.8	10273	0.14	14.7	267
Odessa	189.6	0.449	1489.1	9021	0.17	16.3	247
Simferopol	198.7	0.455	1581.1	8211	0.19	18.8	269

To reduce losses through the glass construction of the passive wall, the analysis of impact of the filler, type of glass and type of grazing on the amount of required energy for heating and cooling systems was carried out.

For the analysis were used glazings with ordinary and energy-efficient glass (Figure 3.14):

- *k*-glass Low-E glass with a "solid" energy-saving coating;
- *i*-glass Double Low-E glass with a "soft" energy-saving coating.

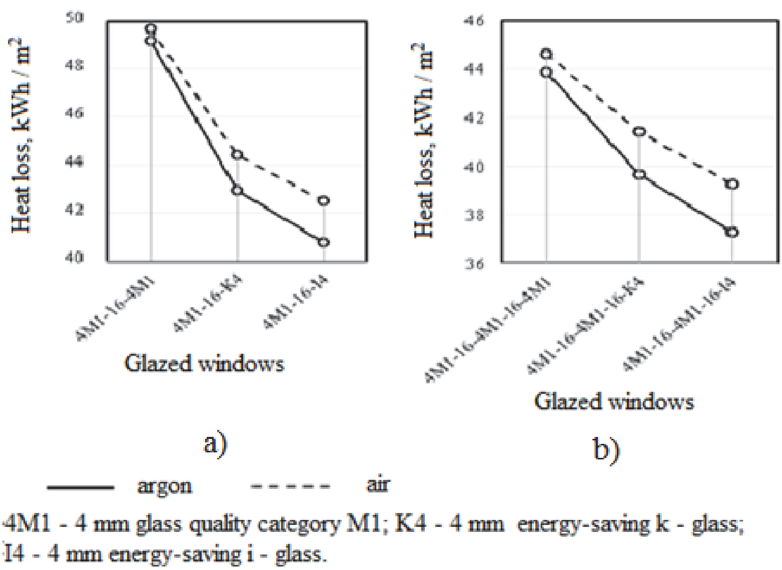

Figure 3.14. Buildings heating demand in Kyiv with installed single-chamber (a) and double-chamber (b) windows

Figure 3.14 shows that single-chamber windows filled with inert gas retain more energy than those filled with air, in case of ordinary glass by 0.8%, *k*-glass by 2.8% and with an *i*-glass by about 3.5%. Compared to double-chamber windows, the difference is: ordinary glass – 1%; *k*-glass – 3.3% and *i*-glass – 6.1%.

The use of double-chamber windows filled with an inert gas-argon and the use of selective coatings can reduce the consumption of heat for heating by 10–26%, but being used in summer, the need for cooling also increases by 10–20%.

Economic feasibility of applying the Trombe wall in combined heating systems with the use of a heat pump or an electric boiler as the main source of heat were studied in the work [20].

The payback period of the passive Trombe wall was: for a system with a heat pump – 10 years and 4 months, for a system with an electric boiler – 2 years and 10 months for Kyiv, and for Odessa – 9 years and 2 years and 8 months, respectively.

3.2. CONCLUSIONS

The given methods for determining the coefficients of substitution of fuel in active solar systems with solar collector provide different values, but on average its value varies in the range of 0.56–0.688, which saves from 200 to 420 m^3 of natural gas, depending on the city of installation, type of collector and service life.

Applying Trombe wall for a private cottage will give an opportunity to save on average more than 250 m^3 of natural gas during the heating season.

Today, active and passive solar installations are expensive for Ukrainian citizens, but their implementation is supported by the state through introducing the "green rate". Expansion of the use of solar systems allows the state to reduce the amount of imported fuel, which is an effective way of energy saving and a step towards Ukraine's energy independence. In addition, application of solar energy improves the ecological state of the environment.

REFERENCES

[1] *Solnechnyie ustanovki goryachego vodosnabzheniya. Posobie po proektirovaniyu*, K., Izd. KievZNIIEP, 2006, p. 26.

[2] Harchenko N.V., *Individualnyie solnechnyie ustanovki*, M.: Atomizdat, 1991, p. 208.

[3] Bekman U., *Raschet sistem solnechnogo teplosnabzheniya*, Bekman U., Kleyn S., Daffi Dzh., M.: Energoizdat, 1982, p. 80.

[4] *Clean energy projecy analysis. RETScreen engineering & cases Textbook*, 3rd edition, <http://www.retscreen.net/>.

[5] Daffi Dzh.A., Bekman U.A., *Teplovyie protsessyi s ispolzovaniem solnechnoy energii*, ed. by Yu.N. Malevsky, M.: “Mir”, 1977.

[6] SNiP 2.01.01-82. Stroitelnaya klimatologiya i geofizika, M., Stroyizdat, 1983.

[7] <http://energy.ast-kairos.ru/komponenty-geliosistemy/geliokollektor/>.

[8] SNiP II-A.6-72. Stroitelnaya klimatologiya i geofizika, M., Stroyizdat, 1973.

[9] NII stroitelnoy fiziki. Rukovodstvo po stroitelnoy klimatologii, M., 1977.

[10] 10 SNiP 2.04.01Vnutrenniy vodoprovod i kanalizatsiya zdaniy.

[11] Nastanova z ulashtuvannia system soniachnoho teplopostachannia v budynkakh zhytlovoho i hromadskoho pryznachennia, DSTU-N B-V.2.5-43:2010, K., MinRehionBud, 2010.

[12] <https://energyplus.net/weather-location/europe_wmo_region_6/UKR.%C2%A0>.

[13] Yaryimbash D.S., Daus Yu.V., *Osobennosti identifikatsii intensivnosti solnechnoy radiatsii pri proektirovanii solnechnyih elektrostantsiy*, “Elektroenergetika” 2014, No. 1, pp. 74–78.

[14] Mak-Veyg. D., *Primenenie solnechnoy energii*, M.: Energoizdat, 1981, p. 216.

[15] Amerhanov R.A., Draganov B.H., *Proektirovanie sistem teplosnabzheniya selskogo hozyaystva: Uchebnik dlya studentov vuzov po agroinzhenernyim spetsialnostyam*, ed. by B.H. Draganov, Krasnodar 2001, p. 200.

[16] DSTU-N B V.1.1 – 27:2010 Budivelna klimatolohiia.

[17] DSTU B V.2.6 – 189:2013 Metody vyboru teploizoliatsiinoho materialu dlia uteplennia budivel.

[18] EnergyPlus Energy Simulation Software, <http://apps1.eere.energy.gov/buildings/energyplus/>.

[19] Dubrovska V.V., Shklyar V.I., Hubska O.V., *The influence of constructive characteristics of the Trombe wall on efficiency of passive heating system*, “Enerhetyka: ekonomika, tekhnolohii, ekolohiia” 2017, No. 2, pp. 61–67.

[20] Dubrovska V.V., Shklyar V.I., Hubska O.V., *Tekhniko-ekonomichna efektyvnist roboty pasyvnoi systemy soniachnoho teplopostachannia v mistakh Ukrainy*. *Ekonomika pidpryiemstva: suchasni problemy teorii ta praktyky: Materialy piatoi mizhnarodnoi naukovo-praktychnoi konferentsii*, Atlant, Odessa 2016, pp. 356–357.

Chapter 4

RESEARCH OF BIOMASS GASIFICATION

Anna M. Slowak

Department of Building Physics and Renewable Energy
Kielce University of Technology

4.1. DESCRIPTION OF THE EXPERIMENTAL INSTALLATION

Experimental research on the biomass gasification process was carried out on the gasification installation with a fluidized bed gasifier. The layout of the installation is shown in Figure 4.1. The experimental setup of the installation is shown in Figure 4.2.

Figure 4.1. General view of the experimental biomass gasification installation

The experimental installation consists of a solid fuel chamber (2), to which the fuel is transported through the opening by a screw conveyor (3). During the gasifier operation, the loading opening is tightly closed in order to avoid sucking in air through the fuel system. Screw conveyor (4) transports biomass from the chamber (2) to the gasifier reactor (1). The screw conveyor is driven by a motor (12) mounted on the conveyor shaft. Fuel consumption was regulated by means of the frequency regulator in which the engine was equipped. The gasifier reactor is equipped with three electric heaters, installed at the reactor height: bottom heating element (13), central heating element (14) and upper zone heating element (15). To monitor and control the gasification process, the reactor is equipped with thermocouples (T) and pressure sensors (P). The reactor also has a system for even distribution of the blow (7). After the reactor, uncleaned generator gas is introduced into the mechanical treatment chamber, where it passes through the graphite filter (9) and is purified of solid particles.

To avoid an uncontrolled process of condensation of water vapor and hydrocarbons with high condensing temperature in the mechanical treatment chamber, an electric heater (20) was installed that maintains the correct temperature in the zone of gases. The generator gas is then injected into the cooling and condensing unit (10) for drying and tar cleaning (high temperature condensing hydrocarbons).

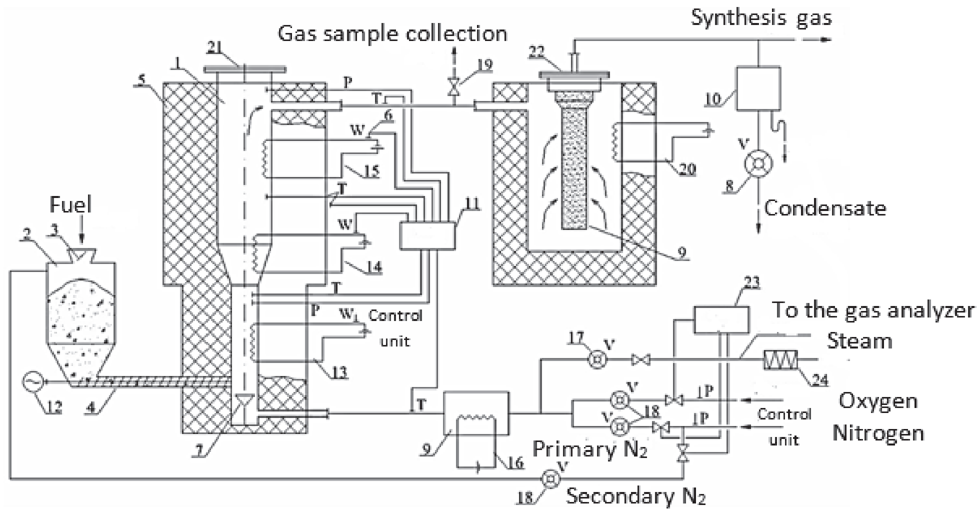

Figure 4.2. Scheme of experimental gasification plant: 1 – biomass gasification reactor, 2 – solid fuel chamber, 3 – gate valve, 4 – screw transporter for fuel transport, 5 – reactor thermal insulation, 6 – installation places for pressure and temperature measuring instruments, electricity consumed, 7 – blowing distribution system, 8 – generator gas flow meter, 9 – graphite gas filter, 10 – cooling and condensing unit, 11 – control and data collection assembly, 12 – screw drive of the fuel transfer system), 13, 14, 15 – electric heaters of different reactor zones (lower, middle with the upper respectively), 16 – electric heater of the pre-heating system, 17 – steam water jet flow meter, 18 – oxygen and nitrogen flow meter, 19 – tap for sampling gas to the filter, 20 – filter assembly heater, 21 – reactor cover, 22 – filter chamber cover, 23 – blowing control unit, 24 – steam superheater

The gas sample was collected for the tar content analysis by means of a tap (19) placed in the purification system. The temperature control of the reactor was controlled by means of the temperature control unit (11).

A blend of components such as nitrogen (N_2), oxygen (O_2) and water vapor (H_2O) was used for blowing. A separate transmission line is provided for each component. The consumption of each constituent of the mixture was controlled by the blowing control unit. The blower was preheated in the heating unit (9) by means of an electric heater (16). The water vapor was generated in the steam generator (24). The consumption of oxygen and nitrogen was measured using flow meters (18).

The ratio of oxygen and nitrogen was controlled by the blowing control unit (23). Part of the nitrogen was introduced into the reactor to form a fluidized bed (primary nitrogen). The remaining part was introduced into the fuel chamber to prevent gasification products or pyrolysis (secondary nitrogen) from entering it. The adjustment of the excess air ratio (a) in the reaction zone of the generator was carried out by changing the oxygen consumption.

Access to the reactor to clean and replace the fluid bed material was effected through the cover (21). Access to the graphite filter for cleaning took place through the filter cover (22). Alumina was used as the fluidized bed material (Al_2O_3).

In order to investigate the composition of the synthesis gas, a C2V-200 Micro GC gas chromatograph was used. Helium (He) and argon (Ar) were used as carrier gases. Gas sampling was carried out for 2 minutes, analysis of the sample lasted another 2 minutes. As a result, the content in the synthesis gas was determined as follows: CO_2.

The diagram of connecting the gas chromatograph to the gasifier is shown in Figure 4.3. After passing the cooling and condensation system, the gas sample passes through an additional purification system, which includes:

- adsorbent of water vapor (2) (phosphorus pentoxide, P_2O_5);
- fine filter for micro-dispersion solid particles (4);
- molecular sieve (5) for the final purification of moisture. After measuring the parameters (6), the gas sample is introduced into the gas chromatograph (1).

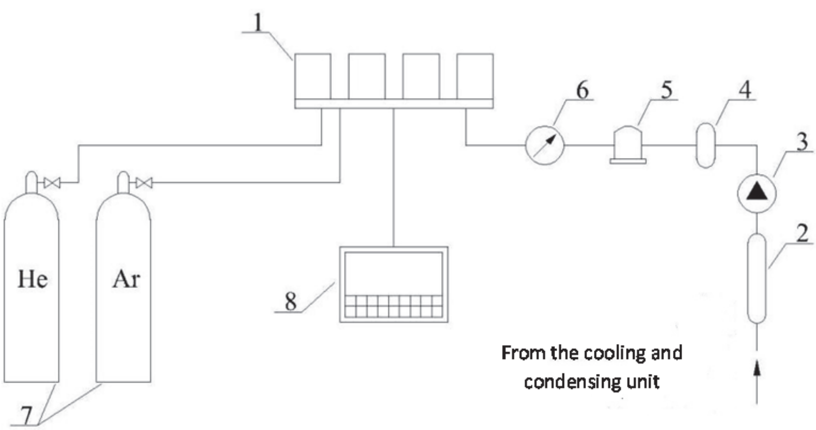

Figure 4.3. Connection diagram for a gas chromatograph

To examine the content and composition of tar in a generator gas under various gasification conditions, gas samples for analysis were taken. Gas samples were taken immediately after the reactor to the purification system. The gas temperature at the point of collection exceeded the condensing temperature of the components. A sample of 100 ml gas was passed through a filter on which all the tars contained in the sample liquefied. After collecting the sample, the filter was rinsed with acetone, and the resulting solution was sent to the gas chromatograph for analysis. Gas analysis allowed to determine the amount and composition of tar under various gasification conditions in the volume of the selected sample.

In order to make an energy balance of a gasifier, during the experiments an instrumental measurement of electricity consumption was made for the heating elements of the external supply system of the rector under different gasification conditions. The consumption of the remaining part of the electricity used to heat the blast air was measured analytically based on the known final air temperature and the level of its consumption.

4.2. METHOD OF CONDUCTING RESEARCH

Experimental tests of biomass gasification processes were carried out in the following conditions:

- excluding (preventing) the impact of variable external factors not included in the experiment;
- using measuring devices with the correct measurement error, which guarantees obtaining the correct error of the test result;
- optimization of the number of variable factors of experimental research by conducting separate univariate studies;
- preparation of the experience plan;
- checking the correctness of the results obtained;
- statistical processing of experimental data.

Among the factors affecting the study, the following was selected: the excess air ratio; process temperature; biomass humidity. The scheme for the organization of experimental research on the biomass gasification process is shown in Figure 4.4.

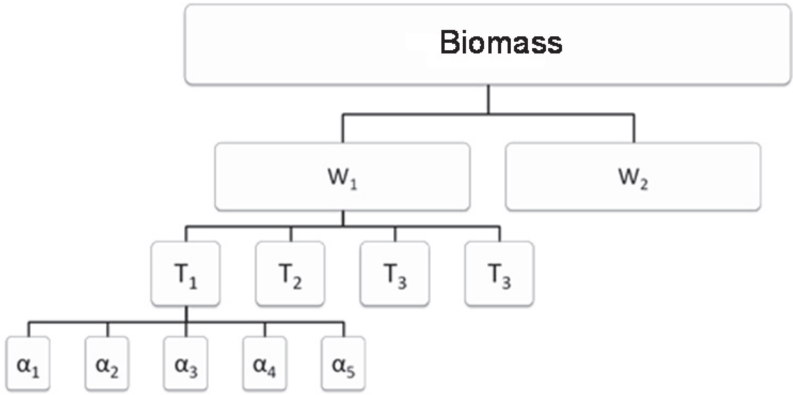

Figure 4.4. Scheme of conducting the experiment regarding biomass gasification (α_i – coefficient of excess air, T_i – temperature in the reactor, W_i – biomass humidity)

The applied scheme allowed for a one-factor analysis of the influence of excess air coefficient, reactor temperature and biomass moisture on the result of the gasification process, in contrast to experimental studies of other authors.

In the process of testing the gasification process, the following process parameters were changed:

a) blow type: dry blow (mixture of oxygen and nitrogen); wet blowing (dry blowing with the addition of steam, $g_{steam} = 0.1$ kg$_{steam}$/kg$_{fuel}$);
b) reactor temperature (T_{react} = 830°C ... 935°C);
c) oxygen consumption (excess air coefficient, α = 0.3 ... 0). Each cycle of experiments was of several stages:
   - warming up the gasifier and setting a fixed set temperature in the reactor;
   - establishing a permanent operating mode after starting the transfer of the blow and biomass;
   - testing the gasification process, measuring the tested parameters, taking gas samples for further analysis;
   - cooling of the gasifier;
   - cleaning the gasifier and preparing for further testing;
   - gas sample testing for tar content and composition;
   - processing of the received data.

During one set of experiments, one type of blow was used and the reactor was kept at a constant temperature. In order to qualitatively assess the effect of the excess air coefficient on the gasification results, in the range α = 0.3 ... 0 experiments were carried out for 4–5 values of α. In order to assess the composition of the generator gas under constant gasification conditions, 5–7 gas samples were selected with a 4-minute break between the samples. The fuel consumption during the gasification process was constant and represented the difference between the mass of fuel in the chamber through and after the experiment. The obtained value concerned the unit of work time of the screw conveyor drive.

The efficiency of the gasification process and the mass of tar were used as optimization parameters. To examine the parameters listed, the following values were measured:

- generator gas composition,
- mass of gas from 1 kg of fuel,
- water vapour mass,
- electricity consumption to maintain the set temperature in the reactor,
- mass of tar.

4.3. ANALYSIS OF THE RESULTS

Generator gas composition and process efficiency

According to the experimental results, the material and energy balance of the gasification process for various gasification conditions was carried out, which allowed to fully assess the efficiency and the quality of the thermochemical treatment of biomass.

After the mathematical processing of the test results, the curves shown in Figures 4.5–4.22 were created.

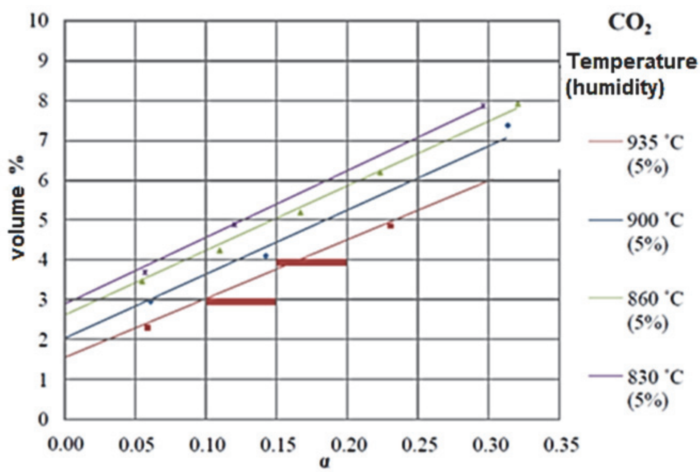

Figure 4.5. CO_2 mass graphs of the generator gas

The graphs in Figure 4.5 show the decrease in acquired CO_2 mass in the generator gas as the process temperature increases and the excess air coefficient decreases. According to the rule of Le Chatelier-Braun, the increase in temperature causes the increase of CO in the endothermic reaction of CO_2 recovery. The smaller coefficient of excess air reduces the amount of carbon that is completely oxidised to CO_2.

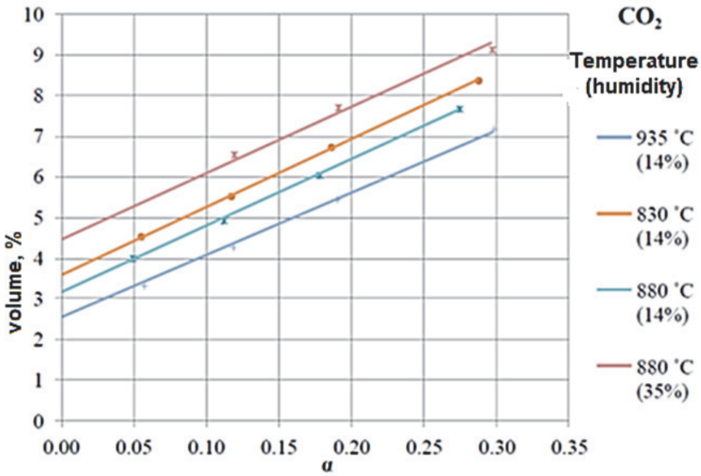

Figure 4.6. CO_2 mass graphs of the generator gas increased humidity increases the CO_2 mass due to the fact that the oxygen in H_2O participates in carbon oxidation processes in reaction

The influence of temperature and the excess air coefficient is similar.

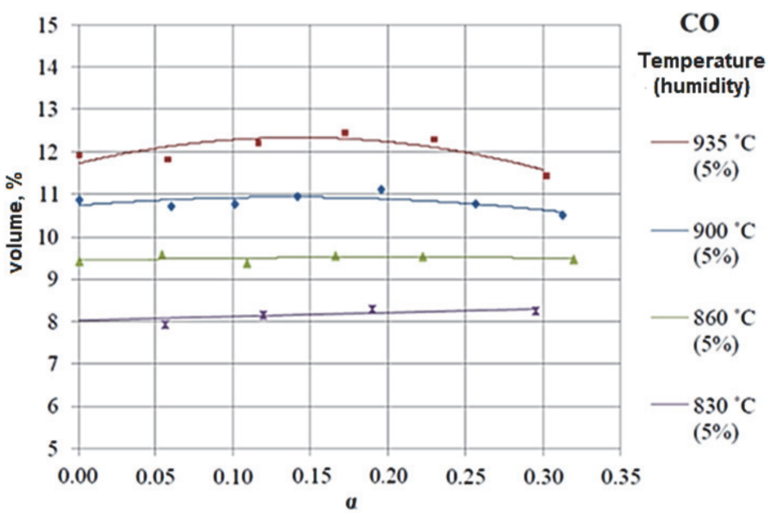

Figure 4.7. CO mass diagrams of generator gas

The graphs in Figure 4.7 show the increase in the CO mass obtained in the generator gas at the increase of the process temperature (see analysis in Figure 4.5). The change of the excess air coefficient does not change the obtained CO mass.

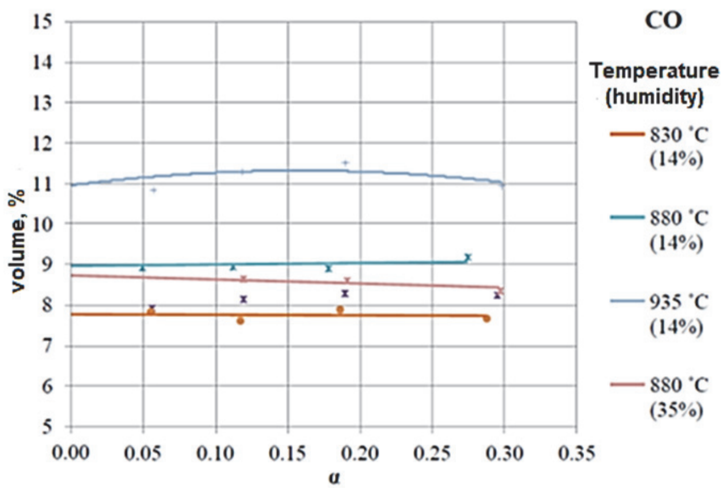

Figure 4.8. CO mass graphs of the generator gas

The increase in the amount of H_2O involved in the reaction reduces the mass of the combustible CO obtained (Figure 4.8). The reduction of the excess air factor also reduces the mass of H_2O as a product of total hydrogen oxidation of fuel or H_2 generated during gasification by reducing the amount of free oxygen in the process (Figure 4.9).

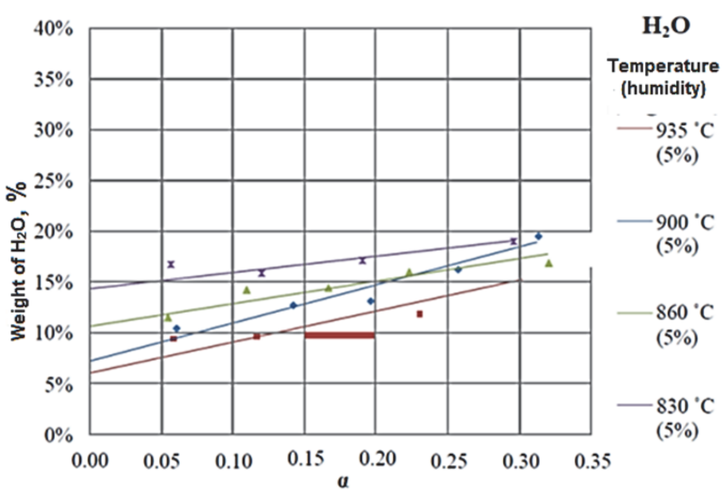

Figure 4.9. H_2O mass graphs of the generator gas

Increasing the amount of H_2O in the system increases its concentration in the generator gas.

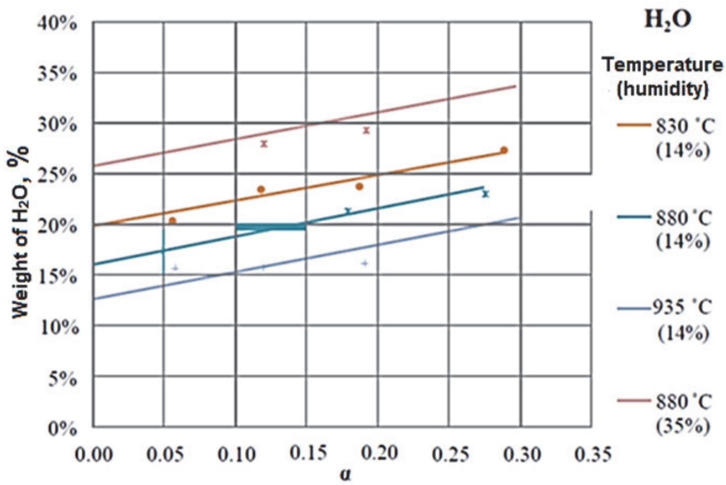

Figure 4.10. H_2O mass graphs of the generator gas

The mass H_2 in the gas increases with increasing temperature (Figure 4.11). This is due to the intensification of the recovery reaction of H_2O on the carbon surface at high temperature. There is also a decrease in the combustible mass H_2 with the increase of the excess air coefficient in the reaction zone due to the higher probability of its combustion (Figure 4.11).

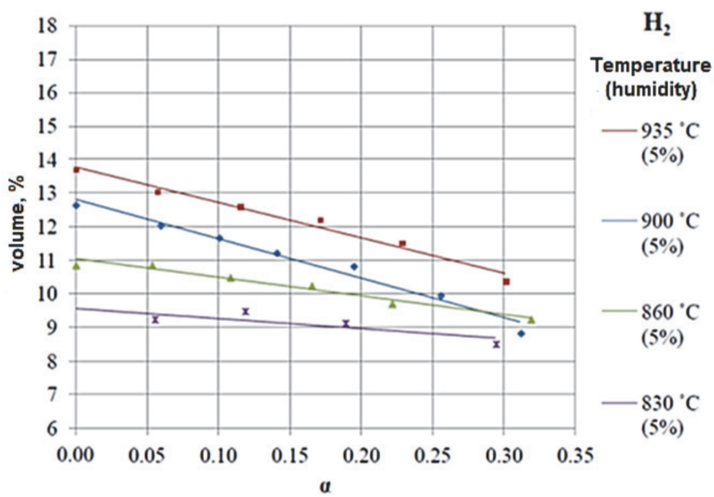

Figure 4.11. H_2 mass graphs of the generator gas

The increase in moisture causes an increase in the mass H_2, because H_2O is an additional source of hydrogen production.

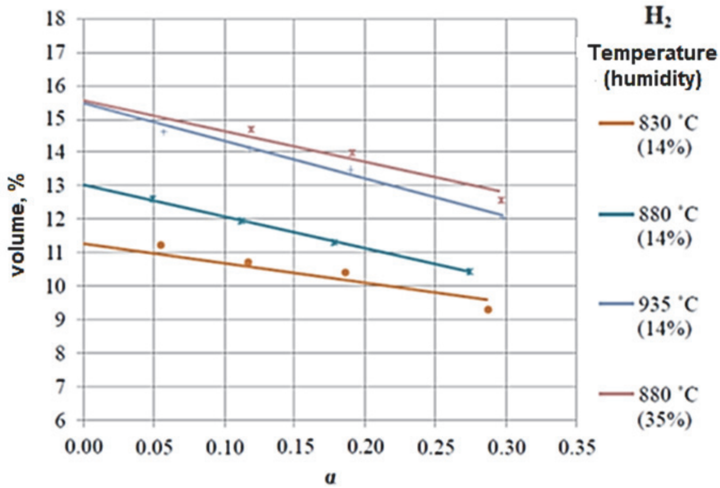

Figure 4.12. H_2 mass graphs of the generator gas

The conversion rate of carbon in combustible gases depends primarily on the efficiency of CO production in the process as the main combustible component containing carbon. Therefore, the nature of the gasification parameters influence on it is similar to the effect on the nature of CO generation – Figures 4.13 and 4.14.

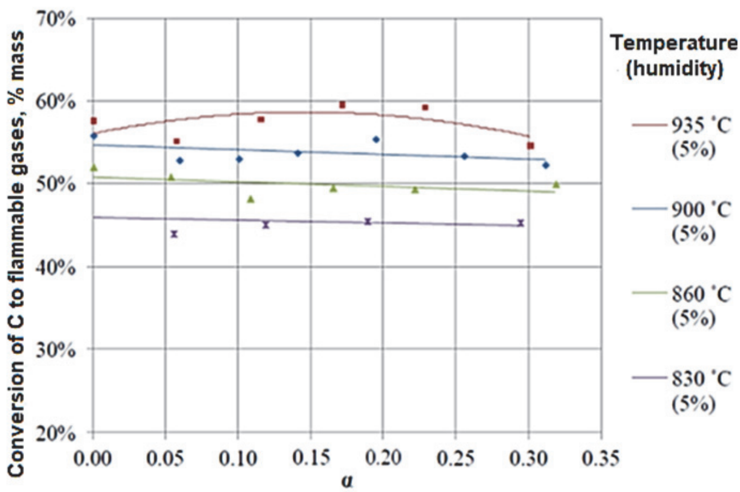

Figure 4.13. Conversion of C to flammable gases, % by mass

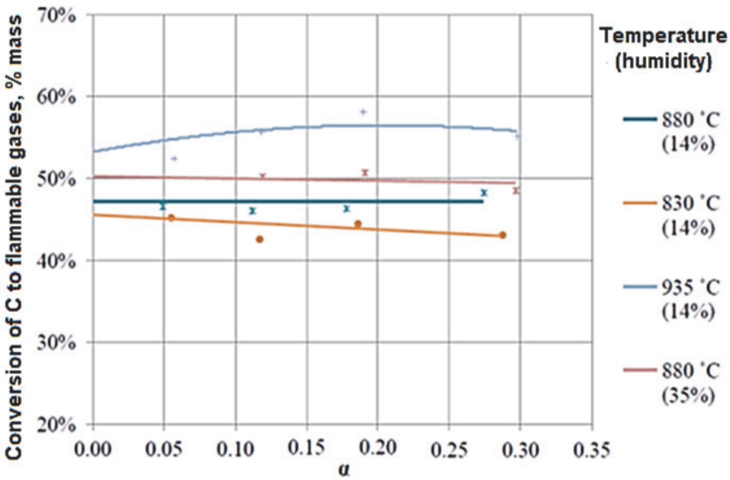

Figure 4.14. Conversion of C into flammable gases, % by mass

The volume of the generator gas mass increases as the process temperature increases due to the increase in the volume of light components (CO and H_2) and the intensification of the recovery reaction H_2O and CO_2 on the surface of the coal residue (Figure 4.15). There is also an increase in gas mass with the increase of the excess air coefficient by additional combustion products production (CO_2 and H_2O) from biomass (Figure 4.15).

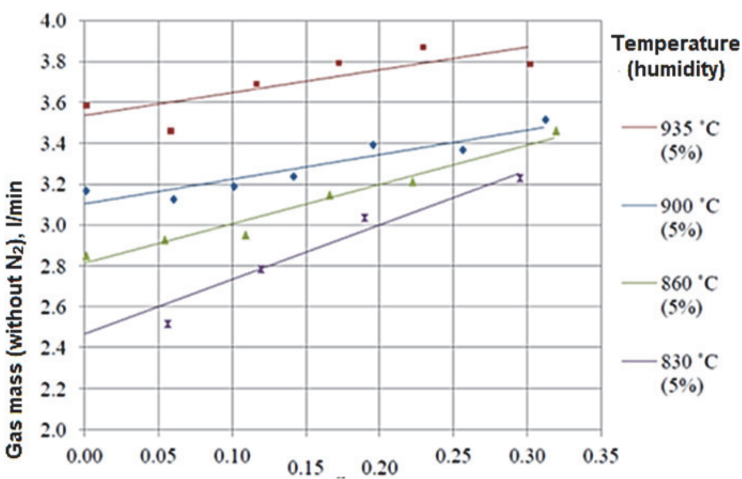

Figure 4.15. Gas mass, l/min

Increasing the humidity also causes an increase in the volume of the producer gas as a result of the creation of an additional amount of H_2 and the passage of the residue H_2O to the generator gas in the form of steam (Figure 4.16).

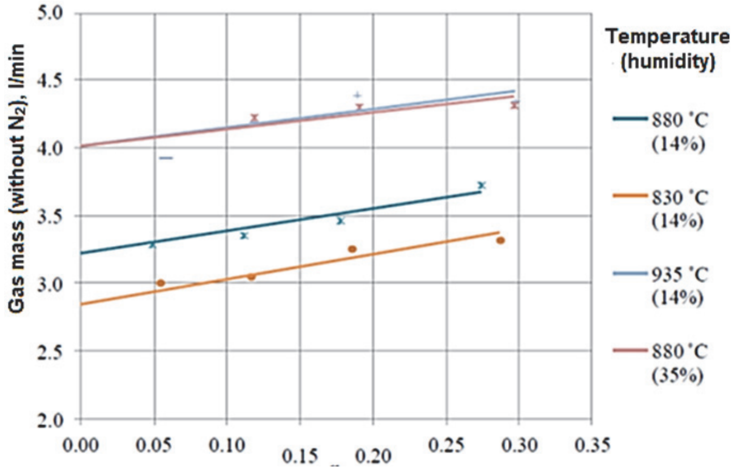

Figure 4.16. Gas mass, l/min

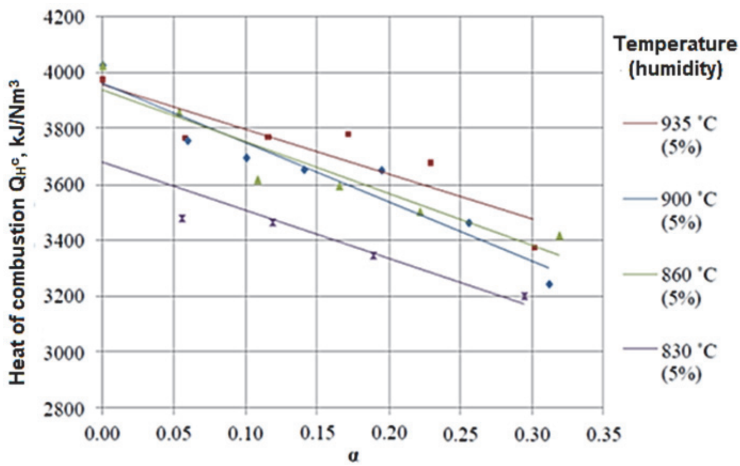

Figure 4.17. Heat of generator gas combustion, kJ/Nm^3

Due to the positive influence of the temperature rise and the reduction of the excess air coefficient on the mass of combustible components, the heat of combustion of the generator gas increases.

The increase of humidity has a differential effect on the composition of the gas. With the increase of the combustible mass of H_2, the non-combustible mass CO_2 and H_2O increases. It causes that the heat of combustion of the generator gas practically does not change (Figure 4.18).

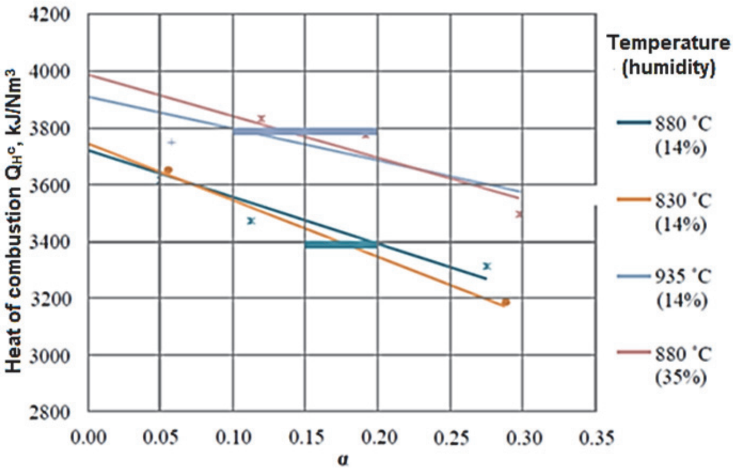

Figure 4.18. Heat of generator gas combustion, kJ/Nm^3

The heat of combustion depends on the nature of the change in the multipliers mentioned. Initial analysis of these values indicates their differential behaviour when the temperature changes and the excess air coefficient. However, the drop in the heat of combustion is not fully compensated by the increase in the mass of the generator gas, which results in the overall efficiency of the installation decreasing – Figures 4.19 and 4.20.

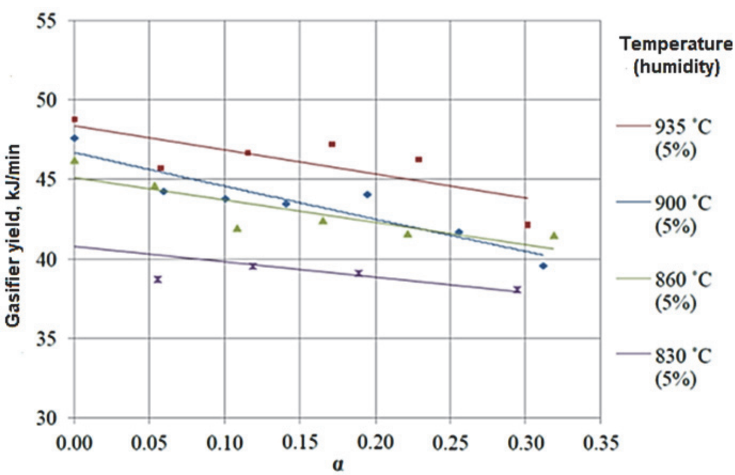

Figure 4.19. Yield of gasifier kJ/min

On the other hand, the increase in humidity increases the efficiency of the gasifier due to the increase in gas mass at its relatively constant heat of combustion – Figure 4.20.

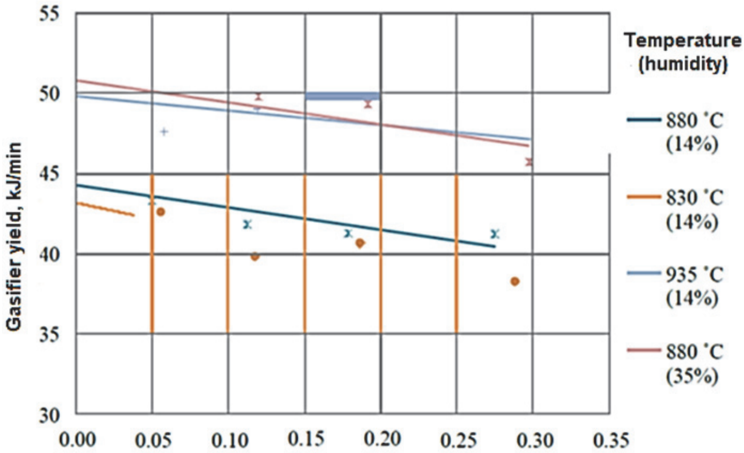

Figure 4.20. Yield of gasifier kJ/min

Analysis of the results gives the opportunity to draw the following conclusions

Increasing the process temperature from 830°C to 935°C affects the gasification results in the fluidized bed gasifier as follows:

- CO mass increases significantly (order of approx. 50% volume);
- CO_2 mass evenly decreases by 20% ... 30% volume;
- CH_4 mass decreases by 13% ... 25% volume;
- the amount of solid unconverted carbon residue (γ) decreases by 15% ... 25% by mass;
- mass of H_2 increases significantly. An increase of 23% ... 47% vol. More significant was the increase in mass of H_2 at low α values;
- H_2O mass decreases 2.5 times at α = 0 and by 25% by mass of fuel at $\alpha = 0.3$;
- total gas mass increases by 6% ... 11% by volume, and nitrogen gas mass by 21% ... 40% by volume;
- the heat of combustion of the generator gas (Q_H^c) increases by 8% ... 9%;
- the weight of the tar decreases by 25% ... 50%; a more significant reduction in tar mass is observed at low α-values.

An increase in fuel humidity from 5% to 14% affects the gasification results as follows:

- CO mass decreases by 5% ... 7% with increasing fuel humidity;
- CO_2 mass increases by 10% ... 30% vol. It is worth noting that the impact is more significant at high temperatures;
- an increase in the moisture content of the fuel practically did not affect the mass of the CH_4;

- the amount of coal residues decreases by 3% ... 5% by mass. This difference is more significant at high temperatures and at high values of α;
- mass H_2 increases by an average of 14% by volume growth at high temperatures is more significant;
- H_2O mass increases 1.5 ... 2.5 times. A significant increase is observed at low α values;
- the total mass of the gas increases by 3% ... 4% by volume, and the mass of nitrogen gas – by 10% ... 14% by volume;
- the heat of gas combustion practically changes with the increase of humidity (mass of H_2 increases and the mass of CO decreases);
- the weight of the tar decreases by 15% ... 20%.

The reduction of the excess air coefficient (α) from 0.3 to 0 results in the gasification process as follows:

- for CO mass at low temperatures, the excess air coefficient had no significant effect, while at high temperatures (over 880°C) an increase in CO mass of 3% ... 5% by volume was observed at $\alpha = 0.15$;
- the effect of the excess air coefficient on the CO_2 mass is significant and has a linear character. The CO_2 mass evenly decreases by 2.7 ... 3.1 times;
- the CH_4 mass increases by 12% ... 25%;
- the amount of coal residues increases significantly. The weight of the residue increases almost twice;
- H_2 mass increases by 10% ... 27% of volume. A more significant increase was observed at high temperatures;
- change in the α indicator at 935°C reduces the mass H_2O three times. At 830°C, the drop is about 30% of the fuel weight;
- total gas mass decreases by 3.5% ... 8% by volume, and the mass of nitrogen free gas – by 12% ... 30% by volume, more significant weight loss takes place at lower temperatures;
- the heat of combustion increases significantly – by 13% ... 14%;
- in high temperatures the influence of the excess of air on the mass of the tar practically does not take place, whereas at 88°C and below – the decrease α causes a significant increase in the tar mass by 60% ... 70%.

In general, according to the results of the analysis, it should be noted that the increase of process temperature and increase of biomass moisture positively affects the composition (quality) of the generator gas. However, the change of the excess air coefficient has ambiguous effects on the gasification process. The α increase worsens the combustible properties of the generator gas, while the reduction α – dramatically increases the mass of tar, which complicates the process of cleaning the generator gas.

Mass and composition of tar in the gasification process

The generator gas is called hydrocarbon complex with high condensing temperature (C_6H_6, C_7H_8, C_9H_8, C_9H_{10}, $C_{10}H_8$, etc.).

The treatment of the results of the tests on the mass and composition of the tar of the gas generator makes it possible to draw the following conclusions:

- increasing the process temperature from 830°C to 935°C reduces the tar mass by 25% ... 50%; a more significant reduction is observed at low α-values;
- increase in fuel humidity from 5% to 14% reduces tar mass by 15% ... 20%;
- at high temperatures, the influence of the excess air factor (α) in the range of 0.3 ... 0 on the mass of tar practically does not occur, whereas at 880°C and below – the decrease α causes a significant increase in tar mass by 60% ... 70%;

The composition of the tar also changes slightly when the process conditions change. The tar pitch test results are shown in Figures 4.21 and 4.22. Figure 4.23 shows the average composition of the resin components of the tar within a constant temperature and humidity. As can be seen on the above figure, the heaviest component of the tar is benzene (C_6H_6) – 60% ... 75% by mass. Three more are: naphthalene ($C_{10}H_8$) – 11% ... 14% by mass, toluene (C_7H_8) – 1% ... 11% by mass and indene (C_9H_8) – 1% ... 5% by mass the other components have a mass fraction below 2%.

It should also be noted that as the temperature decreases, the volume of benzene (C_6H_6) gradually decreases (from 74% to 58% by mass), while naphthalene, toluene and indene increases ($C_{10}H_8$ – from 11% to 13% by mass C_7H_8 – from 1% to 11% by mass, C_9N_8 – from 1% to 5% by weight).

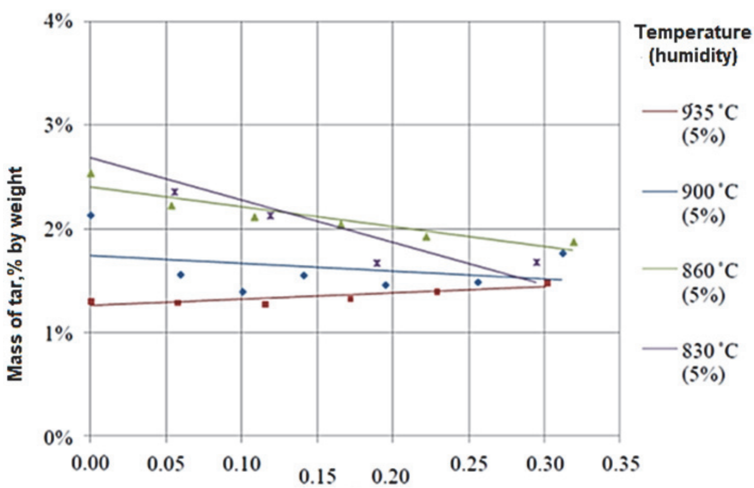

Figure 4.21. Mass of tar, %

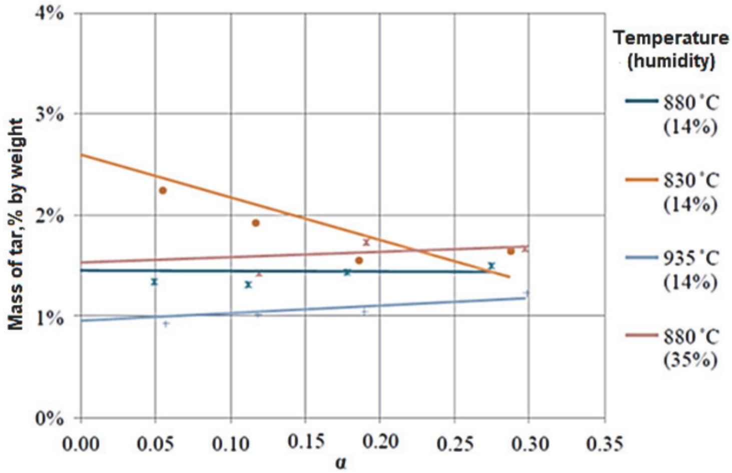

Figure 4.22. Mass of tar, %

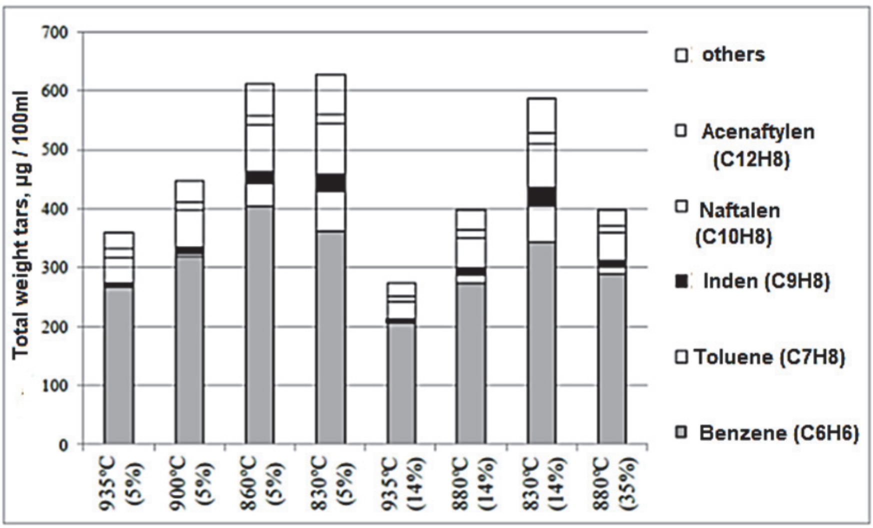

Figure 4.23. Histogram of tars composition at different temperatures and humidity

In order to analyse the influence of tar produced during the biomass gasification process on process organization, physicochemical properties of the basic tar components will be considered (Table 4.1).

Since all of the mentioned components are carcinogenic and practically insoluble in water, they require separation from the producer gas (cooling and condensation) and then carrying out the disposal. However, since all these chemical compounds are flammable compounds, their combustion in a generator gas without treatment and disposal is possible, which greatly simplifies the generator gas cleaning system. In this case, the gas temperature should not be lowered below the condensing temperature of the tar components with the largest fractions. The analysis of tar composition and physicochemical properties of its individual components makes it possible to draw the following conclusions on the fact that the gas temperature before transmission to a gas-fired device must be maintained at a level not lower than 220°C ... 250°C.

Table 4.1. Some physicochemical properties of hydrocarbons with high condensing temperature

Name	**Pattern**	t_{boil}, °C	**Carcinogenic effects**	**Solubility in water**
Benzene	C_6	80.1	Yes	No
Toluene	C_7H_8	110.6	Yes	No
M – xylene (dimethylbenzene) (1.3 dimethylbenzene)	$C_6H_4(CH_3)_2$	139.1	Yes	No
O – xylene (1.2 dimethylbenzene)	$C_6H_4(CH_3)_2$	144.4	Yes	No
Indan (2.3 dyhidroinden)	C_9H_{10}	354	Yes	No
Inden	C_9H_8	182.4	Yes	No
Naphthalene	$C_{10}H_8$	217.9	Yes	No
2-methylnaphthalene	$C_{11}H_{10}$	241	Yes	No
1-methyl naphthalene	$C_{11}H_{10}$	270	Yes	No
Diphenyl	$C_{12}H_{10}$	255.9	Yes	No
Acenaphthylene	$C_{12}H_8$	536	Yes	No
Acenaphthene	$C_{12}H_{10}$	279	Yes	No
Flouren	$C_{13}H_{10}$	293	Yes	No
Phenanthrene	$C_{14}H_{10}$	340	Yes	No
Anthracene	$C_{14}H_{10}$	340	Yes	No
Fluraten	$C_{16}H_{10}$	375	Yes	No
Pyrene	$C_{16}H_{10}$	392	Yes	No

4.4. MATHEMATICAL MODELING OF PROCESSES GASIFICATIONS OF THE BIOFUEL

Purpose of the work

The purpose of the work is to develop a mathematical model of the biomass gasification process for predicting the composition of the generator gas and the technological parameters of the gasification plant operation using a complex parameter – maximum thermodynamic efficiency. To achieve this goal, it is necessary to solve the following tasks:

- to carry out research of the processes occurring during the gasification of biomass in installations with fluidized bed;
- perform a physico-chemical analysis of gasification processes;
- perform an experimental check of the mathematical model.

The development of a mathematical model and its solution

The real process of gasification depends on many factors. Existing mathematical models of this process usually take into account only some of them, so the accuracy of modeling remains rather low. A significant number of models are based on experimental data or hypotheses and are correct only for certain process conditions.

Among all the existing approaches to mathematical modeling of the gasification process, attention should be paid to the method of minimizing the Gibbs free energy. It does not require the specification and selection of certain gasification reactions [10] and considers only the initial and final products of the process. Therefore, this method is more suitable for considering complex systems in which a large number of reactions take place. The method is based on the study of the equilibrium state between all participants in the reactions of the gasification process.

The essence of the method is the use of the thermodynamic potential of the system, the change of which tends to the minimum value under the condition of its equilibrium [10]. Let us write the general equation for determining the isobaric and isothermal potential (Gibbs energy) of a system of ideal gases:

$$G_{tot} = \sum x_i \cdot \mu_i \tag{4.1}$$

where: G_{tot} – the Gibbs energy of the system, kJ/kmol; x_i – the amount of substances in the component of the system, kmol; μ_i – the chemical potential of the component of the system, kJ/kmol:

$$\mu_i = G\ RT\ P^0{}_{fi} + \ln P_i \tag{4.2}$$

where: P_i – the partial pressure of the ith component of the system, Pa; R – the universal gas constant, kJ/(kmol · °C); T – the temperature of the system, K; G_{fi}^0 – the standard free Gibbs energy of the formation of the component, kJ/kmol.

Assuming that the pressure in the gasification chamber is 1 ata, the properties of the gases are close to those of an ideal gas, we write equation (4.2) in expanded form:

$$G_{tot} = \sum x_i \cdot \left(H_{fi}^0 - TS_i^0\right) + RT\sum x_i \ln \frac{x_i}{\sum x_i} \tag{4.3}$$

where: H^0_{fi} – enthalpy of formation of the *i*-th component of the system, kJ/kmol; S^0_i – entropy of the *i*-th component of the system, kJ/(kmol · K).

The problem of determining the composition of a synthetic gas at an equilibrium state of the system reduces to the search for a composition that corresponds to the minimum value of the function expressed by equation (4.3) ($G_{tot} \rightarrow$ min), under certain limiting conditions. The limiting conditions for this method of modeling the gasification process will be the equations of the mass balances of the elements of the system and energy.

Simplifying conditions for considering the problem

Using the thermodynamic equilibrium method involves a number of simplifications, the main ones of which are presented below:

- the time of passage of all gasification reactions is sufficient to establish an equilibrium state between all the gasification products;
- all gases taking part in the gasification process have the properties of an ideal gas;
- components of biomass, the proportion of which does not exceed 1%, and ash are not taken into account;
- the components of the generated synthesis gas are only CO_2, CO, H_2, H_2O, CH_4, C_2H_4, C_6H_6, N_2.

Features of the developed model

1. Accounting for air moisture. In most studies of the gasification process, the authors do not take into account the moisture of the air supplied to the gasifier, citing the fact that its share will not be significant. However, the amount of moisture coming in with the blast air can reach 7% relative to 1 kg of fuel. This amount of moisture will have a significant effect on the efficiency of the gasification process and should be taken into account in the mathematical model of the gasification process.

The w_{air} is determined by the dependence:

$$w_{air} = \frac{d_{air}\alpha_{bio}m_{bio}\left(M_{\mathrm{O}_2} + 3.76\ \mathrm{M}_{\mathrm{N}_2}\right)}{M_{\mathrm{H_2O}}1000} \tag{4.4}$$

where: d_{air} – moisture content of air, g/kg; α_{bio} – coefficient of excess air in the process of gasification; m_{bio} – the amount of oxygen for stoichiometric combustion of 1 km of biomass, kmol; M_i – molecular mass of the i-th component, kg/kmol.

2. The presence of an unconverted carbon residue. In [11] it was experimentally proved that with increasing temperature in the gasification process, while maintaining the remaining process parameters, the concentration of CO_2 decreases in favor of CO. To form 1 kmol of CO, you need twice as much oxygen as for the formation of 1 kmol of CO_2, with the same amount of carbon. Therefore, oxygen will enter the composition of other gas components (H_2O) or remain in the free form (O_2). But gasification products practically do not contain free oxygen in their composition under different gasification conditions [11], and the H_2O concentration decreases with increasing temperature in favor of H_2. Therefore, it is advisable to talk about an increase in the conversion of carbon with increasing temperature. Also, an increase in the conversion rate of carbon occurs with an increase in the amount of moisture entering the reactor [12–14].

   In the proposed model, the amount of non-gasified carbon residue is proposed to be determined by empirical relationships obtained on the basis of the results of the conducted experimental studies.

   The obtained dependence has the following form:

$$\gamma = 1 - \left\{0.63\left(0.589\alpha_{bio} + 0.641\right)\left(0.001T + 0.51\right)\left(0.0003W' + 0.963\right)\right\} \tag{4.5}$$

   where: W' – the total mass of H_2O is given by 1 kg of dry gasified fuel, kg (H_2O)/kg (dry biomass); γ – amount of carbon that remained in the ash residue, kmol.

3. Empirical determination of the yield of hydrocarbons. The output of such components as methane and other hydrocarbons (C_nH_m) can not be accurately predicted using a stoichiometric model. But neglecting even the relatively low yield of hydrocarbon compounds has a significant effect on predicting the yield of other components of the synthetic gas. Since part of the hydrogen (H) and carbon (C) does not lead to the formation of molecules of the (C_nH_m) type, but to the formation of other gas components, this leads to an overestimation of the

concentration of the combustible components of the synthesis gas in the stoichiometric model. gasification. Therefore, it is proposed to determine the yield of some hydrocarbons using empirical relationships, compiled from the results of experimental studies. The obtained dependence for the molar yield of CH_4 is:

$$CH_4 = 0.0678\left(0.0722 - 0.0314\alpha_{bio}\right)\left(23.34 - 0.0097T\right)\left(0.0003W' + 0.9626\right) \quad (4.6)$$

4. There are non-adiabatic process conditions. Most papers consider the gasification process under adiabatic conditions (without loss of heat or additional heat input). But under real operating conditions, heat losses are unavoidable, and with a small power of the gas generator, heat losses can significantly affect its efficiency.

   In the developed mathematical model, such components as heat losses in the gas generator are introduced into the energy balance equation, which gives the possibility of a more accurate and broader assessment of the gasification process.

Equations of mass balances

As noted above, the process of gasification can be considered without dividing it into stages and taking into consideration only the initial and final products of the process. To do this, let's make a general equation of the gasification process:

$$\begin{aligned} &CH_bO_cN_d + \alpha_{bio}m_{bio}\left(O_2 + 3.76N_2\right) + wH_2O + qV_{SG} \\ &\quad + f\left\{V_{FG} + \left(\alpha_{sg} - 1\right)m_{sg}\left(O_2 + 3.76N_2\right)\right\} = \gamma C + x_1H_2 \\ &\quad + x_2CO + x_3CO_2 + x_4H_2O + x_5CH_4 + x_6C_2H_4 + x_7C_6H_6 + zN_2 \end{aligned} \quad (4.7)$$

where: x_1, x_2, x_3, x_4, x_5, x_6, x_7, z – predicted yield H_2, CO, CO_2, H_2O, CH_4, C_2H_4, C_6H_6, N_2, relatively, kmol; V_{SG} – total yield of volatile components in the gasification process, kmol; q – synthesis gas recycling ratio in gas generator, units; m_{sg} – amount of oxygen for stoichiometric combustion of 1 kmol of generator gas, kmol; V_{FG} – amount of combustion products during stoichiometric combustion of 1 kmol of synthesis gas, kmol; w – total H_2O entering the gas generator, kmol.

In general, the mass balance equation for each j-th element in the system containing M elements will look like:

$$\sum_{i=1}^{N} h_{ji}n_i^{out} + A_j^{out} = \sum_{i=1}^{N} h_{ji}n_i^{in} + A_j^{in} \quad (4.8)$$

where: h_{ji} – the number of atoms of the j-th element in the i-th gas or liquid component of the system; n_i^{in}, n_i^{out} – the amount of substance of the i-th gas or liquid component at the entrance to the system and at the output from the system, kmol; A_j^{in}, A_j^{out} – the number of atoms of the j-th element in the solid form, per 1 kmol of biomass at the entrance to the system at the output of the system, respectively.

Equation of energy balance

The generalized equation of the energy balance of the gasification process is as follows:

$$\sum_{i=1}^{n} Q_i^{in} = \sum_{i=1}^{n} Q_i^{out} \tag{4.9}$$

where: Q_i^{in} – energy flow at the entrance to the gasification plant, W; Q_i^{out} – energy flow at the outlet from the gasification unit, W.

In expanded form, equation (4.9) can be written as follows:

$$\begin{aligned} \mathrm{H}_{bio}^{in} &= w_{bio}\mathrm{H}_{w_{bio}}^{in} + w_{air}\mathrm{H}_{w_{air}}^{in} + w_{steam}\mathrm{H}_{w_{steam}}^{in} + \alpha_{bio} m_{bio}\left(\mathrm{H}_{\mathrm{O}_2}^{in} + 3.76\mathrm{H}_{\mathrm{N}_2}^{in}\right) + \\ &+ q\mathrm{H}_{SG}^{in} + f\mathrm{H}_{FG}^{in} + Q_{ex} = \gamma \mathrm{H}_{\mathrm{C}}^{out} + x_1\mathrm{H}_{\mathrm{H}_2}^{out} + x_2\mathrm{H}_{\mathrm{CO}}^{out} + x_3\mathrm{H}_{\mathrm{CO}_2}^{out} + \\ &+ x_4\mathrm{H}_{\mathrm{H}_2\mathrm{O}}^{out} + x_5\mathrm{H}_{\mathrm{CH}_4}^{out} + x_6\mathrm{H}_{\mathrm{C}_2\mathrm{H}_4}^{out} + x_7\mathrm{H}_{\mathrm{C}_6\mathrm{H}_6}^{out} + z\mathrm{H}_{\mathrm{N}_2}^{out} + Q'_{ach} + Q_{loss} \end{aligned} \tag{4.10}$$

where: H_{bio}^{in} – total energy of the dry part of the biomass, kJ; $\mathrm{H}_{w_{bio}}^{in}$ – total energy of moisture of biomass, kJ; $\mathrm{H}_{w_{air}}^{in}$ – the total energy of the water of the blown air supplied to the gas generator kJ; $\mathrm{H}_{w_{steam}}^{in}$ – total energy of water vapor for gasification, kJ; $\mathrm{H}_{\mathrm{O}_2}^{in}$, $\mathrm{H}_{\mathrm{N}_2}^{in}$ – total energy O_2 and N_2 of air, kJ; H_{SG}^{in} – total energy of the recycled generator gas, kJ; H_{FG}^{in} – the total energy of the combustion products entering the gas generator, kJ; Q_{ex} – additional energy entering the gas generator from external sources, kJ; $\mathrm{H}_{\mathrm{C}}^{out}$ – the total energy of the carbon residue, kJ; $\mathrm{H}_{\mathrm{H}_2}^{out}$, $\mathrm{H}_{\mathrm{CO}}^{out}$, $\mathrm{H}_{\mathrm{CO}_2}^{out}$, $\mathrm{H}_{\mathrm{H}_2\mathrm{O}}^{out}$, $\mathrm{H}_{\mathrm{CH}_4}^{out}$, $\mathrm{H}_{\mathrm{C}_2\mathrm{H}_4}^{out}$, $\mathrm{H}_{\mathrm{C}_6\mathrm{H}_6}^{out}$ – total energy H_2, CO, CO_2, H_2O, CH_4, C_2H_4, C_6H_6 as gasification products, kJ; Q'_{ach} – loss of heat with ash, kJ; Q_{loss} – loss of heat to the environment (from the body of the gas generator), kJ.

The total energy of the element of the system consists of its energy of formation and physical heat:

$$H_i = \Delta H_{fi}^0 + Q'_i \tag{4.11}$$

where: ΔH_{fi}^{0} – standard enthalpy of formation of 1 kmol of the *i*-th component, kJ/kmol. Standard enthalpy of substance formation; Q_i' – physical heat of 1 kmol of the *i*-th component of the system, kJ/kmol.

We write in general form the Lagrange function, which is a Gibbs function and bounds the conditions in a general form:

$$L = G_{tot} - \sum_{j=1}^{M} \lambda_j \left(\sum_{i=1}^{N} h_{ji} x_i^{out} + A_j^{out} - \sum_{i=1}^{N} h_{ji} x_i^{in} - A_j^{in} \right) \tag{4.12}$$

where: L – the Lagrange function of the system; λ_j – the Lagrange multiplier at the j-th element.

The partial derivatives for each component of the generator gas equal to zero form a system of equations (4.12) whose solution makes it possible to determine the composition of the generator gas under certain conditions of gasification. Since the mole yield of CH_4, C_2H_4, and C_6H_6 is determined by empirical relationships, they will enter the system (4.13) as constant values for certain gasification conditions.

In the system of equations (4.13), in addition to the variables x_1, x_2, x_3, x_4, the value of the free Gibbs energy (G^0_{fi}), the value of which depends on the temperature, is also taken into account. In this case, the temperature of the system can be determined from the general equation of the energy balance (4.10) and is a function of the final composition of the generator gas.

The solution to this task is performed by an iterative method.

$$\begin{cases} \dfrac{\partial L}{\partial x_1} = RT \cdot \ln\left(\dfrac{x_1}{\sum x_i + z} \right) + G^0_{f\mathrm{H_2}} + \lambda_{\mathrm{H}} (2q - 2) = 0; \\ \dfrac{\partial L}{\partial x_2} = RT \cdot \ln\left(\dfrac{x_2}{\sum x_i + z} \right) + G^0_{f\mathrm{CO}} + \lambda_{\mathrm{C}} (q - 1) + \lambda_{\mathrm{O}} (q - 1) = 0; \\ \dfrac{\partial L}{\partial x_3} = RT \cdot \ln\left(\dfrac{x_3}{\sum x_i + z} \right) + G^0_{f\mathrm{CO_2}} + \lambda_{\mathrm{C}} (q - 1) + \lambda_{\mathrm{O}} (2q - 1) = 0; \\ \dfrac{\partial L}{\partial x_4} = RT \cdot \ln\left(\dfrac{x_4}{\sum x_i + z} \right) + G^0_{f\mathrm{H_2O}} + \lambda_{\mathrm{H}} (2q - 1) + \lambda_{\mathrm{O}} (q - 1) = 0; \\ 1 - \gamma + q(1 - \gamma) + f(1 - \gamma) = x_2 + x_3 + x_5 + 2x_6 + 6x_7; \\ (b + 2w)(1 + q + f) = 2x_1 + 2x_4 + 4x_5 + 4x_6 + 6x_7; \\ c + 2\alpha_{bio} m_{bio} + w + q(c + 2\alpha_{bio} m_{bio}) + \\ \quad + f(c + 2\alpha_{bio} m_{bio} + w + 2\alpha_{SG} m_{SG}) = x_2 + 2x_3 + x_4 \end{cases} \tag{4.13}$$

Experimental studies of the gasification process were carried out in a gasification plant with a fluidized bed generator. Based on the results of experimental studies, the material and energy balances of the process for various gasification conditions were compiled, which allowed to fully assess the efficiency of the gas generator and the quality of thermochemical treatment of biomass.

After the mathematical processing of the research results, the graphs shown in Figures 4.24–4.27. The lines marked with the letter „S" characterize the humidity of the biomass 14%, „S+" – humidity 35%.

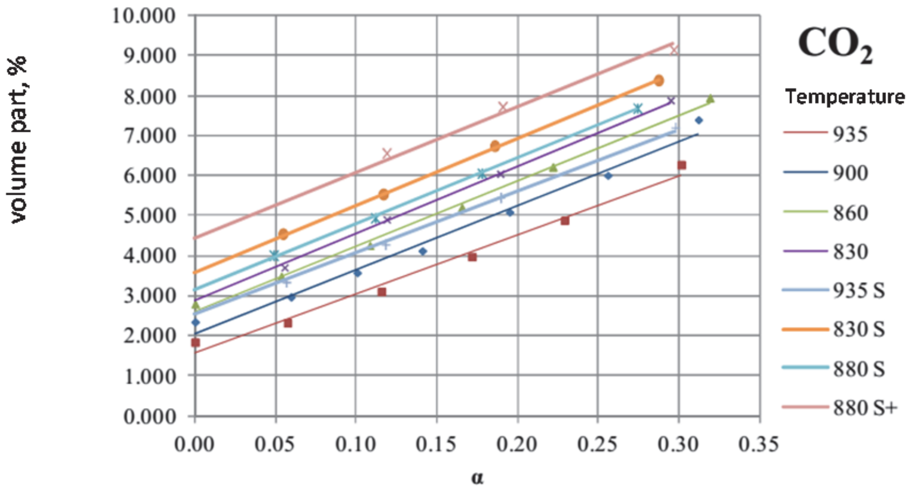

Figure 4.24. Graphs for the CO_2 output at the warehouse generating gas

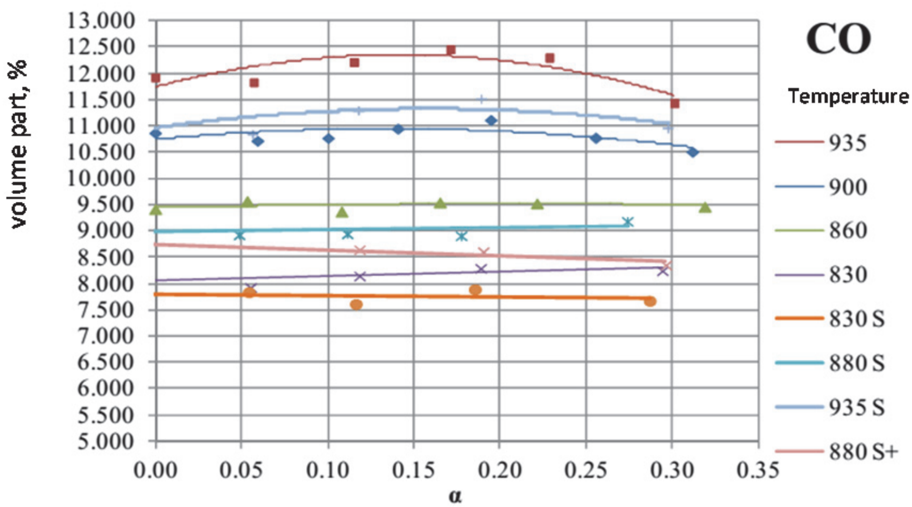

Figure 4.25. Graphs for the CO output at the warehouse generating gas

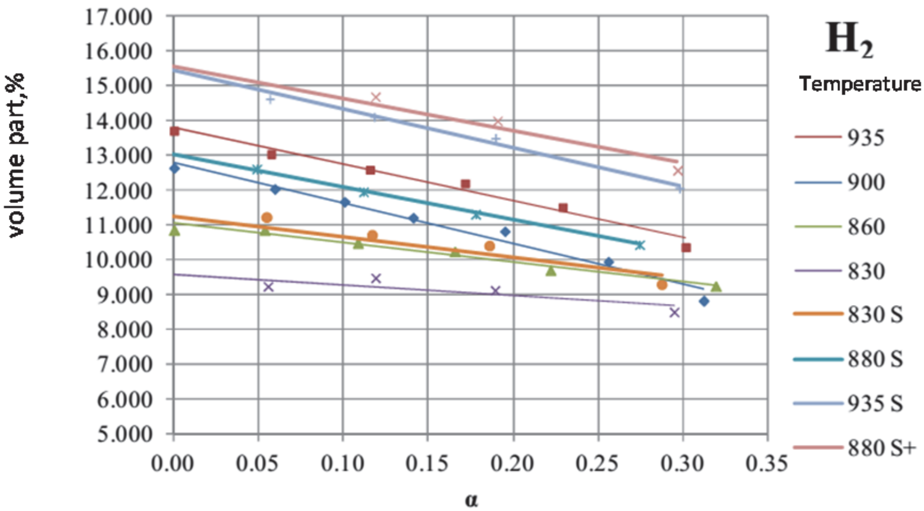

Figure 4.26. Graphs for the H_2 output at the warehouse generating gas

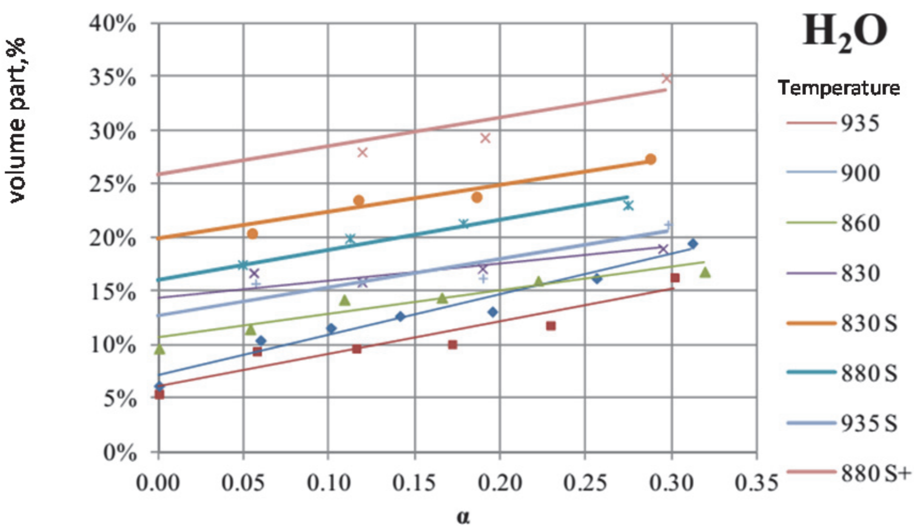

Figure 4.27. Graphs for the H_2O output at the warehouse generating gas

Checking the accuracy of the simulation

Checking the accuracy of the mathematical model of the gasification process is performed using the experimental data. For this, the correlation coefficients between the experimental and simulation results under the same gasification conditions and the relative error of the obtained data were determined.

The output data accepted for modeling are identical to the conditions for carrying out experimental studies of biomass gasification. The results of the comparison are shown in Figures 4.28–4.31.

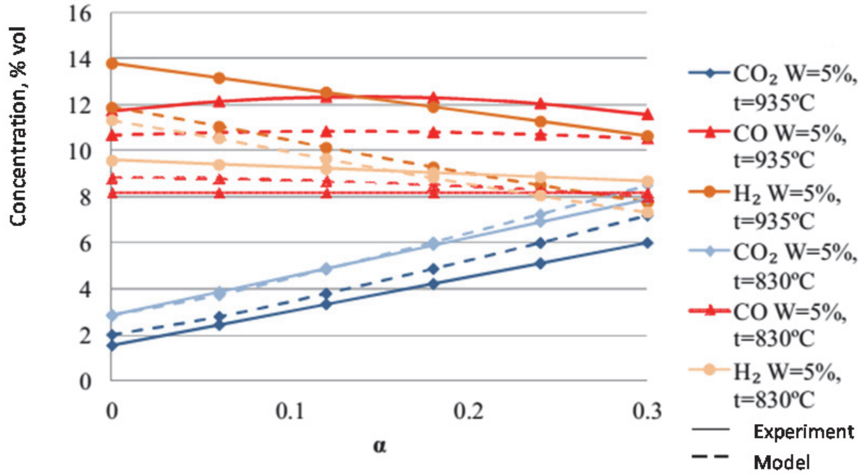

Figure 4.28. Component output graphs generator gas with variable α

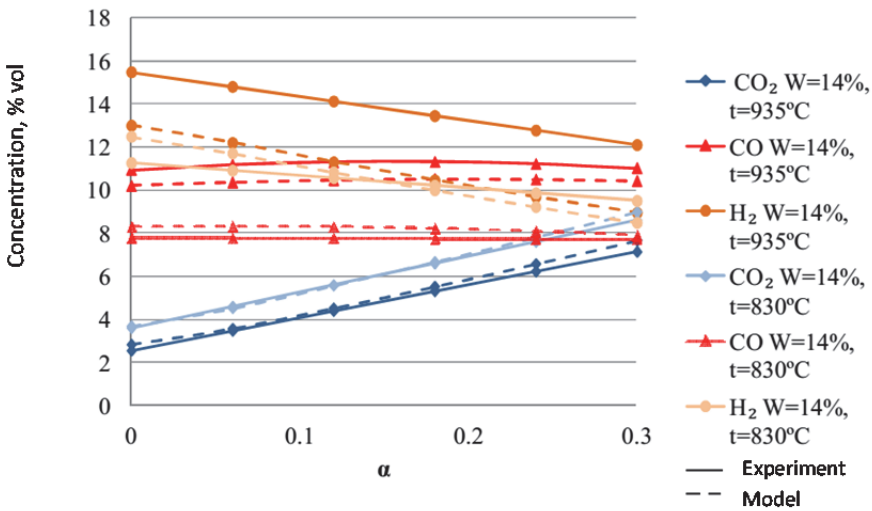

Figure 4.29. Component output graphs generator gas with variable α

Analysis of the results shows that correlation coefficients between experimental data sets and arrays of simulation results for the absolute majority of studies are 0.99 and higher, and only for some 0.85 ... 0.95. It is worth noting the high accuracy of modeling for low gas generation temperatures, the relative error in modeling the output of the components of the generator gas is 5% ... 10%. And a somewhat higher error at high temperatures is 15% ... 20%. Characteristic is a certain underestimation of the yield of the combustible components of the generator gas at high temperatures from the simulation results.

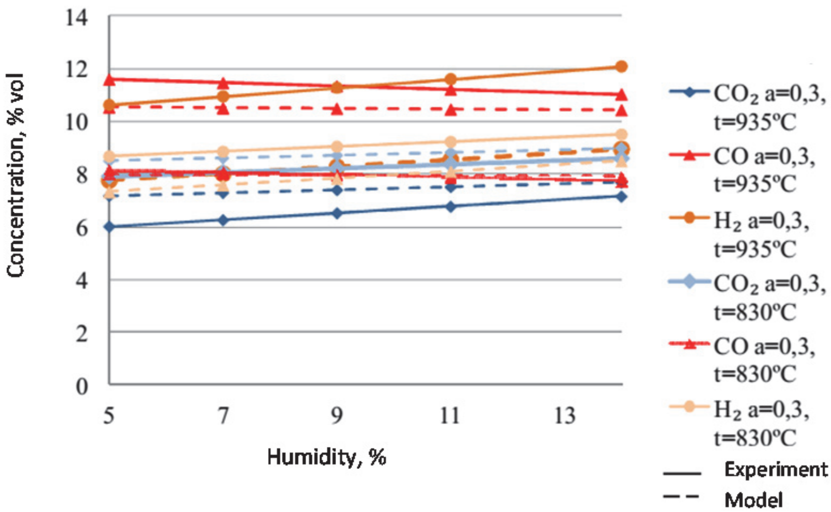

Figure 4.30. Component output graphs generator gas with variable humidity

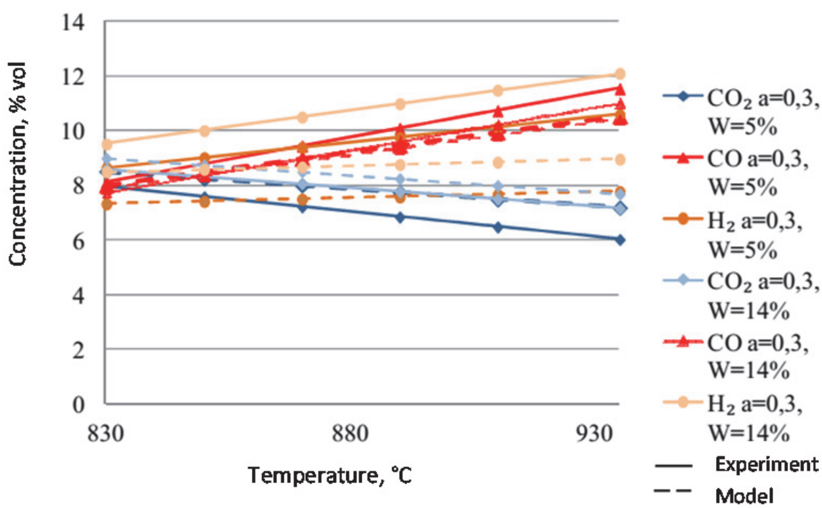

Figure 4.31. Component output graphs generator gas at variable temperature

This accuracy is quite high and allows us to objectively assess the effect of the parameters of the gasification process on its result.

4.5. CONCLUSIONS

1. The experimental test of the biomass gasification process was carried out in accordance with the methodology and with the use of equipment that allows the assessment of individual impacts of various gasification parameters on the process, and consequently the gas composition and efficiency of the installation. Biomass moisture (W_p), excess air coefficient of the process (α_{bio}) and reactor temperature (T_{react}) were chosen as the impact factors.
2. During the tests, the basic indicators of the gasifier operation were measured, in particular the biomass moisture, process temperature, mass and composition of the producer gas, the mass and composition of the tar, fuel consumption and electricity for the needs of process maintenance.
3. The processing of the received data allowed to create the mass and energy balance equation and to determine the impact of gasification parameters on the process's efficiency.
4. The tar mass analysis in the gasification process showed that the mass of tar largely depends on the process parameters. The tar composition test made it possible to determine the critical temperature of the generator gas in which the basic components of the tar condense.

A wide range of single and multifactor experimental studies of biomass gasification under various conditions was carried out. Experimental setup with compensation of energy losses of gas generator and taking into account the dynamics of exothermic reactions of oxidation of combustible components of biomass made it possible to investigate the effect of separate regime factors of the gas generator on the composition of the generator gas.

A mathematical model of the biomass gasification process was developed on the basis of minimizing the isobaric-isothermal potential (Gibbs energy) function to predict the composition of the generator gas and the technological parameters of the gasification plant. The obtained model gives high reliability of the predicted composition of the generator gas, the process temperature and the excess air factor in the reaction zone of the gas generator.

The obtained results can be used in the development of industrial installations for gasification of biomass.

REFERENCES

[1] Kaosol T., Sohgrathok N., *Enhancement of biogas production potential for anaerobic codigestion of wastewater using decanter cake*, Am. J. Agric. Biol. Sci., 7, 2013, pp. 494–502.

[2] Malakahmad A., Nasrudin S.B., Zain S.M., *Anaerobic transformation of biodegradable waste; simultaneous production of energy and fertilizer*, Am. J. Environ. Sci., 9, 2013, pp. 113–119.

[3] Puah C.W., Choo Y.M., Ong S.H., *Production of palm oil with methane avoidance at palm oil mill: A case study of cradle-to-gate life cycle assessment*, Am. J. Applied Sci., 10, 2013, pp. 1351–1355.

[4] Singh V.Ch.J., Sekhar J.S., Thyagarajan K., *Performance studies on downdraft gasifier with biomass energy sources available in remote villages*, "American Journal of Applied Sciences" 2014, 11 (4), pp. 611–622.

[5] Koroneos C., Lykidou S., *Equilibrium modeling for a downdraft biomass gasifier for cotton stalks biomass in comparison with experimental data*, "Journal of Chemical Engineering and Materials Science" 2011, Vol. 2(4), pp. 61–68.

[6] Kantorovich B.V., *Osnovy teorii goreniya i gazifikatsii tverdogo topliva*, M.: Izdatelstvo Akademii Nauk CCCP, 1958, p. 593.

[7] Lavrov N.V, *Fiziko-khimicheskiye osnovy goreniya i gazifikatsii topliva*, M.: Metallurgizda, 1957, p. 288.

[8] Zainal Z.A., Ali R., Lean C.H., Seetharamu K.N., *Prediction of performance of a downdraft gasifier using equilibrium modeling for different biomass materials*, "Energy Conversion and Management" 2001, Issue 42, pp. 1499–1515.

[9] Yang W., Ponzio A., Lucas C., Blasiak W., *Performance analysis of a fixed-bed biomass gasifier using high-temperature air*, "Fuel Processing Technology" 2006, No. 87, pp. 235–245.

[10] Jarungthammachote S., Dutta A., *Equilibrium modeling of gasification: Gibbs free energy minimization approach and its application to spouted bed and spout-fluid bed gasifiers*, "Energy Conversion and Management" 2008, Issue 49, pp. 1345–1356.

[11] Li X., Grace J.R., Watkinson A.P., Lim C.J., Ergudenler A., *Equilibrium modeling of gasification: a free energy minimization approach and its application to a circulating fluidized bed coal gasifier*, Fuel., Vol. 80, Issue 2, 2001, pp. 195–207.

[12] Skoulou V., Zabaniotou A., Stavropoulos G., Sakelaropoulos G., *Syngas production from olive tree cuttings and olive kernels in a downdraft fixed-bed gasifier*, "International Journal of Hydrogen Energy" 2008, Issue 33, pp. 1185–1194.

[13] Miao Q., Zhu J., Miao Q., Barghi Sh., Wu Ch., Yin X., Zhou Zh., *Modeling biomass gasification in circulating fluidized beds: Model sensitivity analysis*, "International Journal of Energy and Power" 2013, Vol. 2, Issue 3, pp. 57– 63.

[14] Pavlenko A., *Dispersed phase breakup in boiling of emulsion*, "Heat Transfer Research" 2018, Vol. 49 (7), pp. 633–641.

Chapter 5

SOLAR POWER SYSTEMS BASED ON STIRLING CYCLE MACHINES AND THERMOMOLECULAR TECHNOLOGY

Victor P. Stoudenets, Nikolay N. Tsyrin, Oleksiy V. Ievtushenko

Department of Heat Engineering and Energy Saving
National Technical University of Ukraine "Igor Sikorsky Kyiv Polytechnic Institute"

One of the ways of converting solar energy into electric is a machine one, in which the dynamic converters are thermal machines working under the cycles of Rankin, Brighton, Stirling. Within the framework of this method, two concepts for the creation of Solar Power Systems (SPS) are being developed:

- with a single general energy converter and a field of concentrating mirrors (heliostats);
- modular principle (including the creation of solar modules with Stirling Engine).

The Stirling Engine (SE) has been recognized as one of the most promising converters for both modular and autonomous SPS.

The perspective of this scientific and technological direction is universally accepted. In particular, the combination of SE with Solar Concentrators (SC) was recognized as one of three promising SPS for the period up to 2020 [1, 2].

5.1. SOLAR DISH/STIRLING SYSTEM BASED ON UDS-1 MACHINE

At the laboratory of the Institute of Energy Saving and Energy Management Igor Sikorsky Kyiv Polytechnic Institute the SPS "Solar Dish Concentrator – Stirling Engine – Generator" was designed. The design procedure is observed and the characteristic analysis of unit component elements is performed. The solar-electrical power conversion in the SPS is considered.

The objective is the analytical and experimental analysis of the key characteristics and efficiency of the SPS and its basic components.

The experimental SPS [3, 4] consists of (Figure 5.1): 1 – Solar Concentrator (SC); 2 – Stirling Engine (SE) UDS-1, with the hot space located in the SC focus; 3 – Electric Generator (EG) DP-2-26, connected via belt drive with SE pulley; 4 – Measuring equipment: Solar radiation, SE hot space and cooling radiator temperatures, SE rotational velocity, EG output voltage and current.

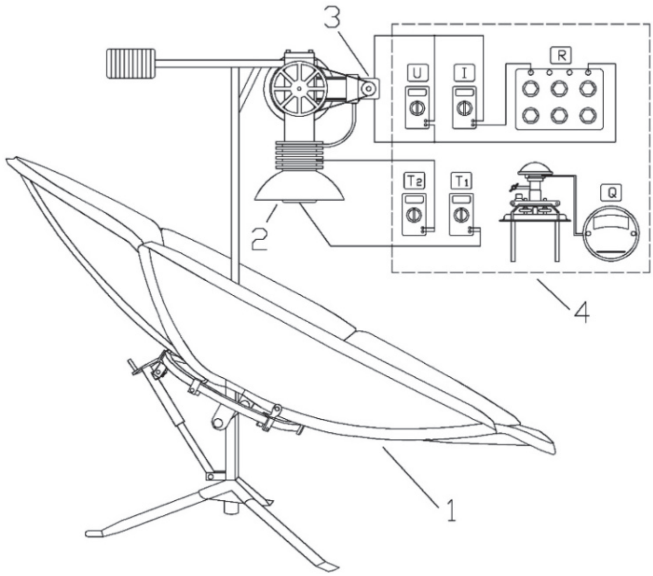

Figure 5.1. The operating solar dish/UDS-1 stirling system

Solar Concentrator

The SC (Figure 5.2) is a six-section (six-petal) dural parabolic dish, covered with the mirror foil, mounted on a tripod base with the ability to turn 360° and to aim. Table 5.1 shows the characteristics of the SC.

Figure 5.2. The solar concentrator

Table 5.1. Characteristics of Solar Concentrator

Midsection diameter	1.5 m
Midsection area	1.77 m^2
Focal length	0.6 m
Diameter/focal length ratio	2.5
Angular aperture	64°
Focal point diameter	0.1 m
Focal point area	$7.85 \cdot 10^{-3}$ m^2
Sun image area	$2.46 \cdot 10^{-5}$ m^2
Concentration ratio	28105
Concentration efficiency	0.235
Max focal point temperature	1000°C
Power	1800 W
Foil thickness	0.4 mm
Foil reflectivity factor	>85%
Gross weight	17 kg

Stirling Engine UDS-1

As a power conversion unit the model of UDS-1 was chosen [5–7]. UDS-1 (Figure 5.3) is a single-acting displacing type machine with power and displacing cylinders, inclined orthogonally (γ – coupling).

Table 5.2. Ratings of Stirling Engine UDS-1

Rated power	5 W
Angular velocity	500 rpm
Number of power cylinders	1
Combustion	External
Cooling	Air
Working fluid	Air
Coupling	Gamma
Weight	8 kg
Dimensions	340×160×170 mm

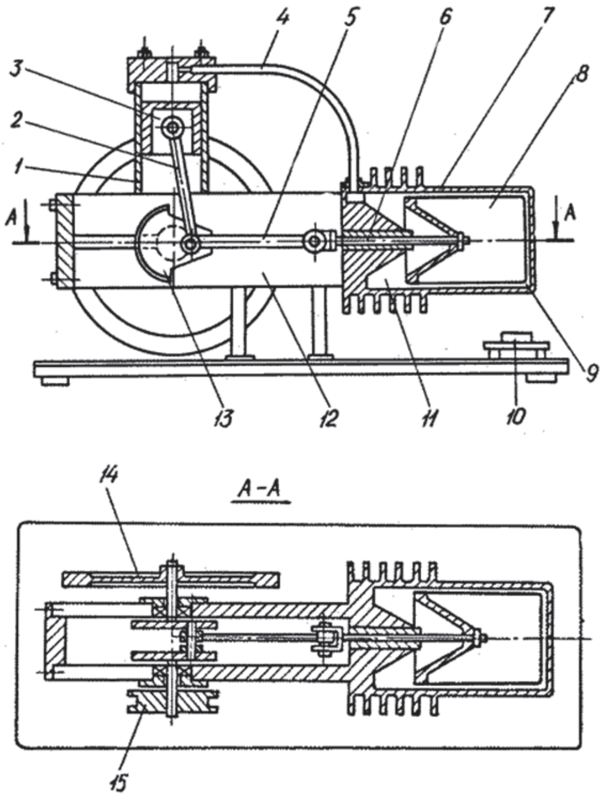

Figure 5.3. The Stirling Engine of UDS-1 model: 1 – power cylinder, 2 – connecting rod, 3 – power piston, 4 – tube of the internal contour, 5 – connecting rod, 6 – hob, 7 – cylinder, 8 – displacer piston, 9 – hot space, 10 – place for external supply of heat, 11 – cold space, 12 – body, 13 – crank, 14 – flywheel, 15 – pulley

Table 5.3. Basic Characteristics of Stirling Engine UDS-1

SE characteristic	Symbol	Magnitude
Power cylinder diameter	D	40 mm
Displacer cylinder diameter	D_d	65 mm
Displacer diameter	d	63.4 mm
Piston and displacer stroke	S	30 mm
Piston stroke/cylinder diameter ratio	SD	0.75
Working volume	V_H	37.68 cm^3
Total volume	V_T	130.86 cm^3
Dead volume	V_D	93.18 cm^3
Minimal pressure in working spaces	$p_{\min}$	0.1 MPa

Electric Generator

Technical characteristics of EG are determined, first of all, by UDS-1 velocity of rotation 500 rpm. EGs with initial voltage of 220 V and such nominal rotational velocity are characterized by considerable size that prevents their using in the construction of SPS. The installing of the multiplier is economically unfeasible. That's why the motor of DC-2-26 type was chosen as a generator, which is a DC machine with excitation from a permanent magnet. Its real image is shown in Figure 5.4, and passport specifications are presented in Table 5.4.

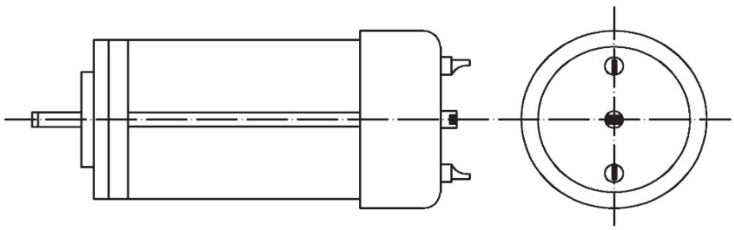

Figure 5.4. The electric motor of DC-2-26 type

Table 5.4. Passport Data of DC-2-26 Motor

Rotational frequency	3800 rpm
Current	1.2 A
Voltage	27 V ±2.7 V
Rated power	12 W
Rated rotary moment	0.0294 Nm
Weight	0.3 kg
Length	90 mm
Diameter	39 mm

5.2. EXPERIMENTAL RESEARCH OF SPS

The series of experiments with SPS based on UDS-1 Stirling machine were conducted in an enclosed space and open air with full reflecting area and without one, two and three SC sections. During the experiments the solar radiation, the SE hot space temperature, the cooling radiator temperature, the SE rotational velocity, the EG output voltage and current were measured. The results of the experiments are represented on the Figures 5.5–5.8.

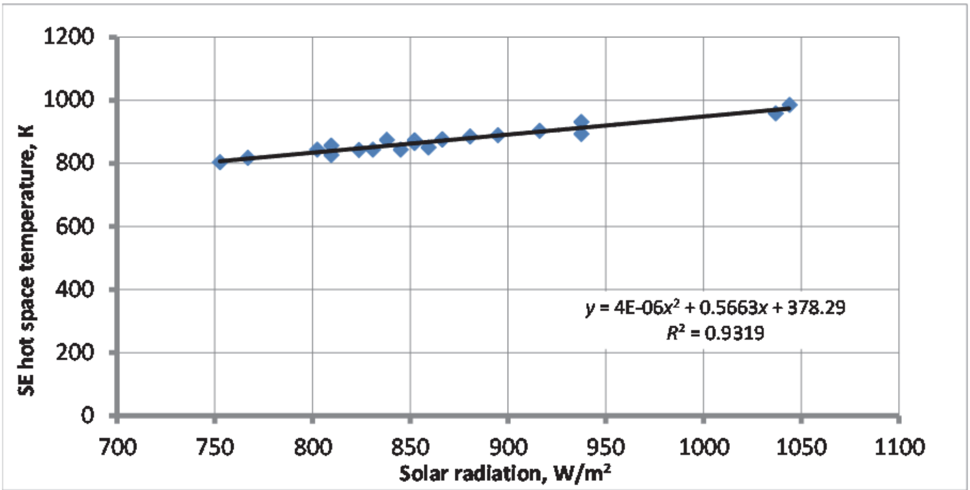

Figure 5.5. The dependence of SE hot space temperature on solar radiation

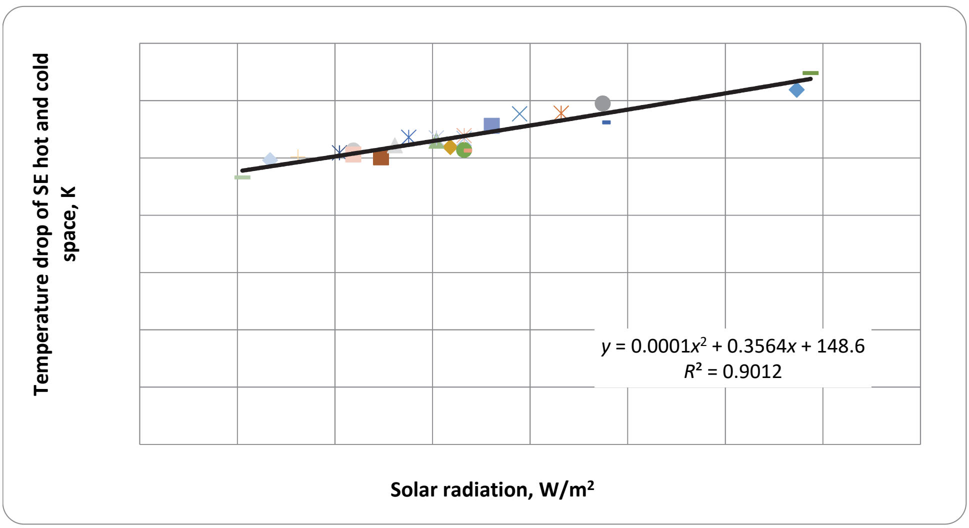

Figure 5.6. The dependence of SE temperature drop on solar radiation

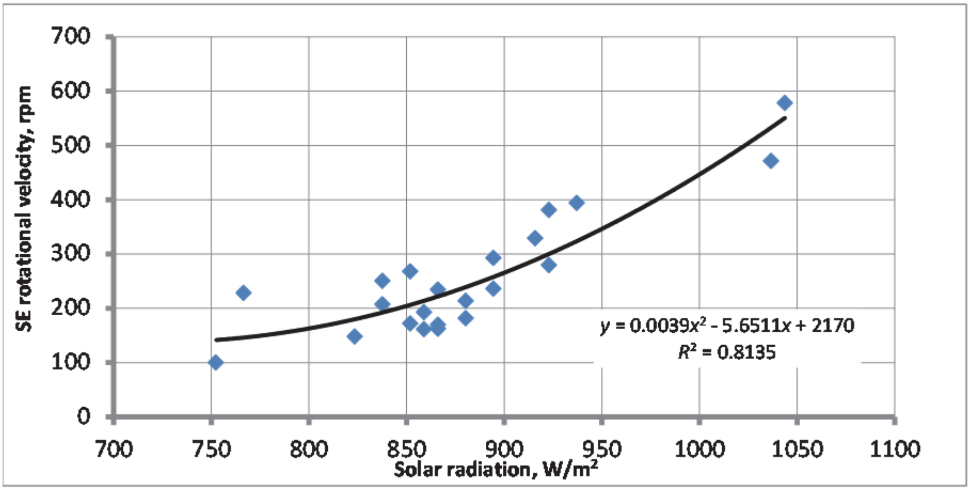

Figure 5.7. The dependence of SE rotational velosity on solar radiation

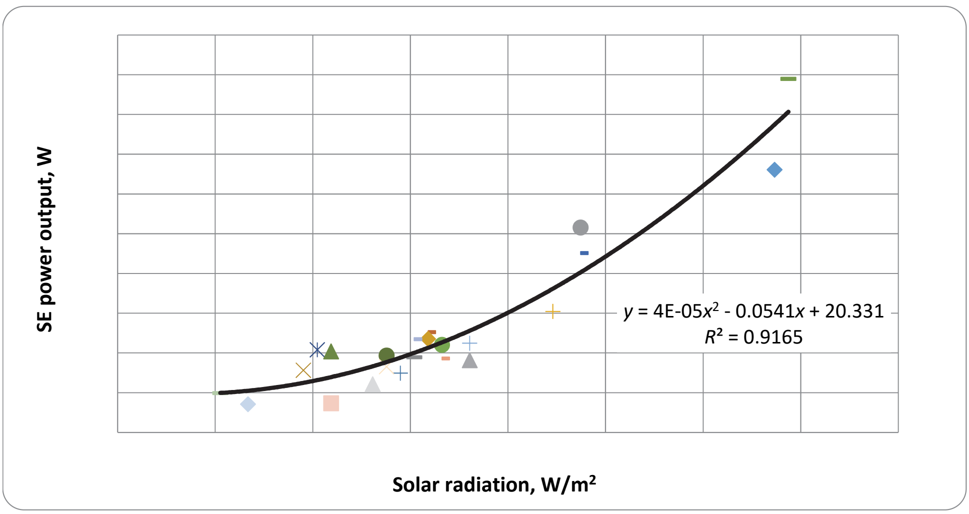

Figure 5.8. The dependence of SE power output on solar radiation

The experimental results establish the dependence between the solar radiation intensity and the temperatures of SE hot and cold space, SE rotational velocity and SE output power. With the increasing of solar radiation all above-mentioned parameters are growing independently on the place where the experiment was made, in the closed or open space, and on the amount of SC sections.

5.3. ANALYSIS OF SC CHARACTERISTICS

Initial parameters of SC

1. Midsection diameter $D = 1.5$ m.
2. Midsection area $A_C = \dfrac{\pi D^2}{4} = 1.77\ \text{m}^2$.
3. Focal length $f = 0.6$ m.
4. Diameter-focal length ratio $\dfrac{D}{f} = 2.5$.
5. Angular aperture $\dfrac{D}{f} = \dfrac{4\sin\theta}{1+\cos\theta}$, $\theta = 64°$.
6. Focal point diameter $d_f = 0.1$ m.
7. Focal point area $F_f = \dfrac{\pi d_f^2}{4} = 7.85 \cdot 10^{-3}\,\text{m}^3$.
8. Sun image area $F_S = \pi\left(\dfrac{f}{214.6}\right)^2 = 2.46 \cdot 10^{-5}\ \text{m}^2$.

Calculation of the Heat Flux [10, 11]

(The Heat Flux that can be achieved on the surface of the SE displacer cylinder).

1. The density of solar radiation $E_S = q_a$ (calculated by the indications of thermocouple pyranometer).
2. Heat flux that falls on the concentrator:

$$Q_F = E_S \cdot A_C = q_a \cdot A_C \tag{5.1}$$

3. Heat flux that falls on heat receiver (potentially available heat flux, passing through the sun image at the focus). Heat receiver has a flat surface (the butt end of the SE displacer cylinder).

$$Q_S = \eta_a \eta_r q_0 \left(\pi f^2\right) \sin^2\theta = \eta_r q_a (214.6)^2 F_S \sin^2\theta = \eta_r (214.6)^2 \sin^2\theta \cdot \frac{F_S}{A_C} Q_F \tag{5.2}$$

where: η_a – fraction of ideal solar constant which is available at the concentrator site, taking into account losses through the atmosphere; η_r – reflectivity efficiency factor taking into account losses by reflectivity or absorptivity of the optical system; q_0 – solar constant; $q_a = E_S$ – actual flux per unit area received at concentrator site.

4. The flux per unit area:

$$q_S = \frac{Q_S}{F_S} = \eta_a \eta_r q_0 \left(214.6\right)^2 \sin^2\theta = \eta_r q_a \left(214.6\right)^2 \sin^2\theta = \\ = \eta_r \left(214.6\right)^2 \sin^2\theta \cdot E_S \tag{5.3}$$

On the other hand:

$$Q_S = AQ_F = \rho_M \eta_P Q_F \tag{5.4}$$

where: A – reflection coefficient of the optical system; ratio of the energy got in the focal area of concentrator, to fallen on a mirror; in fact SC efficiency ($A \approx 0.45$); ρ_M – reflectivity factor of concentrator mirror surface ($\rho_M \approx 0.8$); η_P – efficiency factor of the concentrator positioning ($\eta_P \approx 0.6$).

$$q_S = \frac{Q_S}{F_f} \tag{5.5}$$

where $F_f = 7.85 \cdot 10^{-3}$ m^2 – focal point area.

5. The concentration ratio; ratio of solar flux in the sun image to the solar flux reflected by the flat concentrator surface, both per unit area, and is a function of the geometrical parameters of concentrator. For a cavity as a black body:

$$C = \frac{q_S}{\eta_r q_a} = \frac{q_S}{\eta_a \eta_r q_0} = \left(214.6\right)^2 \sin^2\theta \approx 46.1 \cdot 10^3 \sin^2\theta \tag{5.6}$$

For a flat plate receiver submits to the Lambert cosine law the ratio is the following:

$$C = 30.7 \cdot 10^3 \left(1 - \cos^3\theta\right) \tag{5.7}$$

6. The concentration efficiency; ratio of the total flux received within the sun image to the total flux which is received by the parabolic mirror. For a cavity as a black body:

$$\eta_C = \frac{Q_S}{\eta_r q_a \pi \left(D^2/4\right)} = \left(\frac{1 + \cos\theta}{2}\right)^2 \tag{5.8}$$

For a flat plate receiver submitting to the Lambert cosine law $\left(\varepsilon = \varepsilon_n \cos\theta\right)$:

$$\eta_C = \frac{\varepsilon_n}{6}\left(1+\cos\theta\right)\left(1+\cos\theta+\cos^2\theta\right) \tag{5.9}$$

where ε_n is the emissivity normal to radiating surface.

7. The heat flux per unit area in the points that lay down out of focal image (on the heating surface diameter) [4]:

$$q_{HS} = \frac{2q_S}{\sin^2\theta_1}\left[\cos\theta_1 - \ln\left(1+\cos\theta_1\right) + \frac{\sin^2\theta_1}{2} - \cos\theta_3 + \ln\left(1+\cos\theta_3\right) - \frac{\sin^2\theta_3}{2}\right] \tag{5.10}$$

where: $\theta_1 = \theta$; $\cos\theta_3 = \dfrac{-1+\sqrt{1+8\dfrac{r_f}{r}}}{2}$; $r_f = 0.05\,\text{m}$ – focal point radius; $r = 0.033\,\text{m}$ – heating surface radius.

8. The total heat flux:

$$Q_{HS} = q_{HS} \cdot F_{HS} \tag{5.11}$$

where $F_{HS} = 3.42 \cdot 10^{-3}\ \text{m}^2$ is heating surface area.

Calculations of Temperature

1. Temperature T_{HS}:

$$T_{HS} = \left(\frac{3q_{HS}}{2\varepsilon_{HS}\sigma_0}\right)^{0.25} \tag{5.12}$$

where $\varepsilon_{HS} = 0.6$ is the heating surface emissivity (brass oxidized by heating to 600°C).

2. The heat flux transmitted to the SE Working Fluid (WF):

$$Q_{WF} = \eta_a \eta_r q_0 2\left(\pi f^2\right)\alpha_n \int_{\theta_1}^{\theta_2} F\left(\theta\right)\sin\theta\cos\theta d\theta a \tag{5.13}$$

$$q_{WF} = \frac{Q_{WF}}{F_{HS}} = 2(214.6)^2 \eta_a \eta_r q_0 \alpha_n \int_{\theta_1}^{\theta_2} F\left(\theta\right)\sin\theta\cos\theta d\theta \tag{5.14}$$

for the particular case $\alpha = \alpha_n \cos\theta$:

$$Q_{WF} = \eta_a \eta_r q_0 \frac{2}{3}\left(\pi f^2\right)\alpha_n\left(1-\cos^3\theta\right) = \frac{2}{3}\alpha_n \frac{1-\cos^3\theta}{1-\cos^2\theta} Q_{HS} \tag{5.15}$$

$$q_{WF} = \frac{Q_{WF}}{F_{HS}} = \eta_a \eta_r q_0 \frac{2}{3}(214.6)^2 \alpha_n\left(1-\cos^3\theta\right) = \frac{2}{3}\alpha_n \frac{1-\cos^3\theta}{1-\cos^2\theta} q_{HS} \tag{5.16}$$

where α_n is the absorbtivity for normal incidence.

3. The heat receiver wall temperature (the WF temperature):
   for a flat plate receiver, when $\varepsilon = \varepsilon_n F(\theta)$:

$$q_{WF} = 2(214.6)^2 \eta_a \eta_r q_0 \alpha_n \int_{\theta_1}^{\theta_2} F(\theta)\sin\theta\cos\theta d\theta = 2\varepsilon_n \sigma T_m^4 \int_0^{\pi/2} F(\theta)\cos\theta\sin\theta d\theta \tag{5.17}$$

for a flat plate receiver, when $\varepsilon = \varepsilon_n \cos\theta$:

$$q_{WF} = \frac{2}{3}(214.6)^2 \eta_a \eta_r q_0 \alpha_n\left(1-\cos^3\theta\right) = \frac{2}{3}\varepsilon_n \sigma T_{WF}^4 \tag{5.18}$$

$$T_{WF} = \left(\frac{3q_{WF}}{2\varepsilon_n \sigma_0}\right)^{0.25} \tag{5.19}$$

Analysis of SE indicated characteristics by the Schmidt Method SE initial parameters

1. Working volume V_h = 37.68 cm^3.
2. Total volume V_a = 130.86 cm^3.
3. Dead volume $V_c = V_a - V_h$ = 93.18 cm^3.
4. Crank phase angle: α = 90°.
5. Volume compression ratio $\varepsilon = \dfrac{V_a}{V_c} = \dfrac{V_a}{V_a - V_h}$ = 1.4.

Schmidt theory assumptions

1. Processes of regeneration are ideal; there is a perfect regeneration.
2. Instant value of system pressure is constant.
3. Conditions of the working fluid are changed as an ideal gas.

4. Gas volume changes are sinusoidal.
5. Temperature of cylinder walls and piston is constant.
6. The expansion-compression processes are isothermal.
7. The amount of working fluid is constant.

Schmidt technique (2-cylinder scheme, γ-coupling) [11–13]

1. Cylinder working volume $V_S = 2rA_P$; where: r – crank radius, A_P – power piston sectional area.
2. Expansion space working volume V_{SE}.
3. Compression space working volume V_{SC}.
4. Power piston working space $V_{SP} = 31.4$ cm^3.
5. Power piston working space ratio $k_p = \frac{V_{SP}}{V_{SE}}$.
6. The total working volume $V_{ST} = V_{SE} + V_{SC} = V_{SE}\,(2 + k_P)$.
7. Dead volume V_D.
8. Dead volume ratio $X = \frac{V_D}{V_{SE}}$.
9. Total volume $V_T = V_{ST} + V_D = V_{SE}\,(2 + k_P + 2X)$.
10. Temperature ratio:

$$\xi = \frac{T_C}{T_E} = -\frac{W_C}{W_E} = -\frac{Q_C}{Q_E} \tag{5.20}$$

11. Pressure (mid, max, min):

$$\begin{gathered} p_{\mathrm{mid}} = p_{\max}\frac{(1-\delta)^{0.5}}{(1+\delta)^{0.5}} = p_{\min}\frac{(1+\delta)^{0.5}}{(1-\delta)^{0.5}} \\ p_{\min} = p_{\max}\frac{1-\delta}{1+\delta} \\ p = p_{\max}\frac{1-\delta}{\left[1+\delta\cos(\phi-\theta)\right]} \end{gathered} \tag{5.21}$$

where: $\delta = \frac{B}{S}$; $B = \left(k_p^2 + 2k_p + 2k\cos\alpha(\xi-1) + (\xi-1)^2\right)^{0.5}$,

$$S = \xi + k_p + 1 + \frac{4X\xi}{\xi+1};\ \theta = \mathrm{arctg}\left(\frac{k\sin\alpha}{\xi + k\cos\alpha}\right).$$

12. Transfer of energy:

$$Q_E = W_E = \frac{p_{\max}\delta V_{SE}\pi\sin\theta(1-\delta)^{0.5}}{(1+\delta)^{1/2}\left[1+\left(1-\delta^2\right)^{0.5}\right]} \tag{5.22}$$

$$Q_C = W_C = \frac{p_{\max}\delta k V_{SE}\pi\sin(\theta-\alpha)(1-\delta)^{0.5}}{(1+\delta)^{0.5}\left[1+\left(1-\delta^2\right)^{0.5}\right]} \tag{5.23}$$

13. Effective cycle work:

$$W_T = W_E - W_C = W_E - \xi W_E = W_E(1-\xi) = Q_E(1-\xi) \tag{5.24}$$

$$W_T = \frac{p_{\max}\delta V_{SE}(1-\xi)\pi\sin\theta(1-\delta)^{0.5}}{(1+\delta)^{0.5}\left[1+\left(1-\delta^2\right)^{0.5}\right]} = \frac{p_{\text{mid}}\delta V_{SE}(1-\xi)\pi\sin\theta}{\left[1+\left(1-\delta^2\right)^{0.5}\right]} \tag{5.25}$$

where: $\sin\theta = \dfrac{k_P\sin\alpha}{B}$; $B = \left[(\xi-1)^2 + 2(\xi-1)k_p\cos\alpha + k_p^2\right]^{0.5}$.

14. Volume compression ratio $r_V = \dfrac{1+k_P+X}{1+X}$.

SE power by Schmidt $P_S = W_T N$; where N is rotational velocity.

SE efficiency $\eta_t = \eta_K = \dfrac{W_T}{Q_E} = 1-\xi$.

Analysis of EG efficiency and SPS overall efficiency

1. EG efficiency $\eta_{EG} = \dfrac{W}{P}$; where: W – EG power, P_S – SE power.
2. SPS efficiency $\eta_{SPS} = \eta_{EG}\cdot\eta_{SE}\cdot\eta_{SC}$.

The analysis can be conducted by two methods: using the experimental or calculated values of working fluid temperature in the SE hot space. The expected parameters of both approaches are represented graphically on Figures 5.9–5.12, where the results of analytical calculation are presented by a black line, and experimentally-analytical by red. In both cases with the increasing of solar radiation the values of working fluid temperature, SE power output, SE efficiency and SPS efficiency are growing.

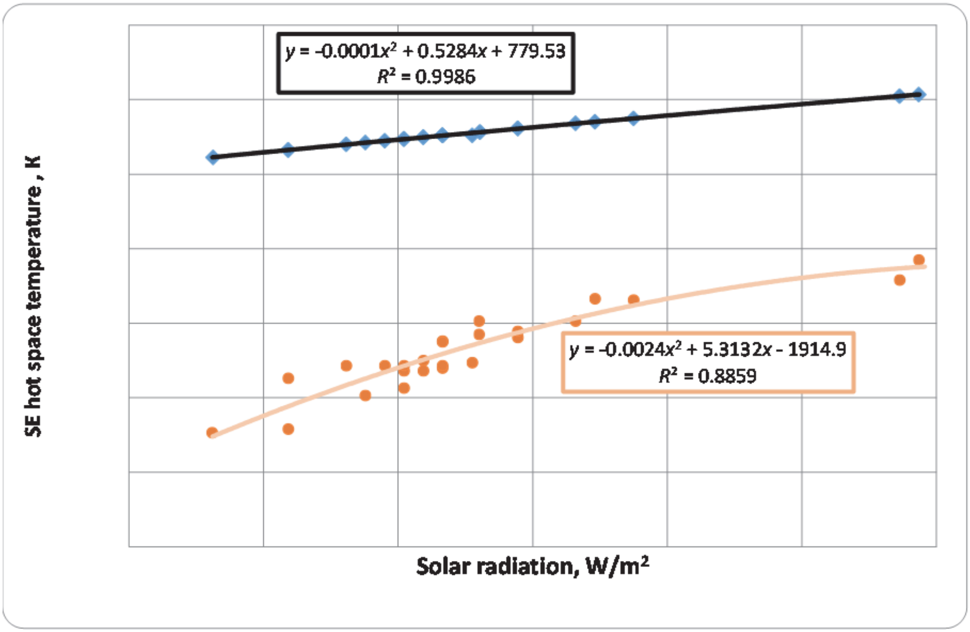

Figure 5.9. Dependence of the SE hot space temperature on solar radiation

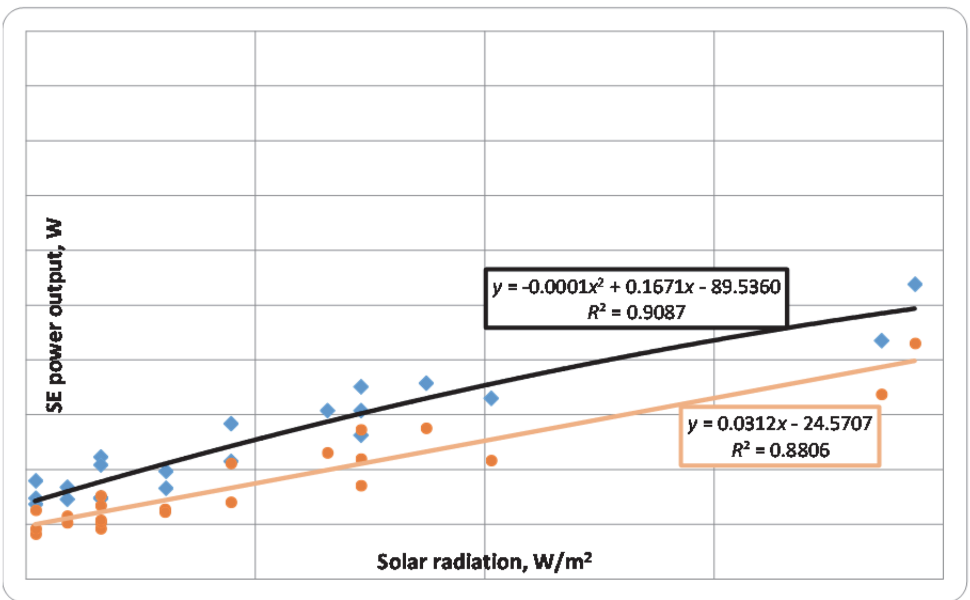

Figure 5.10. Dependence of the SE power output on solar radiation

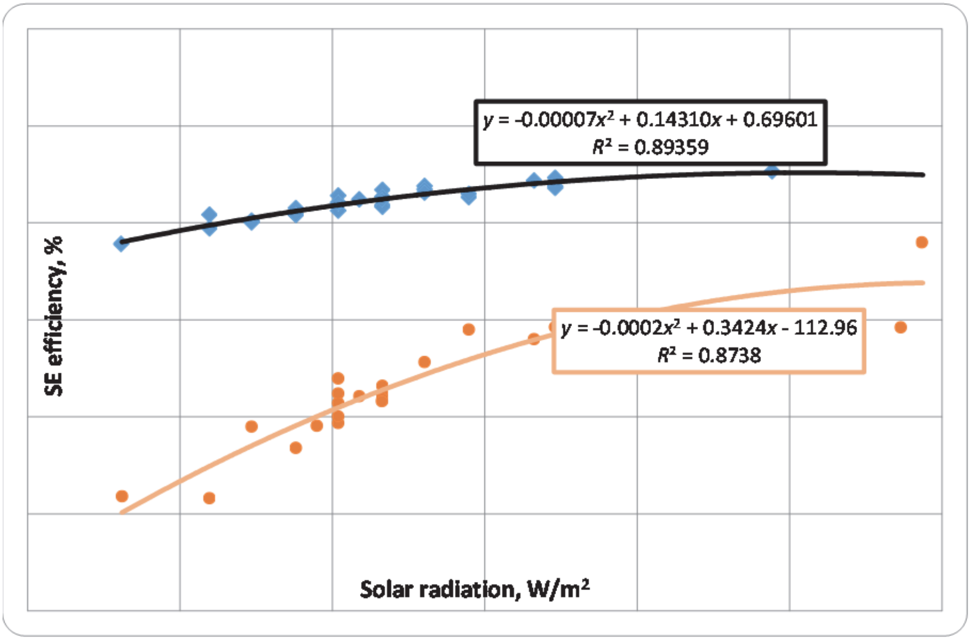

Figure 5.11. Dependence of the SE efficiency on solar radiation

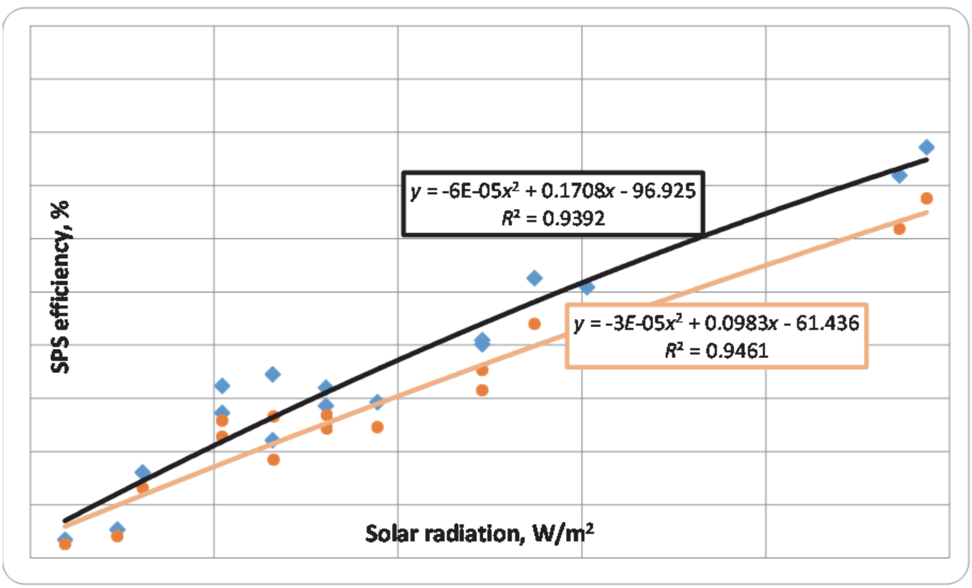

Figure 5.12. Dependence of the SPS overall efficiency on solar radiation

Conclusions

The effect of solar radiation intensity on SE temperature drop and consequently SE power output and SPS electric power is obtained by two approaches: using the experimental or calculated values of working fluid temperature in the SE hot space.

It is shown that the analytical values of SE hot space temperature are seriously above the experimental values. As a result using the hot space temperature experimental data make the SPS characteristic analysis more adequate to real work of SPS and its unit components.

The final calculated parameters of SPS (solar radiation range 753–1044 W/m^2):

– SC efficiency is 45%;
– SE efficiency is 55–68%;
– EG efficiency is 5–44%;
– SPS overall efficiency is 1–14%.

The SPS efficiency can be increased by the lowering of the SE cold space temperature (for example, by air cooling the SE radiator) and by the increasing of working fluid pressure in the SE internal contour.

5.4. SOLAR DISH/STIRLING SYSTEM BASED ON UDS-1 MACHINE WITH REJECTED HEAT RECOVERY

In the process of improving the functioning of the SPS based on UDS-1 and parabolic SC, a constructive upgrade of the SPS was carried out at the laboratory of the Institute of Energy Saving and Energy Management, which was to transfer the UDS-1 from air cooling to water. For that, the water circuit consisting of the water jacket in the engine cooling fins zone, the inlet and outlet water pipes, the water tank and the solar water pump were added to the SPS design. Constructively the water jacket with the pipes and the tank is, respectively, the transparent plastic volume, containing fins, plastic water hoses and the plastic container with a volume of 5 liters.

The modernization allows, firstly, to lower the temperature of the engine cold space and, thus, to increase its efficiency, and secondly, to get heated water, which can be used for household needs.

The main element of the UDS-1 water cooling system is the water pump on SP2-320607 solar battery (Figure 5.13). Passport characteristics are given in Table 5.5.

Figure 5.13. Solar Water Pump on SP2-320607 Solar Battery

Table 5.5. Passport Data of Solar Water Pump

Voltage max, V	5.76
Current max, mA	347
Rated power, W	2
Performance max, l/h	175

The series of experiments was conducted to determine the main operating characteristics of the SPS. During the experiments the solar radiation q, the SE hot space temperature T_1, the cooling water temperature T_2, the SE rotational velocity n, the EG output voltage V and current I were measured. The results of the experiments are represented in Table 5.6 and Figures 5.14–5.19.

Table 5.6. Experimental Data

No.	q, W/m^2	t_1, grad	t_2, grad	dt, grad	n, rpm	R, Ohm	I, mA	U, V	P, W
1.	795.2	523	37	486	153	15	69.7	1.07	0.1475
2.	802.3	528	38	490	181	15	76.7	1.02	0.1665
3.	809.4	532	39	493	192	15	81.6	1.25	0.2019
4.	822.6	545	41	504	203	15	82.5	1.26	0.2060
5.	837.8	555	40	515	252	15	82.7	1.33	0.2126
6.	844.9	569	42	527	263	15	87.1	1.35	0.2314
7.	852.0	580	44	536	276	15	87.6	1.38	0.2360
8.	859.1	591	45	546	278	15	92.1	1.31	0.2479

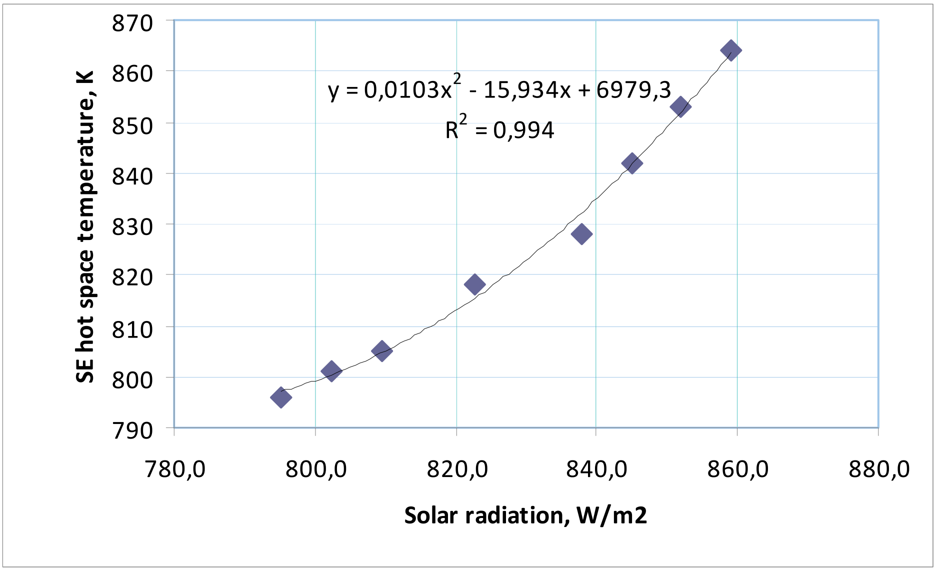

Figure 5.14. Dependence of the SE hot space temperature on solar radiation

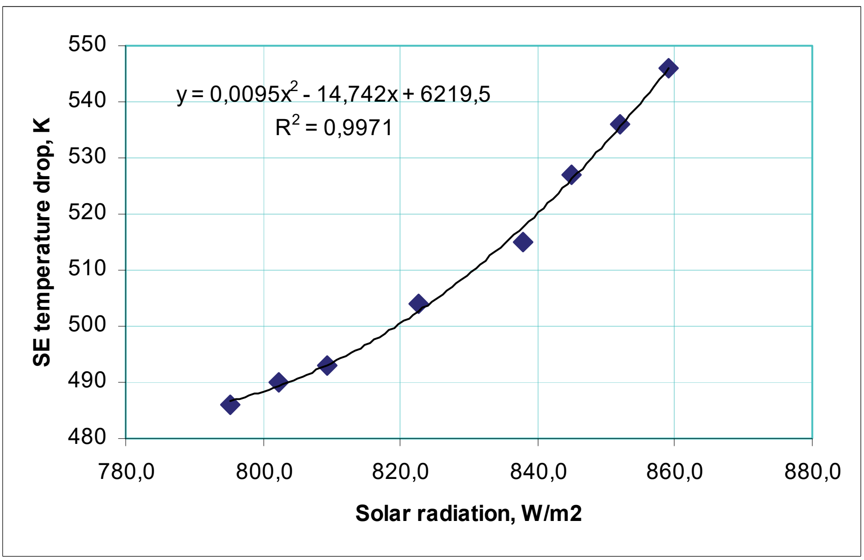

Figure 5.15. The dependence of SE temperature drop on solar radiation

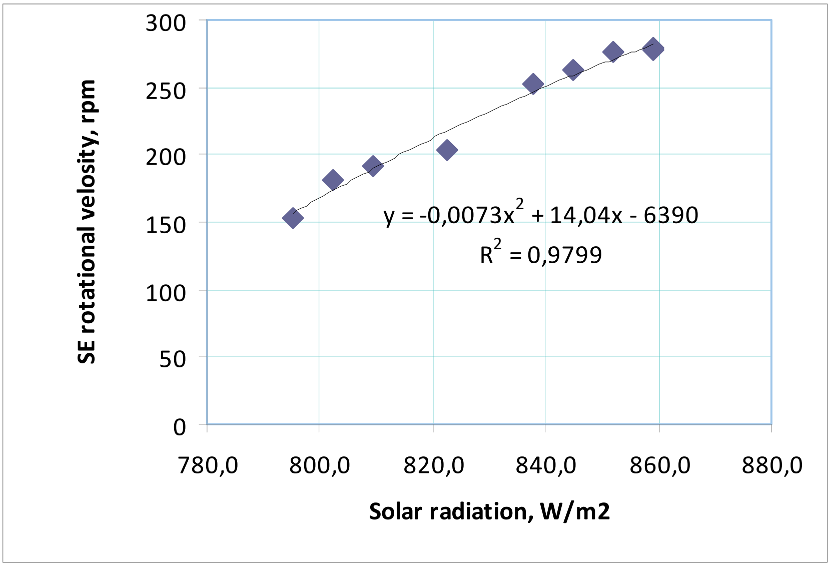

Figure 5.16. The dependence of SE rotational velosity on solar radiation

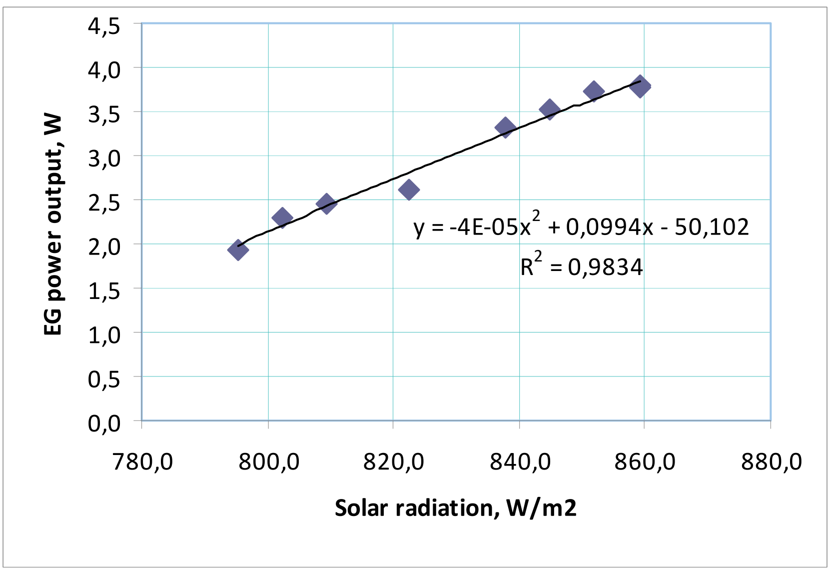

Figure 5.17. Dependence of the SE power output on solar radiation

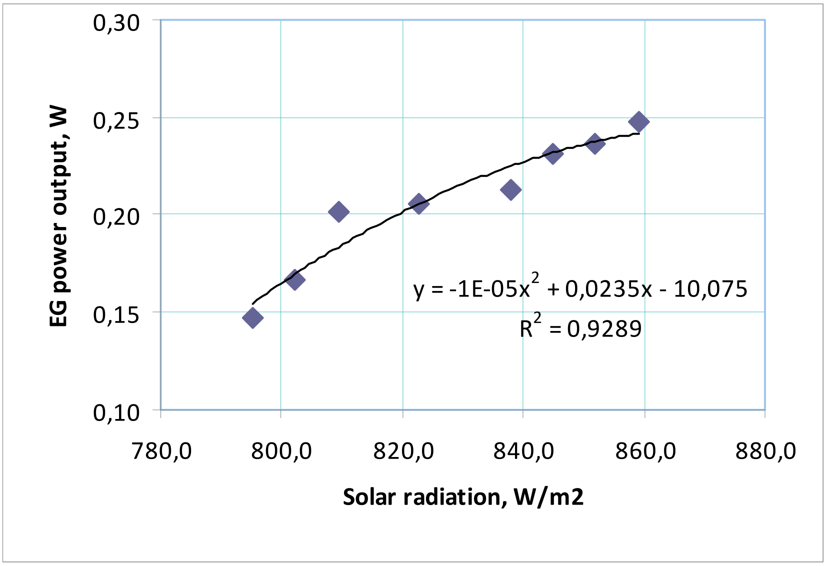

Figure 5.18. The dependence of EG power output on solar radiation

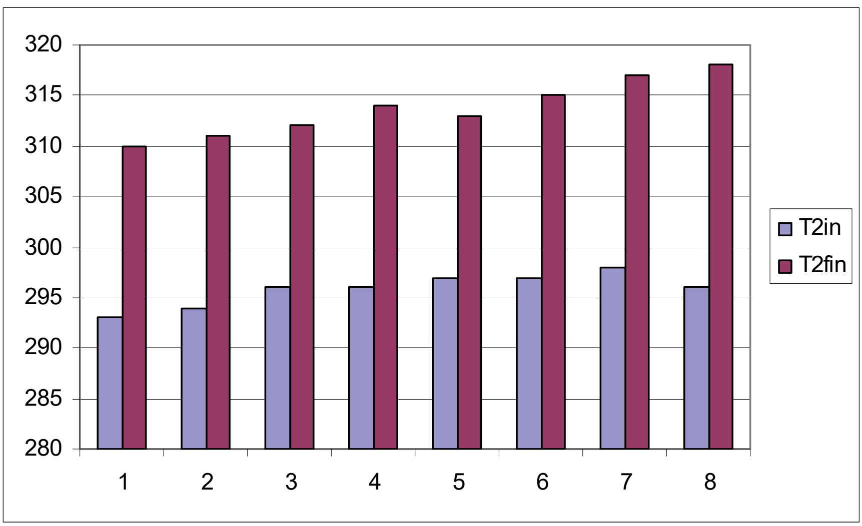

Figure 5.19. Increase in SE cooling water temperature after 5 minutes of SE operation

5.5. SOLIDWORKS SIMULATION OF THE REJECTED HEAT OF THE SPS BASED ON UDS-1

General information and simulation tasks

The working fluid of UDS-1 is an air whose thermophysical properties can be considered as of ideal gas for the modeling process. During the UDS-1 operation the working fluid is heated to the high temperature, so that the expansion takes place and the power piston moves while doing work. To return the piston to its original state, it is necessary to cool the working fluid. The larger the difference between the SE hot and cold spaces, the better the process takes place. Therefore, one of the tasks of SE efficient operation is the heat removal from the SE cold space. There are some fins to increase the heat transfer area. And when the fins are washed with water, the heat removal process is improved.

That process was modeled in SolidWorks software. Due to that it can be seen clearly how the temperature of the fins and the SE cold space changes.

For simulation a real object was taken, the fins are made of steel in the amount of 6 with a thickness of 5 mm, a height of 15 mm, and a step of 5 mm between them. The limiting condition was the temperature inside the cylinder 1000°C.

The task was to simulate the process of changing the SE fin surface temperature, depending on the change in the washing substance velocity. And the comparison of the amount of heat removed of the SE fins with the air and water [14, 15].

Modeling of heat removed of the SE fins at air washing

Experiments have been carried out for different velocities of air supply to the SE fins. The following speeds were used: 0.1 m/s, 0.3 m/s, 0.5 m/s.

With the help of the program, one can observe how the temperature of the air, fins and fin free spaces changes after air passing through the SE fins. Figures 5.20–5.22 show the change in the air temperature after passing through the fins.

As can be seen from the above figures, air after passing through the fins and fin free spaces is heated, taking part of heat from the fins, while cooling the air inside the SE cylinder.

Modeling of heat removed of the SE fins at water washing

For the next research, instead of the air that washes the cylinder, water was used. At the same time, the cylinder itself was placed in a jacket in which through the canal the water was fed.

The design of the cylinder has not changed. The boundary conditions under which the calculation was made were changed. The following mass flow rate of water at the entrance to the jacket was given: 0.001 kg/s; 0.0015 kg/s; 0.0017 kg/s.

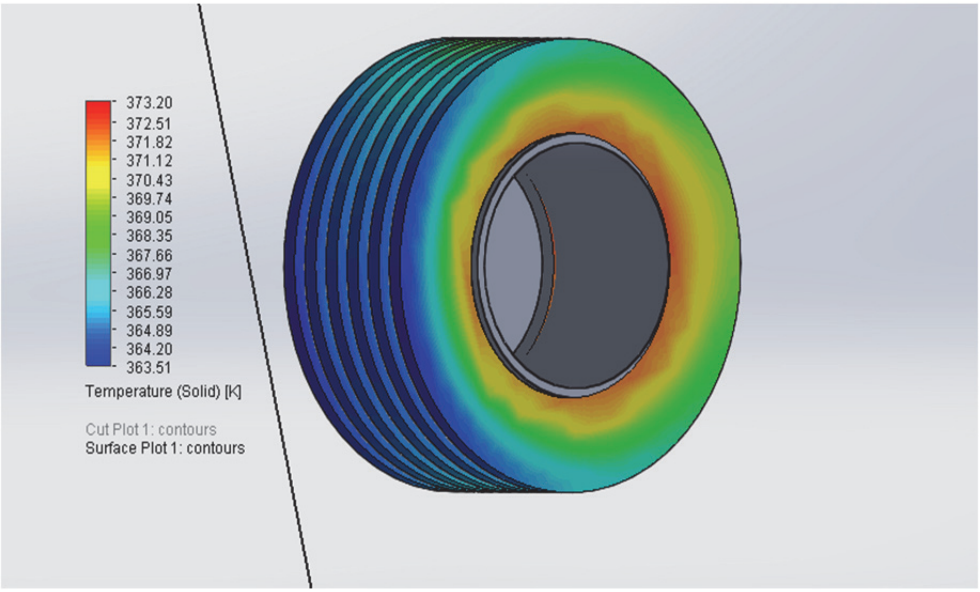

Figure 5.20. Temperature change of the SE fins

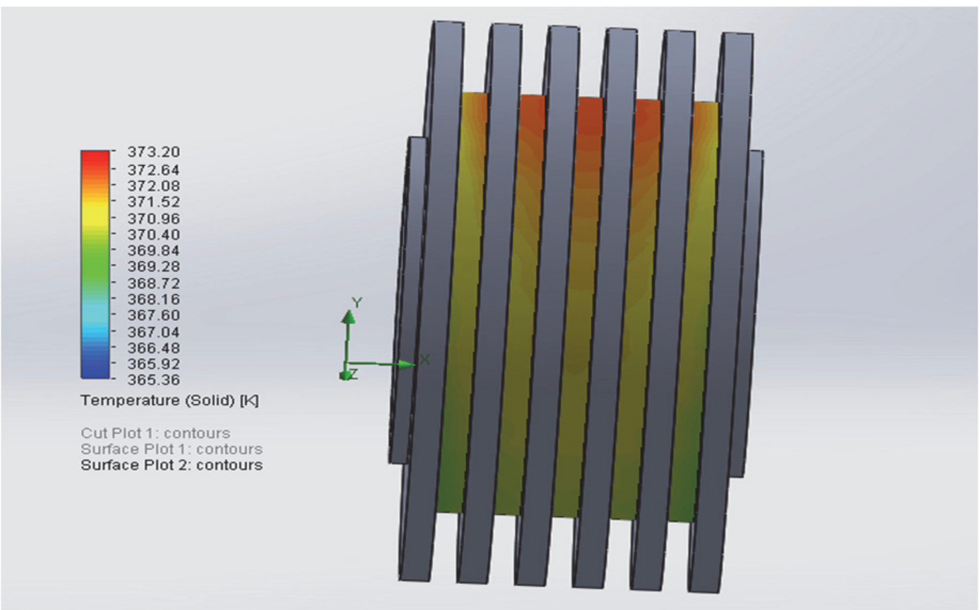

Figure 5.21. Changes in temperature in the fin free spaces

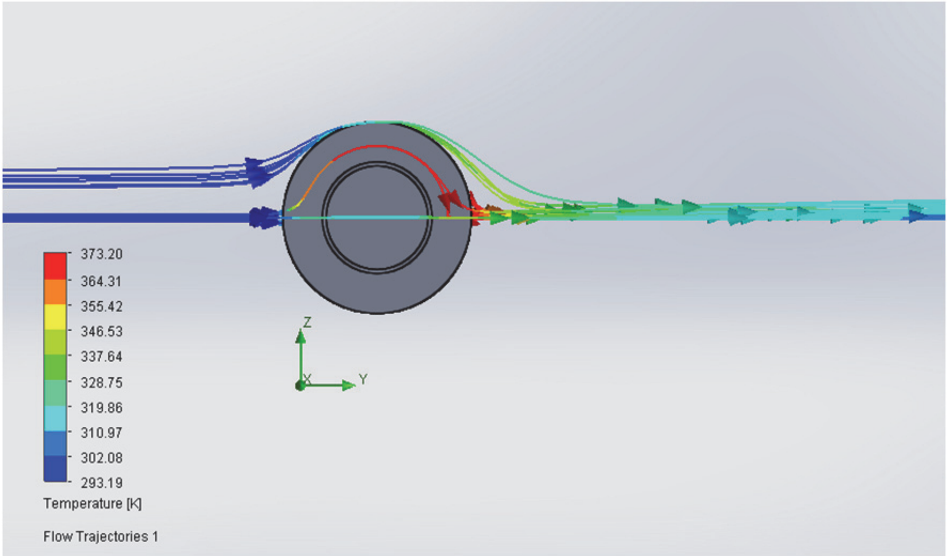

Figure 5.22. Path and change in air temperature

Figures 5.23–5.25 show the change in the water temperature after passing through the fins. Water supply was carried out at a temperature of 20°C. After washing the fins of the cylinder, the water removed part of the heat and warmed up. According to this simulation, the water heated to 60°C. Further it can be used for household purposes.

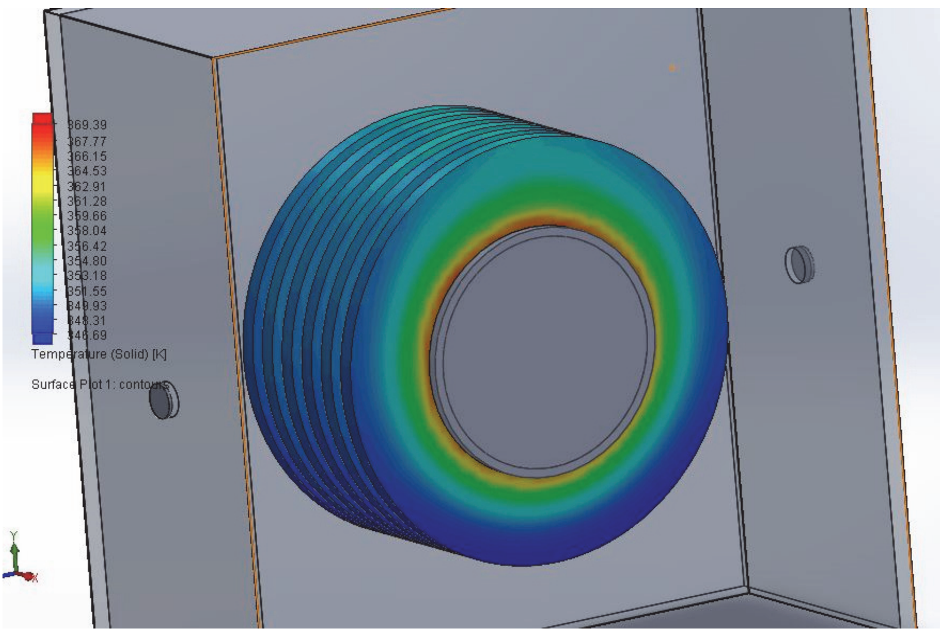

Figure 5.23. Temperature change of the SE fins

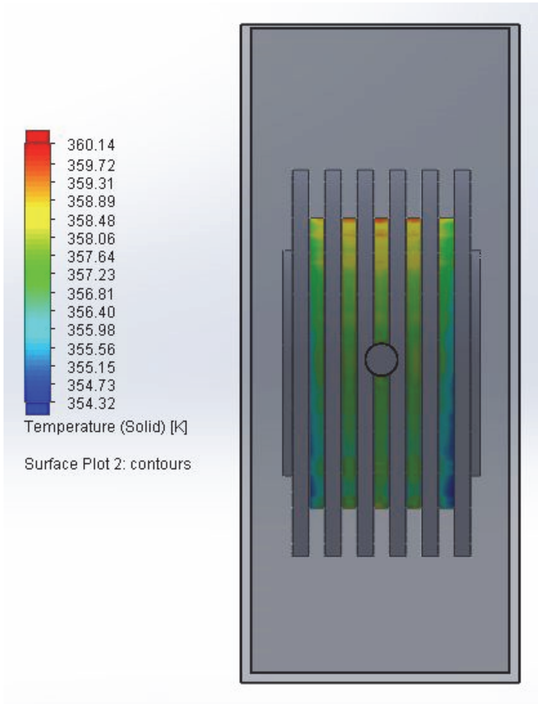

Figure 5.24. Changes in temperature in the fin free spaces

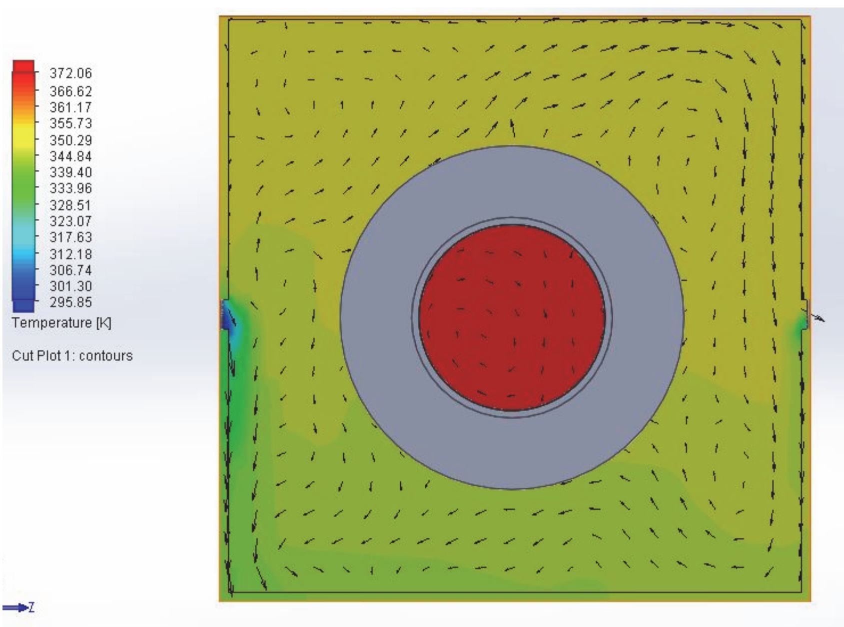

Figure 5.25. Path and change in water temperature

The results of the simulation are given in Tables 5.7 and 5.8 and are presented in the form of comparative graphs (Figures 5.26 and 5.27).

Table 5.7. The value of the surface heat flux in the fin free spaces

Exp.	Surface heat flux (air), W/m^2	Surface heat flux (water), W/m^2
1.	1269.2	3001.8
2.	1396.4	3351.3
3.	2026.9	4154.2

Table 5.8. The value of the surface heat flux on the fins of the SE cylinder

Exp.	Surface heat flux (air), W/m^2	Surface heat flux (water), W/m^2
1.	1872.3	3698.1
2.	2357.7	4588.7
3.	2790.5	5787.0

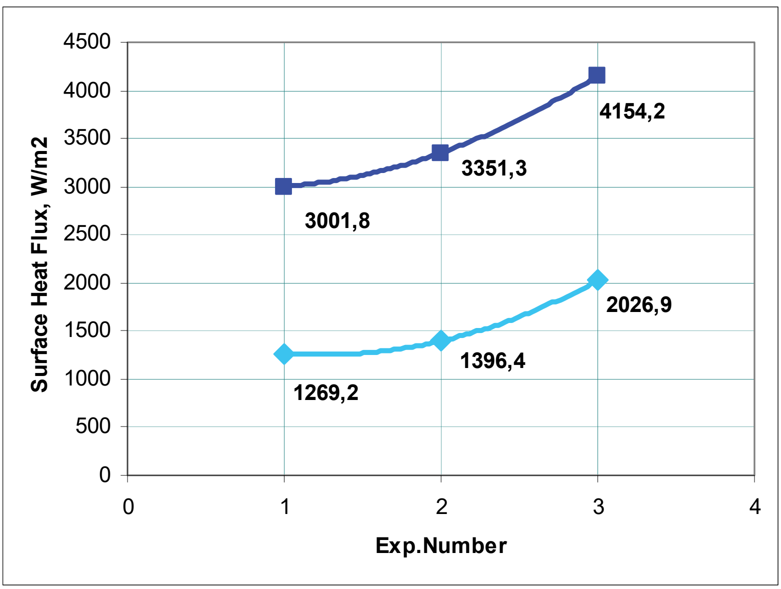

Figure 5.26. Comparison of the surface heat flux in the fin free spaces

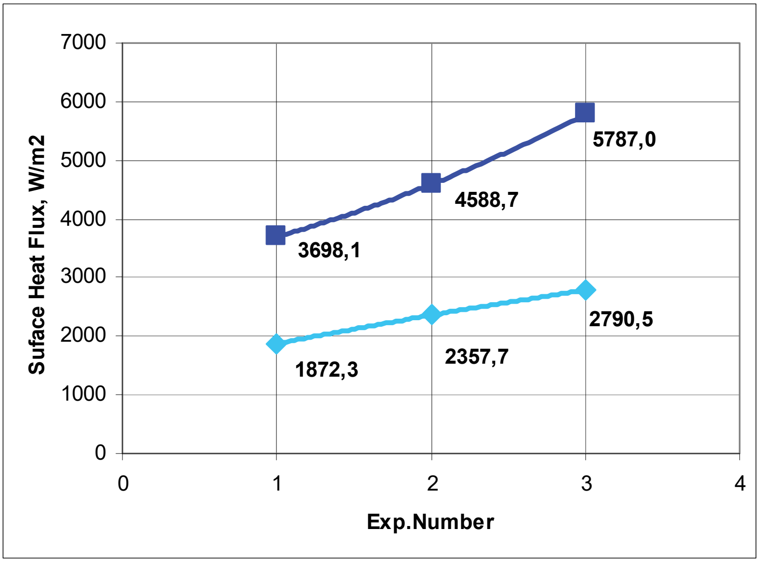

Figure 5.27. Comparison of the surface heat flux on the fins of the SE cylinder when washed with air and water

Thus, the increase in the intensification of heat removal from the SE finned surface depends on the fluid heat capacity and on the fluid speed of washing the surface.

According to the results of the modeling above, the conclusion is made that the use of water cooling improves the process of heat recovery in 2–2.2 times.

Calculation of the SPS overall efficiency, depending on solar radiation

In accordance with the methodology given above (see analysis), the calculations of the SPS elements basic characteristics and the conversion process efficiency were performed. The results are presented in Table 5.9.

Table 5.9. SPS elements efficiency and overall efficiency

No.	η_{SC}	η_{SE}	η_{EG}	η_{SPS}
1.	0.45	0.611	0.076	0.021
2.	0.45	0.612	0.072	0.020
3.	0.45	0.612	0.082	0.023
4.	0.45	0.616	0.079	0.022
5.	0.45	0.622	0.064	0.018
6.	0.45	0.626	0.066	0.019
7.	0.45	0.628	0.064	0.018
8.	0.45	0.632	0.065	0.019

SPS overall efficiency:

$$\eta_{SPS} = \eta_{SC} \cdot \eta_{SE} \cdot \eta_{EG} \tag{5.26}$$

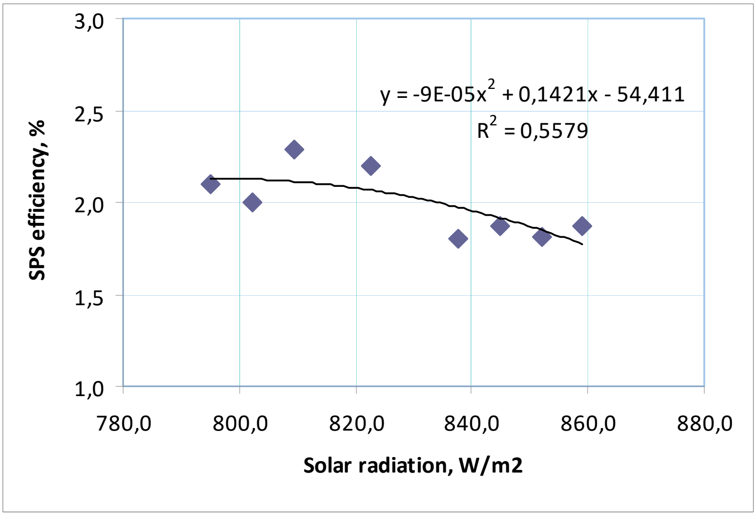

Figure 5.28. Dependence of the SPS overall efficiency on solar radiation

Estimation of the SPS with Heat Recovery overall efficiency, depending on solar radiation

The amount of heat obtained by cooling water during the SPS operation (τ = 5 min):

$$Q = c_{H_2O} m_{H_2O} \left(T_{2fin} - T_{2in}\right) \tag{5.27}$$

where c_{H2O} = 4.19 kJ/kg·K is specific heat capacity of cooling water; m_{H2O} = 2.2 kg – mass of cooling water.

Heat flow to cooling water:

$$Q_{H2O} = Q_{\tau} / \tau \tag{5.28}$$

where τ = 300 sec. is operation time.

SPS with Heat Recuperation overall efficiency:

$$\eta_{SPS(HR)} = \frac{E_{\Sigma}}{Q_F} = \frac{W_{EG} + Q_{H_2O}}{Q_F} \tag{5.29}$$

The estimated values of the SPS with Heat Recovery efficiency are given in Table 5.10.

Table 5.10. Estimation of the SPS with Heat Recovery overall efficiency

T_{2in}, K	T_{2fin}, K	Q_F, W	Q_{H_2O}, W	W_{EG}, W	Q_Σ, W	$\eta_{SPS(HR)}$
293	310	795.2	522.4	0.147	522.50	0.66
294	311	802.3	522.4	0.166	522.52	0.65
296	312	809.4	491.6	0.202	491.83	0.61
296	314	822.6	553.1	0.206	553.29	0.67
297	313	837.8	491.6	0.213	491.84	0.59
297	315	844.9	553.1	0.231	553.31	0.65
298	317	852.0	583.8	0.236	584.04	0.69
296	318	859.1	676.0	0.248	676.23	0.79

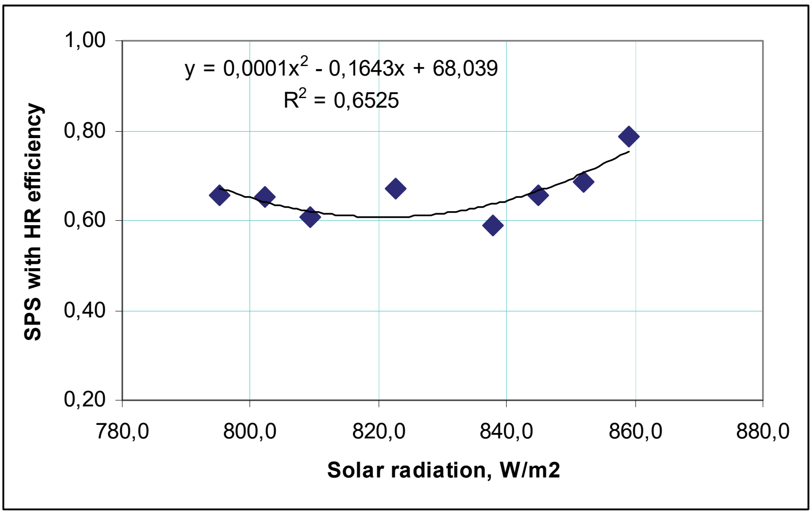

Figure 5.29. Dependence of the SPS with Heat Recovery overall efficiency on solar radiation

Conclusions

After the constructive upgrade of the SPS, which was to transfer the UDS-1 from air cooling to water, the new experiments were carried out and the following results were obtained that characterize the efficiency of the SPS elements:

– SC efficiency is 45%;
– SE efficiency is 61–63%;
– EG efficiency is 6.4–8.2%.

For SPS as a unit the following results were obtained (without recuperating heat): SPS overall efficiency is 1.8–2.3%.

Taking into account that the solar radiation rang in the experiments was 790–860 W/m^2, the obtained efficiency values correlate with the results obtained before at the higher solar radiation (see Part I).

Taking into account the work of the heat recovery system, the estimation of the SPS overall efficiency gave the following result: SPS with HR overall efficiency is 59–79%.

Thus, the transition to UDS-1 water cooling and the water heating system availability significantly improved the work of the SPS.

5.6. SOLAR WATER-HEAT SUPPLY SYSTEM WITH ACTIVE THERMODYNAMIC CIRCUIT BASED ON HYDRAULIC PISTON CONVERTER

Further development of SPSs with solar concentrators and dynamic converters based on Stirling cycle heat machines may be associated with the new class of thermodynamic converters operating under the Stirling cycle with liquid pistons, which was developed at the Republic of Uzbekistan Academy of Science Institute of Physics and Technology on the basis of the new technology for the transformation of thermal energy, implemented on the principle of pneumohydraulic self-oscillating systems.

The hydraulic piston converter (HPC) thermodynamic cycle is the combined steam and gas cycle and can operate from various heat sources with working temperature of 70–95°C, including flat solar collectors [16, 17].

Various schemes of using the HPCs in solar systems for water lifting and hot water supply with flat collectors and with a parabolic-cylindrical concentrator have been developed. The inclusion of HPC in the system increases the efficiency of solar energy conversion by 8–10% [17].

Currently, the Institute for Physics and Technology is developing designs for solar-thermal systems of multifunctional purpose with a thermodynamic active circuit (TAC) based on the use of HPC and SC – flat and parabolic-cylindrical (Figure 5.30).

SPSs of this type can provide simultaneous rising of cold water from a source and heating a part of the water to the temperature of 50–60°C, and also can produce desalination of saline waters [18].

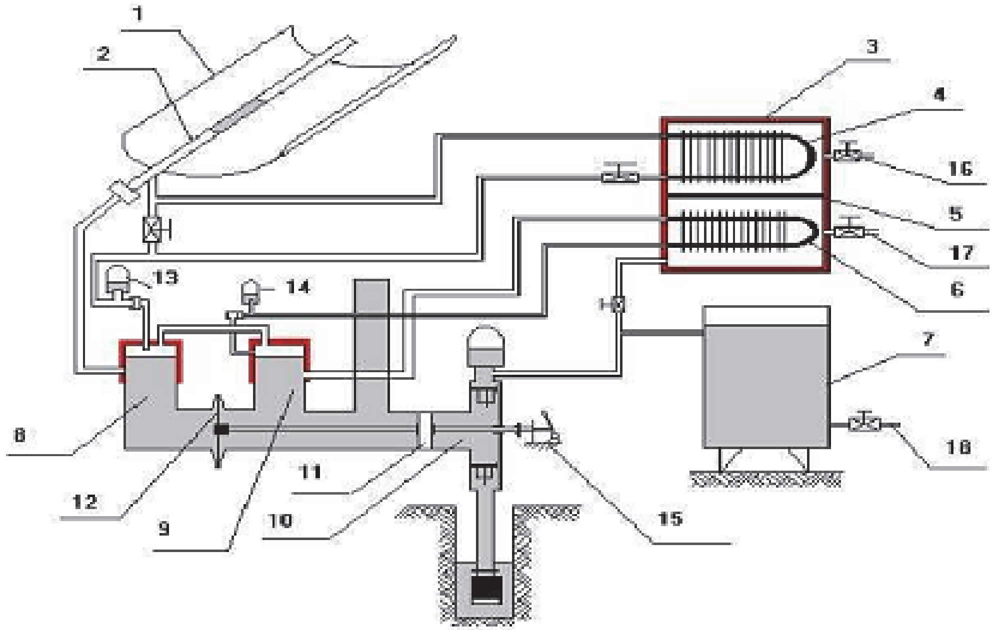

Figure 5.30. SPS of combined cold and hot heat supply with active thermal circuit and parabolic-cylindrical concentrator

The SPS consists of the following elements:a parabolic-cylindrical concentrator (1) with a linear solar heat receiver (2), a hot water tank (3) with a heat exchanger (4) in the upper part, with a partition (5) and with a heat exchanger 6 in the lower part, a cold storage tank (7), a hydraulic piston converter (HPC), including a hot cylinder (8), a cold cylinder (9), a pump unit (10), a piston of the pump unit (11), rigidly connected to the membrane piston (12) and a manual starting device (15). The heat exchanger of the hot water tank (4) is connected at one end to the heat receiver, and the other through a circulation pump (13) with a gas cavity of a hot cylinder (8) of a HPC. The heat exchanger of the cold water tank (6) is connected at one end to the liquid cavity, and the other through the circulation pump (14) with the gas cavity of the cold cylinder (9). One end of the heat receiver (2) is connected by a hydraulic line with a liquid cavity of hot cylinder (8), and the other end with heat exchanger (4) and through the bypass line and a circulation pump (13) with a gas cavity of a hot cylinder (8). A piston (11) of a pump unit is rigidly connected to the manual starter (15). The hot water tank (3) is provided with a tap of hot water (16) and the tap of warm water consumption (17), and the cold water tank (7) is equipped with cold water tap (18).

The principle of operation of the SPS is described in [18].

When heat is supplied to the gas cavity of the HPC hot cylinder and heat is removed from the gas cavity of the HPC cold cylinder the temperature difference between the gas cavities of hot and cold cylinders in the HPC is established, providing the work of thermodynamic cycle, while there is a self-oscillating process of liquid columns in HPC cylinders, and there is excitation and maintenance of the cyclic process of liquid oscillating motion in solar heat receiver (2), heat exchangers (4) and (6), as well as in connecting lines. At the same time, the pressure in the operating circuit varies cyclically, and when increasing the pressure the liquid is pumped into the pneumohydraulic accumulators of the circulating pumps (13), (14) of the hot and cold HPC cavities. With decreasing pressure in the working circuit due to the pneumatic energy stored in the pneumohydraulic accumulators, some of the liquid is injected into the hot and cold HPC cavities. Thus, the liquid circulation is organized along two contours:

- heat receiver (2) – heat exchanger (4) – pump (13) – gas cavity of hot cylinder (8) – liquid cavity of hot cylinder (8) – heat receiver (2);
- heat exchanger (6) – pump (14) – gas cavity of cold cylinder (9) – liquid cavity of cold cylinder (9) – heat exchanger (6).

Thus, the SPS, due to the solar radiant flux, provides the pumping of water from a well or other pond and the production of hot water, i.e. the consumer can be provided with cold and hot water.

Unfortunately, there are no technical specifications or results of experimental studies of the described SPS [18] in the literature. There are only operating data of the previous laboratory sample of the hydraulic piston converter [17].

Hydraulic Accumulators

Since SPSs with HPC are heat-hydraulic systems by nature, there are traditional hydrodynamic devices, in particular, circulation pumps with pneumohydraulic accumulators (PHA) among their structural elements [18]. Consequently, in addition to the technical advantages acquired by SPSs due to the use of the hydraulic devices, they also have the traditional disadvantages accompanying the use of such elements, in particular, PHA.

It is known that the PHA is a pressurized vessel that allows accumulating the energy of the compressed gas and transferring it to the hydraulic system with a flow of fluid under pressure.

With a slow change in pressure in the hydraulic system (>3 min), the gas compression process is close to the isothermal one, when the heat exchange between the gas and the surrounding environment completely takes place, and the product of the gas pressure p on its volume V is constant. With a sharp change in pressure (<1 min) the process is close to adiabatic. In the real case, the process is between these states. To increase the efficiency of the work, the PHAs are filled with gas (nitrogen) under a certain pressure (pressure of charge). Extreme pressure charging is recommended to take [19–21]: at accumulation of energy $0.9 \cdot p_{min}$; at hydraulic shock absorbing $(0.6...0.9) \cdot p_{mid}$; when damping the pulsations $0.6 \cdot p_{mid}$), where p_{mid} is the average working pressure.

For all types of PHAs, with all uses, including energy-saving systems of recuperative type [18], there are three principal disadvantages that can not be eliminated within the traditional approach to designing a PHA: the variability of the pressure of the hydraulic system in accordance with the change in the amount of accumulated energy, low specific energy capacity than in other in other branches of power engineering, explosion hazard due to the presence of the gas phase. Even the new technological improvements do not lead to a fundamental improvement.

Traditionally, the leading countries in which more than 40 firms (in each country) are involved in the development and production of PHA are the United States and Germany. The main world producers of PHA are the companies such as Bosch Rexroth AG, ROEMHELD GmbH, HYDAC International [19–25]. Piston PHAs produced by leading foreign firms have a capacity of V_{nom} = 0.16...400 L and pressure $p \leq 37.5$ MPa, membrane PHAs – V_{nom} = 0.075...10 L and pressure $p \leq 30$ MPa, cylinder PHAs – V_{nom} = 0.16...455 L and pressure $p \leq 55$ MPa. It is seen, that the pressures range is rather limited, because the safety conditions dictate a mandatory three-fold safety margin. However, Hydac supplies cylinder accumulators at a pressure up to 100 MPa, V_{nom} = 1.5 L or 10 L under a special order.

Thermomolecular Accumulators

It should be pointed out once again that one of the basic elements of the modern hydraulic systems are pneumohydraulic accumulators, the improvement of which, in particular, increasing energy efficiency, is problematic as it occurs due to a detailed study and improvement of their working process and constructive parameters, that is, factors that are traditionally well known and studied. This problem is proposed to be solved by developing the new types of accumulators using the fundamentally new working media.

The Laboratory of Thermomolecular Energetics deals with the investigations in the new scientific trend named “the thermomolecular energetics (TME)” (the author and the founder of the Laboratory is prof. V. Eroshenko (1940–2015)). The investigations are directed on researching the physical, chemical and thermodynamic properties of the new non-traditional heterogeneous working medium (HWM) “nonwetting liquid – capillary-porous matrix” (repulsive clathrates (RC)). The successive HWM compression-expansion process allows accumulating and releasing the significant surface energy due to the forced formation and spontaneous reduction of interphase surface (performance of the Gibbs work of surface formation, see Figure 5.31).

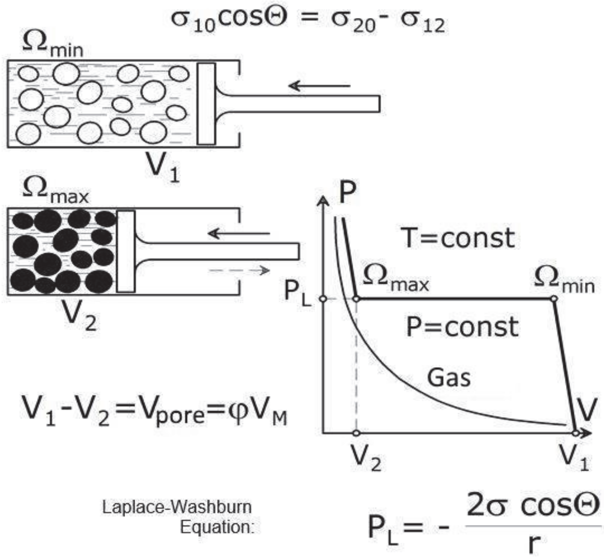

Figure 5.31. The principle of thermomolecular accumulator operation

As the result there is a possibility of creating new compact HWM energetic devices of different classes [26–28], such as:

- hydro-capillary accumulators of mechanical (hydraulic) energy,
- dampers, bumpers and shock-absorbers,
- energetically autonomous devices of different types.

The basis of the work of thermomolecular devices is the idea of using the Gibbs thermodynamic method for surface phases, the laws of molecular physics and colloidal chemistry in the creation of new thermodynamic working media for power devices of various classes, in particular, accumulators based on the principles of thermomolecular energetics.

The essence of this idea concerns the peculiarities of the behavior of heterogeneous lyophobic systems (HLS) used as the new, heterogeneous working medium, which consists of two main components: fluid and capillary-porous body (CPB), which is not wetted by this fluid. In the process of compression-expansion of the HLS there is a forced development and spontaneous reduction of the interphase-surface. From the point of view of thermodynamics, the working-medium is actually the interphase developed surface with the large free surface energy (the Gibbs potential) capable of performing the useful mechanical work.

Thus, it is possible to design the highly effective multifunctional TME-accumulators with technical characteristics, much higher than the traditional counterparts.

The TME-accumulator working medium is the HLS “liquid-porous matrix”, which uses micro-mesoporous materials: superhydrophobic zeolites with pore space of 0.2–0.3 ml/g and a specific surface (1–2)·10^3 m^2/g. The TME-accumulator operating chamber is a volume filled with HLS, where the pore space remains free of fluid in the absence of external action due to the non-wetting of the porous body by the liquid.

The process of energy accumulation is the forced development of the interphase surface by forced intrusion of the liquid into the porous space under the external pressure, which is determined by the Laplace capillary pressure (Figure 5.31).

The value of the accumulated energy is equal to the product of the surface tension of the liquid on the interphase surface area (the Gibbs work, surface energy, capable of performing mechanical work).

Recuperation of energy is the spontaneous release of liquid from the pore space under the Laplace capillary pressure. For a synthesized matrix, the working pressure can be ~600 bars. Taking into account the designed matrix, the specific (volumetric) energy capacity can reach 25–30 MJ/m^3 of HLS.

Hydraulic Accumulators vs Thermomolecular Accumulators (Calculations)

In the absence of the technical characteristics of the above mentioned SPS with HPC in general and used PHAs in particular, comparison of two types of the accumulators can be based on the traditional PHA technical characteristics spectrum, taken from the PHA data sheets and operating instructions of the most well-known PGA producers [19–25]. The comparison is carried out within the same mass-dimensional characteristics for accumulators of different types. The results are shown in Tables 5.11, 5.12 and Figure 5.32.

Basic Hydraulic Accumulator Terms

p_0 – gas pre-charge pressure,

p_1 – min operating pressure (min allowed pressure),

p_2 – max operating pressure (max allowed pressure),

Δp_{dyn} – working pressure range,

V_{nom} – nominal volume (gas volume),

V_0 – effective gas volume (internal working volume),

$V_{1(gas)}$ – gas volume at p_1,

$V_{2(gas)}$ – gas volume at p_2,

$V_{1(oil)}$ – oil volume at p_1,

$V_{2(oil)}$ – oil volume at p_2,

V_S – accumulated volume (oil volume at max working pressure),

M_0 – net weight,

M – total weight,

E – energy capacity,

e_V – specific energy capaciity per unit nominal volume,

e_M – specific energy per unit mass.

Table 5.11. The calculation results for traditional PHAs of the different models

Model	p_0	p_1	p_2	Δp_{dyn}	V_{nom}	V_0	$V_{1(gas)}$	$V_{2(gas)}$
	bar	bar	bar	bar	liter	liter	liter	liter
HAD 1,0-200-1X/10G04E-1N111-BA	10,0	85,0	200,0	115,0	1,0	1,0	0,93	0,40
HAD 3,5-350-1X/10G05E5-1N111-CE	10,0	220,0	350,0	130,0	3,5	3,5	3,05	1,95
HYDROKOMP 8200-03	100,0	125,0	500,0	375,0	0,075	0,075	0,060	0,015
ROEMHELD 9605_611	100,0	110,0	500,0	390,0	0,075	0,075	0,068	
SBO 750-0,25A6/342U-750AK	75	83,3	750,0		0,25	0,246	0,221	0,025
Model	$V_{1(oil)}$	$V_{2(oil)}$	V_S	M_0	M	E	e_V	e_M
	liter	liter	liter	kg	kg	kJ	kJ/l	kJ/kg
HAD 1,0-200-1X/10G04E-1N111-BA	0,07	0,60	0,53	3,5	4,0	6,76	6,76	1,70
HAD 3,5-350-1X/10G05E5-1N111-CE	0,45	1,55	1,10	16,0	17,0	31,15	8,90	1,83
HYDROKOMP 8200-03	0,015	0,060	0,045			1,04	13,86	
ROEMHELD 9605_611			0,059	2,4	2,5	1,14	15,14	0,46
SBO 750-0,25A6/342U-750AK			0,197	9,0	9,2	4,05	16,20	0,44

Basic Thermomolecular Accumulator Terms

V_{pore} – pore volume,

V_{pm} – porous matrix volume,

V_m – material volume,

V_{rc} – repulsive clathrate volume ($V_{rc} = V_{nom}$),

φ – porosity (V_{pore}/V_{pm}),

m_l – liquid mass,

m_m – material mass,

m_{rc} – repulsive clathrate mass,

M – total mass (rc+container),

p_i – pressure of intrusion ($p_i = p_2$),

E – energy capacity,

e_V – specific energy capacity per nom. volume unit,

e_M – specific energy capacity per mass unit.

Table 5.12. The calculation results for TME-accumulators with CPB of the different porosity

φ	V_{rc}	V_{pore}	V_m	m_l	m_m	m_{rc}	M	p_i	E	e_V	e_M
cm³/cm³	liter	liter	liter	g	g	g	kg	bar	kJ	kJ/l	kJ/kg
0,5	1,0	0,33	0,33	333,3	733,3	1066,7	4,57	200,0	6,67	6,67	1,46
0,5	3,5	1,17	1,17	1166,7	2566,7	3733,3	19,73	350,0	40,83	11,67	2,07
0,5	0,075	0,025	0,025	25,0	55,0	80,0		500,0	1,25	16,67	
0,5	0,075	0,025	0,025	25,0	55,0	80,0	2,48	500,0	1,25	16,67	0,50
0,5	0,250	0,083	0,083	83,3	183,3	266,7	9,27	750,0	6,25	25,00	0,67
φ	V_{rc}	V_{pore}	V_m	m_l	m_m	m_{rc}	M	p_i	E	e_V	e_M
cm³/cm³	liter	liter	liter	g	g	g	kg	bar	kJ	kJ/l	kJ/kg
0,65	1,0	0,39	0,21	393,9	466,7	860,6	4,36	200,0	7,88	7,88	1,81
0,65	3,5	1,38	0,74	1378,8	1633,3	3012,1	19,01	350,0	48,26	13,79	2,54
0,65	0,075	0,030	0,016	29,5	35,0	64,5		500,0	1,48	19,70	
0,65	0,075	0,030	0,016	29,5	35,0	64,5	2,46	500,0	1,48	19,70	0,60
0,65	0,250	0,098	0,053	98,5	116,7	215,2	9,22	750,0	7,39	29,55	0,80

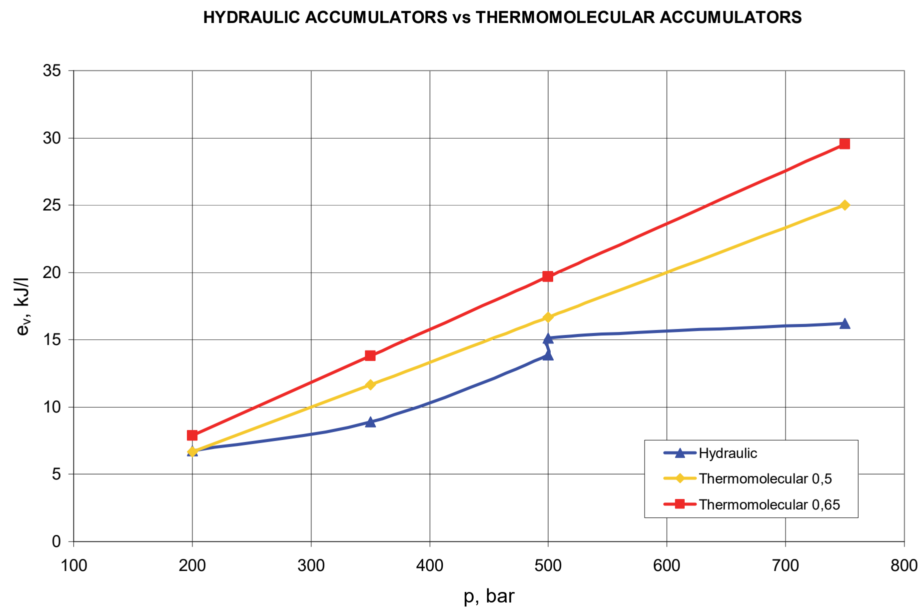

Figure 5.32. The specific energy capacity for PHA and TME-accumulators

5.7. CONCLUSIONS

The thermodynamic and thermophysical peculiarities of the functioning of some constructions of the solar power systems (SPS) with solar concentrators on the basis of converters operating in the Stirling cycle are considered. The result of the work of the considered SPSs is the receipt of heat and electric energy. The parameters of their productivity and efficiency are determined; ways of their work further improvement are analyzed.

For the multifunctional SPSs with active thermodynamic circuit, as an option to improve the basic characteristics, the use of structural elements, in particular, thermo-molecular accumulators, whose work is based on the heterogeneous lyophobic systems (HLS) as the new type of working media, is proposed.

REFERENCES

[1] Jacobson M.Z., Delucchi M.A., *A path to sustainable energy by 2030*, "Scientific American" 2009, Vol. 301, No. 5, pp. 38–45.

[2] Rannels J., *The DOE office of solar energy technologies vision for advancing solar technologies in the new millennium*, "Solar Energy" 2000, Vol. 69, No. 5, pp. 363–368.

[3] Stoudenets V.P., Dovgyi S.S., Yemanova N.O., *Solar Power System Based on Stirling Engine*, Proceedings of the international conference "UKR-POWER 2012", "Energy saving, energy efficiency, ecology – a strategic direction of energy development, "Investments and Innovations", Kyiv, IEE NTUU "KPI", 06–07 December 2012, pp. 42–45.

[4] Stoudenets V.P., Dovgyi S.S., Yemanova N.O., *The Characteristics of Solar Dish/Stirling System Based on UDS-1 Machine*, Proceedings of the 8th International Green Energy Conference (IGEC-8), Kyiv, 17–19 June 2013, pp. 214–216.

[5] Dolganov K.Y., Lisitsa V.P., *Educational-demonstrational Stirling engine UDS-1*, "Dvigatelestroyeniye" 1989, No. 5, pp. 28, 33.

[6] Fedienko A.V., Stoudenets V.P., *Efficiency of the heat pump system based on the Stirling machine UDS-1*, "Energy Technologies and Resource Saving" (Energotechnologii i Resursosberegenie) 2011, No. 3, pp. 76–78.

[7] Stoudenets V.P., Fedienko A.V., *Characteristics of the cycle of the heat pump system based on the Stirling machine UDS-1*, "Industrial Heat Engineering" ("Promyshlennaya Teplotekhnika") 2011, Vol. 33, No. 8, pp. 126–130.

[8] Hiester N., Tietz T., Loh E., Duwez P., Nevin K., *Theoretical considerations on performance characteristics of solar furnaces*, "Journal of Jet Propulsion" 1957, Vol. 27, No. 5, pp. 507–513.

[9] Duwez P., *Utilization of solar furnaces in high-temperature research*, "Transactions of ASAE" (Am. Soc. Agric. Eng.) 1957, Vol. 79, No. 5, pp. 1019–1023.

[10] Simon A., *Calculation of the concentration of energy at points outside the focal spot of a parabolic condenser*, "Solar Energy" 1958, Vol. 2, No. 2, pp. 22–24.

[11] Walker G., *Stirling engines*, Oxford: Clarendon Press, 1980.

[12] Reader G.T., Hooper C., *Stirling Engines*, E. & FN Spon, London 1983.

[13] Kongtragool B., Wongwises S., *A review of solar-powered Stirling engines and low temperature differential Stirling engines*, "Renewable and Sustainable Energy Reviews" 2003, Vol. 7, No. 2, pp. 131–154.

[14] Zadiora A.T., Stoudenets V.P., *Modeling Heat Recovery of SPS Based on Stirling Engine in SolidWorks*, Materials of the XV International Scientific and Practical Conference of Postgraduates, Graduates and Students "Modern Problems of Scientific Supply of Energy", Kyiv, Igor Sikorsky Kyiv Polytechnic Institute, 25–28 April 2017, Vol. 2, 2017, Vol. 1, p. 129.

[15] Zadiora A.T., Stoudenets V.P., *Solar Power System Based on UDS-1 Machine with Heat Recovery*, Materials of the IX scientific and technical conference "Energy. Ecology. Man" (conference of young researchers – graduate students and masters), 25 May 2017, IEE, Igor Sikorsky Kyiv Polytechnic Institute, 2017, pp. 118–122.

[16] Orda E.P., Trukhov V.S., Tursunbaev I.A., *Solar hydro-piston water lift*, "Geliotechnika" 1991, No. 5, pp. 11–14.

[17] Orda E.P., Trukhov V.S., Tursunbaev I.A., *Analysis of the working process of the solar hydro-piston converter*, "Geliotechnika" 1995, No. 6, pp. 43–49.

[18] Trukhov V.S., Tursunbaev I.A., Orda E.P., *Solar water and heat supply systems with active thermodynamic circuit*, Materials of the Conference dedicated to the 60th anniversary of the foundation of the Republic of Uzbekistan Academy of Science Institute of Physics and Technology, Tashkent, 27–28 November 2003, pp. 94–99.

[19] *Diaphragm-type accumulator. Type HAD*/RE 50150/02.05. Data sheet/Hydraulics/Bosch Rexroth AG.

[20] HYDROKOMP 8200-03/Data sheet/*Hydraulic accumulators*/HYDROKOMP GmbH/Issue 05.14/600-2.

[21] ROEMHELD 9605_600 Operating instructions/*Hydraulic accumulator*/ROEMHELD GmbH/Issue 04.2004/B061EN01.

[22] ROEMHELD 9605_611 Data sheet/*Hydraulic accumulators*/ROEMHELD GmbH/issue 9.14/F9.601.

[23] HYDAC International. *Accumulators: Bladder, Piston, Diaphragm*/HYDAC International. Accumulator Catalog #02068195/08.03.

[24] HYDAC International. *Accumulators: Bladder, Piston, Diaphragm*/HYDAC International. Innovative Solutions. Accumulator Brochure #02068195/7.08.

[25] HYDAC International. *Accumulators: Bladder, Piston, Diaphragm*/HYDAC International. Innovative Fluide Power. Accumulator Catalog #02068195/04.13.

[26] Eroshenko V., Piatiletov I., Coiffard L., Stoudenets V., *A new paradigm of mechanical energy dissipation*, Part 2, *Experimental investigation and effectiveness of a novel car damper*, "Proceedings of the Institution of Mechanical Engineers, Part D: Journal of Automobile Engineering" 2007, Vol. 221, No. 3, pp. 301–312.

[27] Ievtushenko A.V., Stoudenets V.P., Eroshenko V.A., *Effective Thermal Conductivity of Heterogeneous Lyophobic Nanosystems for Use in Thermomechanical Energy Devices*, "International Journal of Thermal Sciences" 2012, 62, pp. 103–108.

[28] Eroshenko V.A., Grosu Y., Tsyrin N., Stoudenets V., Nedelec, J.M., Grolier J.P.E., *Exceptionally Large and Controlled Effect of Negative Thermal Expansion in Porous Heterogeneous Lyophobic Systems*, "The Journal of Physical Chemistry C" 2015, 119, No. 19, pp. 10266–10272.